Regulation of *Drosophila* Motor Axon Pathfinding by the Metalloprotease Tolloid-related 1 (Tlr1) and the Collagen *Drosophila* multiplexin (Dmp)

Dissertation

der Mathematisch-Naturwissenschaftlichen Fakultät

der Eberhard Karls Universität Tübingen

zur Erlangung des Grades eines

Doktors der Naturwissenschaften

(Dr. rer. nat.)

vorgelegt von

Dipl.-Biol. Frauke Meyer

aus Hamburg

Tübingen

2011

Tag der mündlichen Qualifikation:	08.12.2011
Dekan:	Prof. Dr. Wolfgang Rosenstiel
1. Berichterstatter:	PD Dr. Bernard Moussian
2. Berichterstatter:	Prof. Dr. Rolf Reuter

‘Scientific research [is] a steering process,
a means by which we find our way about,
and try to make sense of, a bewildering
and complex world.’

Peter Medawar
‘Advice to a Young Scientist’
1979

Acknowledgements

First and foremost, I would like to thank my supervisor Bernard Moussian for his constant and invaluable support. Furthermore, I thank Hermann Aberle and Christiane Nüsslein-Volhard for the opportunity of joining MPI Department 3, for their support and useful discussions, and specifically Hermann Aberle for the introduction to the subject and methods of motor axon pathfinding research, for letting me work with his *tlr1* mutant, his help in quantifying larval phenotypes and for performing several *tlr1* rescue experiments. I thank current and former members of Department 3, especially the 'fly people' Dirk Beuchle, Uwe Irion, Iris Koch, Jana Krauss, Andrea Mahr, Nina Vogt, and Ines Wolff for listening to my sorrows and for their help and advice. Similar thanks go to the former 'fish people' Petra Haas and Kajori Lahiri. Last not least I thank friends and family who provided lots of non-scientific support.

Table of Contents

Zusammenfassung

Axone folgen stereotypen Wegen zu ihren Zielen, und die Wegfindung von Motorneuronen bei *Drosophila* ist ein gängiges Modellsystem, um die zugrunde liegenden molekularen Mechanismen zu erforschen. In der Vergangenheit wurden zahlreiche Rezeptoren und ihre diffusiblen oder membrangebundenen Liganden als steuernde Faktoren für axonale Wachstumskegel identifiziert. Ein vollständiges funktionelles Bild des Prozesses fehlt jedoch noch, und es ist zu erwarten, dass weitere Faktoren noch unentdeckt sind. In der vorliegenden Arbeit werden zwei solcher Faktoren identifiziert.

Die extrazelluläre Protease Tolloid-related 1 (Tlr1) wurde durch einen Mutagenesescreen als Faktor für die Wegfindung von Motorneuronen entdeckt. Sowohl *tlr1*-mutante L3-Larven, als auch Embryonen im Stadium 16 - 17 zeigen häufig einen fehlerhaften Verlauf aller fünf motorischer Nerven. *tlr1* wird embryonal in mehreren Geweben exprimiert, und entsprechend konnte der mutante Phänotyp durch Expression von transgenem Tlr1 mittels unterschiedlicher Gal4-Treiberlinien gerettet werden. Dies schloss solche mit ein, die zu einer ektopischen Expression von Tlr1 führten. Dies zeigt, dass Tlr1 nicht zellautonom agiert.

Die extrazelluläre Matrix ist das Umfeld, in dem die axonale Wegfindung stattfindet, und es ist daher zu erwarten, dass sie bei diesem Prozess eine wichtige Rolle spielt. Mutanten des *Drosophila* Multiplexins (Dmp), eines Homologs von Collagen XV/XVIII, wurden durch zielgerichtete Deletionen erzeugt, und es wurden moderate, jedoch statistisch signifikante Effekte auf die axonale Wegfindung beobachtet. Es entstanden Defekte, die qualitativ ähnlich denen in *tlr1*-Mutanten waren, aber sich quantitativ unterschieden. Multiplexine besitzen eine C-terminale Endostatin (ES)-Domäne, die monomer oder trimer vorkommen kann. Transgen exprimiertes monomeres ES und Dmp in voller Länge, aber nicht trimeres ES, konnten den mutanten Phänotyp retten, jedoch senkte trimeres ES signifikant die normalerweise auftretende Fehlerrate im wildtypischen Hintergrund. *dmp* wird vor allem im Dorsalgefäß und im ventralen Nervensystem exprimiert. Die zur Rettung des mutanten Phänotyps führende Überexpression erfolgte jedoch mesodermal und in einigen einzelnen Zellen des

ventralen Nervensystems, so dass Dmp vermutlich nicht zellautonom wirkt. Die unterschiedlichen Effekte, die sich für die verschiedenen Dmp-Fragmente beobachten liessen, legen nahe, dass Dmp ein vielseitiges Molekül ist, das Wegfindungsprozesse in mehrere Richtungen beeinflussen kann. Andere Ergebnisse zeigen, dass Dmp eines von mehreren Substraten von Tlr1 sein könnte.

Summary

Axons follow stereotyped and reproducible pathways to their targets, and *Drosophila* motor axon pathfinding is a popular model system for investigating underlying molecular mechanisms. In the past, a good number of receptors and their diffusible or membrane-bound ligands have been identified as factors that steer axonal growth cones. However, a complete functional picture of the process is missing, and it is conceivable that additional axon pathfinding factors remain to be discovered. Two of them are contributed to the list by this work.

The extracellular protease Tolloid-related 1 (Tlr1) was identified as motor axon guidance factor through a mutagenesis screen. In both *tlr1* mutant L3 larvae and stage 16-17 embryos, all five motor nerves exhibit pathfinding errors at high frequencies. *tlr1* is embryonically expressed in several tissues, and likewise, transgenic rescue of the mutant phenotype was possible using several different Gal4 driver lines, including such that lead to ectopic Tlr1 expression. This indicates that Tlr1 acts cell non-autonomously.

The extracellular matrix is the environment in which axon pathfinding takes place, and as such conceivably plays an important role in the process. Mutants for *Drosophila* multiplexin (Dmp), a collagen XV/XVIII homologue, were generated by targeted deletion, and moderate, yet statistically significant effects on axon pathfinding were observed, that were similar in quality but not in penetrance to those of *tlr1* mutants. Multiplexins have a C-terminal endostatin (ES) domain, which can occur in monomeric or trimeric versions. Transgenically expressed monomeric ES, as well as full-length Dmp, was able to rescue the mutant phenotype, unlike trimeric ES, but trimeric ES significantly lowered the pathfinding error rate that is normally present in a wild type background. *dmp* is mainly expressed in dorsal vessel and ventral nerve cord, but rescue expression was driven in mesoderm and ventral nerve cord, indicating that the role of Dmp is cell non-autonomous. The differences in effect seen by different Dmp fragments imply that Dmp is a versatile molecule that can modulate pathfinding processes in different ways. Results suggest that Dmp may be one of several substrate molecules of Tlr1.

1. Introduction

A characteristic organ in the animal kingdom is the nervous system, which has to fulfil a variety of tasks. One of them is to orchestrate the use of muscles. Connectivity within the nervous system as well as neuromuscular connectivity are key to coordinated movement, and thus to all animal behaviours, like translocation, food uptake, hunting of prey, defence against enemies, flight from danger, mating behaviour and childcare. Neuromuscular connectivity thus has a biological significance at least equal to that of connectivity between neurons within the nervous system.

Neuromuscular connectivity depends on secure navigation of motor axons' growth cones to defined target muscles during development, and the navigation process of a motor axon can also serve as a model for axons that will form neuron-neuron connections, and vice versa. *Drosophila melanogaster* and *Caenorhabditis elegans* are invertebrate model systems that offer two advantages for analysing axon guidance mechanisms. First, they have a simple nervous system architecture, and second, they are easily amenable to classical genetic analysis. As a result, many axon guidance molecules were initially identified in invertebrates and their functional conservation in vertebrate axon guidance confirmed afterwards (Araujo and Tear, 2003).

Genetic and biochemical studies largely focused on transmembrane molecules of adhesive or signalling function and their diffusible or membrane-bound ligands, like Robo and Slit, semaphorins and their plexin-containing receptor complexes, netrins and DCC/frazzled receptors, ephrins and their receptors, fasciclinII/NCAM and DsCam (Araujo and Tear, 2003; Dickson, 2002; Tessier-Lavigne and Goodman, 1996). The contributions of other components of the extracellular matrix (ECM) to axonal pathfinding mechanisms have received much less attention (Hartmann and Maurer, 2001; Matani et al., 2007; Van Vactor et al., 2006).

1.1. Guidance cues can be categorized according to their mode of action

A large number of different guidance cues act at once on any individual growth cone. The growth cone has to integrate this information in order to react with the appropriate

guidance decision (Araujo and Tear, 2003; Chilton, 2006; Raper and Mason, 2010; Tessier-Lavigne and Goodman, 1996).

In order to systematically approach the question how guidance decisions are made, it can be useful to categorize individual guidance cues according to their effect. A classic approach by Tessier-Lavigne and Goodman (1996) categorizes the mechanisms involved into four types: Growth cones can either be attracted (1) or repelled (2) and the molecular cues involved can either act in a short-range (3) fashion (contact attraction and repulsion) or long-range fashion (4) (chemoattraction and –repulsion; here a cue bridges the distance between its site of synthesis and the growth cone by diffusion). The existence of all these mechanisms has been demonstrated in neuronal cell cultures, and many examples exist for their *in vivo* relevance (Tessier-Lavigne and Goodman, 1996). While some cues clearly fall into one or the other class, cases are known where a molecule has different effects on different axons. Most prominently, Netrin-1 and its orthologues can both attract and repel axons from the ventral midline, depending on the direction in which respective axons need to grow (Colamarino and Tessier-Lavigne, 1995; Hong et al., 1999).

A more modern system categorizes guidance molecules into tropic guidance cues, adhesive cues, trophic signals, and modulatory cues (Raper and Mason, 2010). Here, tropic guidance cues are such that impart a directional valence to growth cone motility. This category is highly similar to the classical system of attractive and repulsive guidance mechanisms, populated by transmembrane receptors and their diffusible or membrane-bound ligands, by Tessier-Lavigne and Goodman (1996), and referred to above. Adhesive cues, according to Raper and Mason (2010), have a permissive influence on axon outgrowth, so that axons prefer permissive substrates over non permissive substrates when given the choice (Letourneau, 1975). They are cell adhesion molecules (CAMs) present on neuronal or non-neuronal surfaces, like Sidestep (Siebert et al., 2009), or extracellular matrix (ECM) components, like laminin (Bozyczko and Horwitz, 1986). Trophic signals mainly promote survival of neurons and their processes, and growth cone motility, like neurotrophins (Reichardt, 2006). Modulatory cues change the way axons respond to tropic cues without carrying directionality information on their own. Laminin has been reported to turn netrin-mediated attraction into repulsion (Hopker et al., 1999).

Neurotrophins can reduce the response of axons to the repellent semaphorin3A (Dontchev and Letourneau, 2002). However, Raper and Mason admit that this categorization is of limited power, since guidance cues can have functions in more than one context, and these different functions can fall into different categories. Examples obvious from the above are laminin, which is categorized as adhesive cue in one case and as modulatory in another, and neurotrophins, which can be trophic cues as well as modulatory cues.

1.2. Motor axon pathfinding is a multi-step process

Motor axon pathfinding is an experimental system that serves as a model the findings of which can also be relevant to pathfinding mechanisms of neurites of other neuronal cell types or model systems, where axon pathfinding targets are dendrites, and even to endothelial cells which form the vascular system, and *vice versa* (Weinstein, 2005). *Drosophila* embryonic motor axon pathfinding, specifically, is a compelling model system due to its limited number of objects involved. In embryonic and larval abdominal hemisegments A2 to A7, 30 body wall muscles per hemisegment are innervated by around 34 motor neurons that are bundled into five nerves. Motor neuron somata positioned in the ventral nerve cord have defined identities, and thus defined tasks of innervating specific muscles via specific nerve routes. The innervation pattern is stereotypically repeated from hemisegment to hemisegment (Landgraf et al., 1997; Sink and Whitington, 1991). This segmental repetition gives the experimenter the opportunity to observe the results of several independent pathfinding processes within one specimen. As a drawback, embryonic motor axons and nerves are very fine structures and therefore not easy to image, especially to single-cell resolution.

Drosophila embryonic motor axon pathfinding can be broken down into separate steps. Initially, a motor axon has to exit the central nervous system in order to project into the periphery. This task involves two guidance decisions: the right rostrocaudal exit position has to be found, and followed by determining the right outgrowth direction away from the midline. The *Drosophila* nervous system is intrinsically segmented (Landgraf et al., 1997), and glial cells seem to play a role in determining the segmental exit points of growth cones (Sepp et al., 2001). *Drosophila* ventral midline axon guidance mechanisms

are well characterized (Dickson and Zou, 2010), and it is easily conceivable that motor axons respond to the same signals as all other midline neurons that direct their neurites towards, across and/or away from the midline.

After exiting the CNS, motor axons have to navigate through the developing periphery to find their muscle targets. In the *Drosophila* embryo, as in vertebrates, several motor axons initially occur in bundles, forming a motor nerve, before they defasciculate from one another in order to pursue their individual targets (Hollyday, 1995; Landgraf et al., 1997; Westerfield et al., 1986). However, these fasciculated axons do not necessarily migrate at the same time. Rather, certain axons pioneer on the path laid out by local guidance cues. Other axons follow this track, either making use of local guidance cues in a similar fashion as the pioneer axon, or rely on cues presented by the pioneer axon. Ablation studies of pioneer neurons have given evidence for both mechanisms (du Lac et al., 1986; Lin et al., 1995; Sanchez-Soriano and Prokop, 2005).

En route to its specific target, each growth cone encounters intermediate targets termed as choice points. At each choice point, certain growth cones have to take the decision to steer away, to defasciculate from other axons (Schneider and Granato, 2003).

At the ventral choice point of the *Drosophila* embryonic muscle innervation system, the five main motor nerves, each of which contains several axons, defasciculate and steer off into individual directions. The ISN is the nerve heading most dorsally to innervate the hemisegment's 10 dorsalmost muscles. The SNa targets six lateral muscles, while the ISNb, SNc and ISNd innvervate the ventral muscle field consisting of 13 muscles altogether (see Fig. 1) (Landgraf et al., 1997; Sink and Whitington, 1991).

The next necessary step after appropriate branching is recognition of the precise synapse target site. After this, synapse development can ensue (Schneider and Granato, 2003).

1.3. Several genes cause similar mutant phenotypes in *Drosophila* motor nerves

A number of *Drosophila* motor axon guidance mutants are known where the defasciculation of ISNb, SNc or ISNd can be impaired, which often results in the

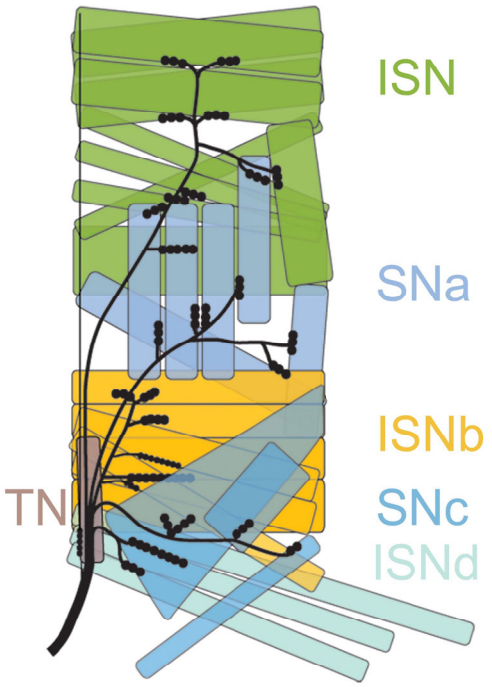

Fig. 1. Larval hemisegmental set of muscles, viewed from the exterior, and the five motor nerves that innervate them. The target muscle fields of the five different nerves are depicted in different colours and the names of the respective nerves are given on the right. Phenotypes studied in this work concern the ISNb, which innervates one of the three ventral muscle fields (yellow) and the ISN, innervating the dorsalmost muscle field (green).

respective nerve continuing along the ISN. This frequent phenotype is termed ventral bypass phenotype, and occurs in several mutants, including those of BeatIa, a molecule of the immunoglobulin superfamily secreted by motor neurons (Fambrough and Goodman, 1996). Mutants for the transmembrane BeatIc show only light ISNb defects, and a *beatIc* mutant background improves the *beatIa* ventral bypass phenotype, suggesting that the two molecules have opposite adhesive functions, with BeatIa positively regulating ISNb defasciculation, and functional BeatIc enhancing the ISNb bypass phenotype caused by BeatIa loss of function (Pipes et al., 2001). Recently, BeatIa was shown to interact with the muscle surface attractant Sidestep in guiding motor axons to muscle targets (Siebert et al., 2009). Side mutants themselves show a strong ventral bypass phenotype (Sink et al., 2001). Loss of the cell adhesion molecule Fasciclin II (FasII), which is present in all motor axon cell membranes, does not lead to a significant ISNb phenotype (Fambrough and Goodman, 1996), but axonal overexpression of FasII produces the characteristic ISNb bypass phenotype (Lin and Goodman, 1994). Motor axon pathfinding phenotypes are never uniform within a particular mutant, and also differ within one individual from hemisegment to hemisegment. The range of ISNb mutant phenotypes comprises different

degrees of ventral bypass, which can apply to some or all of the three ventral nerves. In particular, an ISNb ventral bypass can be partial, with some but not all ISNb axons detaching from the ISN. A full ventral bypass can be fused, i.e. the ISNb can remain completely fasciculated with the ISN, or can be parallel, also called split, with the ISNb detaching from the ISN, but travelling in parallel with it. In addition, stall phenotypes occur where the ISNb apparently comes to a halt near the ventral muscle field. These different ISNb phenotypes have been nicely described and quantified in a series of publications concerning the axonally expressed *Drosophila* receptor protein tyrosine phosphatase (RPTP) family. The mutant phenotype of the RPTP LAR exhibits a full ventral bypass penetrance of around 60%, and around 30% partial bypass penetrance, leaving only about 10% of ISNb nerves to correctly enter the ventral muscle field (Krueger et al., 1996). The strongest mutant allele of *Ptp69D* exhibits 25% full and 15% partial bypass (Desai and Purdy, 2003). For all other RPTPs, the single mutant phenotype does not differ from wild type, but the full ISNb phenotype terminology can be used to describe double and triple mutant combinations of the different genes (Desai et al., 1997; Jeon et al., 2008; Schindelholz et al., 2001; Sun et al., 2001). Their genetic interactions are complex, including a proposed counteraction of LAR through PTP99A (Desai et al., 1997).

Mutants for *beatIa*, *side*, different RPTP mutant combinations, and animals axonally overexpressing FasII also exhibit misinnervations of lateral muscles through the SNa as well as dorsal ISN phenotypes. Cases where the anterior SNa branch outgrows its target muscles have been termed an SNa bypass. Another recurring SNa phenotype is a failure to bifurcate, as well as ‘stalls’. The ISN usually exhibits the least severe guidance defects. In some cases, the ISN stops short of its final target muscles, or outgrows them, including misrouting (Fambrough and Goodman, 1996; Lin and Goodman, 1994; Schindelholz et al., 2001; Sink et al., 2001; Sun et al., 2001). Interestingly, a complete failure of the ISN to innervate its target muscle field has never been described.

1.4. The extracellular matrix provides the substratum for growing axons

The extracellular matrix (ECM) is a supramolecular assembly of collagens, laminins, metalloproteinases and proteoglycans that holds cells together (Bosman and

Stamenkovic, 2003). Axonal pathfinding occurs in close contact to the ECM, produced by various cell types (Raper and Mason, 2010). Hence, the molecules present in this environment can potentially provide direct guidance cues, or be the background that supports and modulates the function of guidance cues, which can be diffusible molecules acting over a distance. Laminin, for example, is known as a permissive substratum for *in vitro* axon outgrowth (Raper and Mason, 2010), and *Drosophila* Laminin A has been implicated in the pathfinding of ocellar axons (Garcia-Alonso et al., 1996) as well as embryonic midline axons (Stevens and Jacobs, 2002).

Proteoglycans can be grouped into different families, an important one of which are heparan sulphate proteoglycans (HSPGs) (Bosman and Stamenkovic, 2003; Iozzo et al., 2009). Different roles in neural development have been allocated to them (Hartmann and Maurer, 2001; Matani et al., 2007; Van Vactor et al., 2006). They have an enormous potential for creating different microenvironments or encoding different guidance cues due to the combinatorial potential that lies within different glycan side chain modifications (Bulow and Hobert, 2004; Esko and Selleck, 2002).

In *Drosophila,* Syndecan (Sdc) and, to a lesser extent, the glypican Dally-like (Dlp), both of them HSPGs, have been shown to function in axonal guidance at the ventral midline via the action of the Slit/Robo signalling system (Johnson et al., 2004; Rawson et al., 2005; Steigemann et al., 2004) and in the visual system (Rawson et al., 2005). However, they seem to play a minor role in the *Drosophila* motor axon guidance system, since in triple mutants of all glypicans and syndecans (*sdc*, *dally*, *dlp*) motor axon pathfinding is accurate (Fox and Zinn, 2005), even though Sdc and Dlp bind to the motor axon guidance receptor LAR *in vitro* (Johnson et al., 2006) and *sdc* mutations also enhance the LAR phenotype (Fox and Zinn, 2005).

1.5. Metalloproteases in axon pathfinding

Matrix metalloproteinases (MMPs) are a group of ECM-shaping and remodelling proteases of the metzincin family, that comprises more than 20 members in vertebrates and exhibits a broad and overlapping set of substrates (Bosman and Stamenkovic, 2003). MMPs, as well as ADAMs ('A Disintegrin and Metalloproteases'), another group of metalloproteases, have been associated with migratory processes in general and also with

axonal pathfinding, and they have been shown to be expressed in the growth cones of vertebrate neurons (McFarlane, 2003; Webber et al., 2002). Recently, *Drosophila* MMP1 and -2 have been shown to be involved in motor axonal adhesion in the embryonic ventral motor axon guidance experimental system (Miller et al., 2008). Here, lack of MMPs resulted in lack of fasciculation, albeit without significant effects on axon pathfinding, while overexpression resulted in overadhesion between axons. ADAMs, in turn, have been implicated in axon extension much earlier. In 1996, Famborough et al. described axon extension defects for the *Drosophila* mutant *kuzbanian*, the ADAM10 ortholog (Fambrough et al., 1996). ADAM10 was shown to interact with ephrinA2 in mouse brain, modulating the interaction of ephrinA2 with its receptor through cleavage of the former (Hattori et al., 2000). At the *Drosophila* embryonic ventral midline, cleavage of the Slit receptor Robo by Kuzbanian seems to be essential for growth cone repulsion through Robo signalling (Coleman et al., 2010).

1.6. Tolloid-related 1 is a member of the BMP1 family of metalloproteases

Part of the work presented here is the first description of Tolloid-related 1 (Tlr1), also known as Tolkin (Tok), as a motor axon pathfinding molecule. *tlr1*, which is the only homologue of *tolloid* (*tld*) in the *Drosophila* genome and its direct genomic neighbour, was discovered using *tld* cDNA to probe *Drosophila* genomic libraries (Nguyen et al., 1994) and using the protease domain of mammalian Bone morphogenetic protein 1 (BMP1) to probe a genomic walk of the *tld* region in the *Drosophila* genome (Finelli et al., 1995). The mammalian genome contains three homologous Tld/BMP1 genes, with mTld and BMP1 being isoforms produced from the same gene. The domain structure of this protein family comprises a protease domain of the astacin type, that coordinates Zn^{2+} for catalytic activity (Sterchi et al., 2008), an N-terminal prodomain that typically needs to be removed in order to activate the protease domain, and a C-terminal region that is composed of three (BMP1) or five (Tld and Tlr1) CUB domains for mediating protein-protein interactions, and one (BMP1) or two (Tld and Tlr1) EGF-like domains that probably contribute to the overall protein tertiary structure (Hopkins et al., 2007).

A well-established function of Tld is cleavage of Sog, a TGF-β homologue, thus acting in embryonic dorso-ventral patterning through the canonical BMP signalling

cascade. This function is conserved between *Drosophila* and vertebrates (Blader et al., 1997; Marques et al., 1997; Piccolo et al., 1997), although, interestingly, cleavage sites for *Drosophila* Sog and the vertebrate homolog Chordin differ both in number and sequence motif (Canty et al., 2006; Scott et al., 1999). Tlr1 has been implicated in Sog degradation as well, both in dorsoventral patterning (Srinivasan et al., 2002) and in crossvein formation in the wing (Serpe et al., 2005).

Initial functional characterization of vertebrate BMP1 defined it as a procollagen C-proteinase, as it processes procollagens I, II and III into mature collagens at their C-termini (Kessler et al., 1996; Reddi, 1996). Later, each of the vertebrate BMP1/TLD-like proteases was shown to C-terminally process procollagens I, II and III *in vitro* (Pappano et al., 2003). The mammalian genome encodes three BMP1/TLD-like proteases in total (Scott et al., 1999; Takahara et al., 1996), with BMP1 and mammalian TLD being isoforms produced from the same gene (Takahara et al., 1994). Later, more collagens were added to the list of molecules being processed by BMP1/TLD-like proteases, either N- or C-terminally, like collagens V, VII, XI (Hopkins et al., 2007; Pappano et al., 2003; Rattenholl et al., 2002; Unsold et al., 2002), as well as other ECM constituents, such as the laminin 5 γ2 chain (Amano et al., 2000) and the HSPG perlecan (Gonzalez et al., 2005).

1.7. Collagens are abundant ECM components

Collagens are the most abundant constituents of all extracellular matrices (Bosman and Stamenkovic, 2003) with the network-forming collagen IV being a main building block of basement membranes (Ricard-Blum and Ruggiero, 2005; Yurchenco et al., 2004). They are a large family of triple helical proteins that are widespread in the body and the organismal world. For vertebrates, currently 29 distinct collagen types are known, that are numbered in the order of their discovery. They are encoded by 44 different genes and appear rich in variations as homo- or heterotrimers (Kadler et al., 2007; Soderhall et al., 2007).

Several vertebrate collagens form fibrils that are principal tensile elements of vertebrate tissues, such as tendon, cartilage, bone and skin, among them being type I, II, and III collagens. Moreover, vertebrates possess relatively short fibril-associated

collagens with interrupted triple helices (FACITs). Transmembrane collagens exist that have a short cytoplasmic N-terminus and long interrupted triple helical extracellular domains. These ectodomains can be proteolytically shed and have paracrine functions. Other collagens form anchoring fibrils or beaded filaments (Kadler et al., 2007).

The endostatin-producing collagens, types XV and XVIII are typically associated with basement membranes (Kadler et al., 2007). In *Drosophila*, this family is represented by only one copy, which was previously uncharacterized, and plays a central role in this work. Remarkably, the *Drosophila* genome harbours only three collagen genes in total, the other two encoding collagen type IV monomers (Mirre et al., 1992; Yasothornsrikul et al., 1997).

1.8. Collagens XV and XVIII share a characteristic domain structure

Collagens XV and XVIII are the two vertebrate members of a collagen family termed multiplexins (for 'multiple triple-helix domains and interruptions'), and each of them is encoded by a single gene (Kivirikko et al., 1994; Muragaki et al., 1994; Muragaki et al., 1995; Oh et al., 1994). While collagen XVIII is an HSPG (Halfter et al., 1998), collagen XV is chondroitin sulfate proteoglycan (CSPG) (Li et al., 2000). Both molecules are characterized by a collagen triple helix region, which is interrupted by several non-collagenous stretches, as well as a C-terminal non-triple helical, 'non-collagenous' domain termed NC1 (Muragaki et al., 1994; Muragaki et al., 1995; Oh et al., 1994; Rehn and Pihlajaniemi, 1994). The NC1 domains are composed of three functionally distinct regions: an association region in its most N-terminal part that trimerizes NC1 monomers, a hinge region that is thought to be sensitive to protease digestion, and the C-terminal globular endostatin (ES) domain (Sasaki et al., 1998).

ES domains of vertebrate types XV and XVIII collagens differ by certain features. At the very beginning of the type XVIII ES domain a Zn^{2+} coordination motif is present, but absent from type XV collagen. Besides, there is a four-residue loop within the type XVIII ES domain that is thought to convey heparin binding properties and is absent from type XV ES (Sasaki et al., 2000).

Both vertebrate collagen XVIII and *C. elegans* collagen XVIII occur in three different isoforms (Ackley et al., 2001; Muragaki et al., 1995; Rehn and Pihlajaniemi,

1995), whereas for vertebrate collagen XV only one isoform has been described (Kivirikko et al., 1994; Muragaki et al., 1994). They all share the triple helical region followed by the C-terminal endostatin-containing NC1 domain. Immediately N-terminally of the triple helix region, vertebrate collagen XV and all isoforms of collagen XVIII contain a domain that is homologous to the N-terminal domain of thrombospondin (TSPN) (Kivirikko et al., 1994; Muragaki et al., 1995; Rehn and Pihlajaniemi, 1995). Two of the three worm isoforms carry this domain as well, while the third does not have any N-terminal globular domains (Ackley et al., 2001). In vertebrates, N-terminal extension with a domain bearing resemblance to the extracellular domain of the *Drosophila* Wnt receptor Frizzled and with an acidic domain generate a middle and a long isoform, respectively (Muragaki et al., 1995; Rehn and Pihlajaniemi, 1995), whereas the longest *C. elegans* isoform carries an N-terminal domain with similarity to the Frazzled familiy of Netrin receptors (Ackley et al., 2001).

1.9. Collagens XV and XVIII have diverse effects on migratory processes

In 1997, a 20 kD protein was identified in conditioned media from murine hemangioendothelioma cells with inhibitory activity on the proliferation of bovine endothelial cells. It also inhibited tumor growth in mouse models. This protein was found to be identical to the C-terminal domain of murine collagen XVIII (O'Reilly et al., 1997). Proteolytic cleavage of collagen XVIII, the exposure of a new N-terminal sequence, and the coordination of Zn^{2+} in the N-terminal region of ES were suggested to be necessary for biologic activity (Boehm et al., 1998; O'Reilly et al., 1997). Subsequently, a series of tissue culture experiments were conducted on the motogenic activity of endostatin. For example, the effect of human multiplexin fragments on angiogenesis was tested in chick chorioallantoic membrane (CAM) assays. VEGF-induced angiogenesis was inhibited by ES-15 and NC1-15, while ES-18 and NC1-18 had no marked effect. In contrast, if angiogenesis was induced by FGF-2, NC1-15 and ES-18 had an inhibitory effect, while the other fragments had none (Sasaki et al., 2000). More results have been found that are similarly contradictory, and confirm differences in effects between monomeric and di- or trimeric ES derived from the same multiplexin within a given experimental system (Clamp et al., 2006; Kuo et al., 2001; Sasaki et al., 1999; Yamaguchi et al., 1999).

First *in vivo* evidence on the function of collagen XVIII or its derivatives came from the respective *C. elegans* mutant (Ackley et al., 2001). In worm *cle-1* mutants, migration defects of several neuronal cell types were observed. Rescue experiments for the migratory phenotype of mechanosensory neurons (MSNs) resulted in a rescue activity for NC1, while ES did not rescue. On the contrary, ES, but not NC1 impaired MSN migration in wild type background. In zebrafish, morpholino knockout of collagen XVIII resulted in a motor axon stall phenotype shortly after spinal cord exit (Schneider and Granato, 2006). Defects of neuronal migration have also been hypothesized as relevant in the etiology of Knobloch syndrome, a condition that affects human patients with a defective collagen XVIII gene and is associated with myopia, macular degeneration and retinal detachment, among other symptoms (Kliemann et al., 2003).

Biochemical work on vertebrate collagen XVIII has identified several proteases that are capable of releasing monomeric ES, including elastase, cathepsin L, matrilysin, MMP-9 and other MMPs (Felbor et al., 2000; Ferreras et al., 2000; Heljasvaara et al., 2005; Wen et al., 1999). Proteolytic ES release has been shown to be necessary to activate biological function *in vitro* (Heljasvaara et al., 2005).

Knowledge of downstream action mechanism of multiplexins or their cleavage products is limited. The antiangiogenic properties of endostatin seem to depend on its binding to heparan sulfates (Gaetzner et al., 2005; Sasaki et al., 1999). The HSPG glypican was identified as a low-affinity binding partner of ES, with the heparan sulfate side chains being critical for the interaction (Karumanchi et al., 2001). Endostatin also seems to interact with integrins, above all $\alpha 5\beta 1$ integrin (Rehn et al., 2001; Sudhakar et al., 2003; Wickstrom et al., 2004).

2. Aim of the thesis

Already a decade ago, a considerable number of extracellular proteins that act as guidance cues in the process of motor axon pathfinding had been identified, but the vast majority of these factors were transmembrane receptors and their diffusible or membrane-bound ligands (Araujo and Tear, 2003; Dickson, 2002). It was conceivable, however, that not all axon pathfinding factors had been identified yet, especially since a coherent picture of how complex guidance decisions are made was not available. For example, there was and still is no exact answer to the question how the axonal processes of *Drosophila* larval motor neurons differentially pathfind to their respective target muscles, with many of the neuron-muscle relationships being exclusive.

Axonal pathfinding takes place in a complex environment, as the extracellular matrix that growth cones have to navigate their way through is formed by a fair number of different components. While such components did not fail to be recognized as factors influencing pathfinding, the relatively small amount of detailed genetic and molecular data available seemed not to do justice to their significance.

With the discovery of the *tlr1* mutant motor axon pathfinding phenotype prior to this thesis work an interesting novel player had been identified that called for phenotypic and functional characterization. Members of the BMP1/TLD-like protease family have frequent roles in ECM formation, and specifically as procollagen-C-proteinases (pCPs) (Hopkins et al., 2007). An extracellular protease is a compelling candidate for modulating extracellular guidance signals or converting extracellular matrix components into signals. It can potentially attenuate a message by activating a cue through cleavage of a precursor form, or inactivate a signal through cleavage, or alternatively convert a signal to a different one. Spatial and/or temporal restriction of proteolytic action has the potential to encode new information about position and developmental time point.

Heparan sulfate proteoglycans (HSPGs) are ECM components that bear a vast potential for fine-tuning of guidance cues, since the number of different sugar side chain modifications that can be added to a HSPG core protein is large (Bulow and Hobert, 2004). The role of the membrane-bound HSPGs syndecans and glypicans in axon pathfinding has been demonstrated in several model systems (Rhiner and Hengartner,

2006). Limited indications for a function of the HSPG core protein collagen XVIII and its homologues in neuronal migration processes existed (Ackley et al., 2001; Kliemann et al., 2003; Schneider and Granato, 2006), but the function of the *Drosophila* gene was entirely uncharacterized. Moreover, a plethora of potential roles of different multiplexin fragments in migratory behaviour of different endothelial cell types was known from studies in vertebrate *in vitro* models (Clamp et al., 2006; Kuo et al., 2001; Sasaki et al., 2000).

In addition to Tlr1 and Dmp being interesting candidates on their own for novel roles in axon guidance mechanisms, also a direct connection between the two could be hypothesized. Dmp was a candidate for being a direct substrate of Tlr1, as members of the BMP1/TLD-like protease family act on several ECM components, including collagens. Vertebrate BMP1 is responsible for the C-terminal processing of fibrillar collagens I, II, and III (Kessler et al., 1996; Li et al., 1996), which are major components of the vertebrate ECM, as well as of lower abundance collagens (Rattenholl et al., 2002; Unsold et al., 2002), and all vertebrate BMP1-like proteases have pCP activity (Pappano et al., 2003; Scott et al., 1999). Since multiplexins are collagens with C-terminally located signalling domains that function while proteolytically released from the triple helical trunk, a specific enzyme-substrate relationship between Tlr1 and Dmp seemed possible.

The work of this Thesis therefore aimed at characterizing the effect of Tolloid-related-1 and the previously unnamed gene CG33171, encoding the only multiplexin in *Drosophila*, on axonal pathfinding in the *Drosophila* motor neuronal model system.

3. Results

3.1 Summary of Publication 1: Frauke Meyer and Hermann Aberle (2006). At the next stop sign turn right: the metalloprotease Tolloid-related 1 controls defasciculation of motor axons in *Drosophila*. Development 133, 4035-4044.

In a large-scale mutagenesis screen that was carried out on L3 larvae (Aberle et al., 2002; Parnas et al., 2001) using the transgenic CD8-GFP-Sh marker for postsynaptic domain of neuromuscular junctions (NMJs) (Zito et al., 1999) four alleles of a new mutant were found that showed missing and mislocalized NMJs. The mutant was initially named *piranha* (*pir*), and the affected gene identified as *tolloid-related 1* (*tlr1*) by meiotic recombination mapping and candidate gene sequencing. Tlr1 and its sequence homolog Tolloid (Tld) are extracellular metalloproteases of the BMP1 family and are composed of a central protease domain that makes use of a coordinated Zn^{2+} ion for catalytic activity, a C-terminal protein interaction domain of several EGF- and CUB-repeats, and an N-terminal prodomain that is usually removed before secretion of the protein (Hopkins et al., 2007). Of the four *tlr1* alleles found in the screen, three were identified to contain premature stop codons at the end of the prodomain. The fourth was a serine to threonine exchange mutation within the Zn^{2+} coordination motif of the protease domain. *tlr1* was shown to be transcribed throughout embryogenesis, beginning in the dorsal blastoderm at stage 5. Further notable expression domains are the mesoderm at stage 13 and ring gland and individual cells of the ventral nerve cord at stage 16.

Based on these CD8-GFP-Sh signals, the misinnervation frequency in L3 larvae of a transheterozygous combination of the premature stop alleles $tlr1^{D427}$ and $tlr1^{K788}$ was determined to be 38.1% and 25% for the two dorsalmost muscles 1 and 9, which are innervated by the intersegmental nerve (ISN), and between 23.9% and 64.3% for ventral muscles 12, 13, 6 and 7, which are innervated by the intersegmental nerve b (ISNb). Misinnervation observed in wildtype was 0% for muscles 1 and 9, and between 0% and 6.8% for muscles 12, 13, 6 and 7. The pattern and degree of misinnervation varied between hemisegments, both across each larva and between different individuals. Antibody stainings for the endogenous postsynaptic marker Discs large (Dlg) strictly

colocalized at NMJs with CD8-GFP-Sh signals, both in wild type and in *tlr1* mutants, indicating that the transgenic marker faithfully reflects NMJ distribution.

Motor nerves of L3 larvae were visualized using anti Fasciclin II (FasII) immunostaining or by selectively expressing a dsRed2 reporter construct in motor nerves using the Gal4/UAS system. Motor nerves due to innervate the ventral region of the hemisegment (ISNb, SNc and ISNd) frequently remained fasciculated with the nerves leading dorsally, the ISN and SNa, instead of branching off into the ventral muscle fields, thus creating a ventral bypass phenotype. In a number of cases, the ISNb and/or other nerves bypassed their designated ventral choice point, but underwent a belated defasciculation from the ISN that occured more dorsally than in wild type. This lead to imperfect innervation of the target muscles from a dorsal direction and at ectopic locations, termed reachback phenotype.

Anti-FasII immunostaining of stage 16-17 embryos revealed that *tlr1* mutants exhibit pathfinding defects that are similar in quality to those observed in L3 larvae. The rate of observed full ISNb bypass events, where no nervous structure can be seen leaving the main nerve tract towards muscles 12, 13, 6, and 7, amounts to 82% and the mutant phenotype thus exhibits a higher penetrance than in L3 larvae based on assessment using the transgenic postsynaptic marker CD8-GFP-Sh. While there are different possibilities to account for these differences, it nevertheless becomes clear that Tlr1 is required during the initial embryonic pathfinding process, and not just for maintenance of synaptic connections during larval development.

The *tlr1* mutant phenotype could be rescued by Tlr1 overexpression from a number of different Gal4 driver lines, expressing Tlr1 in somatic muscles, postmitotic neurons, fat body, hemocytes or ubiquitously after heat shock, indicating that Tlr1 acts in a cell non-autonomous way. In contrast, neither the closely related paralogue Tolloid (Tld) nor the midline guidance protease Kuzbanian were able to substitute for Tlr1 function.

A double mutant of *side*, encoding the muscle surface guidance molecule Sidestep, and *tlr1* showed a more penetrant phenotype than either of the single mutants, suggesting that Side and Tlr1 do not act in the same linear pathway.

In summary, Tlr1 is an extracellular protease important for embryonic motor axon pathfinding, and especially for the defasciculation of ventral motor nerves to occur at the

right place in space and time. The mechanism of action is cell non-autonomous, and Sidestep is not a direct substrate of Tlr1.

3.2 Summary of Publication 2: Frauke Meyer and Bernard Moussian (2009). *Drosophila* multiplexin (Dmp) modulates motor axon pathfinding accuracy. Development, Growth and Differentiation 51, 483-498.

Multiplexins are heparan- or chondroiotin sulfate proteoglycan collagens containing a C-terminal endostatin domain that is involved in the regulation of migratory processes of many epithelial and endothelial cell types. Effects on nervous system development have also been described (Ackley et al., 2001; Kliemann et al., 2003; Schneider and Granato, 2006).

CG33171 encodes the only multiplexin in the *Drosophila* genome. CG8647, another predicted gene upstream of CG33171, and encoding a domain similar to the N-terminal domain of thrombospondin (TSPN), was shown to be part of the multiplexin open reading frame. A plethora of alternative transcripts are produced from the locus, and three main sequence variants differ in the domain composition of the encoded protein. The long isoform N-terminally contains the TSPN domain, which is absent in the middle isoform. The short isoform is a single endostatin domain, which lacks the trimerization motif present in all other isoforms. Sequence analysis of the gene shows that it shares characteristic homologies with both vertebrate multiplexins, collagen XV and XVIII. Therefore it was named *Drosophila* multiplexin (*dmp*).

Expression of *dmp* starts only late in embryogenesis, about the time point when growth cones of the ISNb steer away from the ISN nerve tract. Expression domains are the dorsal vessel and individual cells of the ventral nerve cord that are arranged in a symmetrical pattern. All of the three different isoforms exhibit the same expression pattern.

Two deletion alleles of *dmp* were generated, one of which, $dmp^{\Delta C12\text{-}25}$ was a null with respect to the protein's C-terminal endostatin and trimerization region. In anti-FasII immunostainings on stage 16-17 embryos, both alleles showed the same phenotype. $dmp^{\Delta C12\text{-}25}$ exhibited the stronger penetrance, with 21.4% of ISNb nerves performing a ventral bypass and sometimes intruding into a neighbouring segment. This compares to a

figure of 7.2% errors in wild type. Similarly, the ISN error rate increased from 1.7% in wild type to 5.8% in *dmp*$^{\Delta C12\text{-}25}$, with the ISN bifurcating and/or fusing with a neighbouring ISN. The ISNb phenotype could be rescued by overexpressing constructs encoding the Dmp middle isoform or the shortest isoform, the endostatin domain only. In contrast, the trimeric ES version encoded by an NC1 construct could not improve the ISNb phenotype in *dmp*$^{\Delta C12\text{-}25}$, but had a dominant beneficial effect on ISNb pathfinding accuracy in wild type background. Here, overexpression of NC1 reduced the wild type ISNb error level of 7.2% to 0.75%. We conclude that ES is the active agent in axon guidance, and is releasable from the full-length Dmp molecule but not from the NC1 domain. An excess of the NC1 domain, in turn, seems to be able to increase the stringency of guidance interactions in a wild type background. We suggest that a higher endogenous NC1 dosage is not used in wild type although beneficial in individual cases, because an ES excess might impair the plasticity of the system that is needed for maintaining a functional error correction mechanism.

In summary, this work characterized the *dmp* genomic locus and its transcripts, and uncovered different roles for different fragments of Dmp in motor axon pathfinding.

4. Discussion

The work for this Thesis aimed at characterizing the role of the extracelluar protease Tolloid-related 1 (Tlr1) and its putative substrate *Drosophila* multiplexin (Dmp) in motor axon pathfinding. Both of these proteins act within the extracellular matrix, which is a compartment of indisputable relevance for axon pathfinding, but so far has received a level of attention clearly inferior to that of cellular factors. Through this work, two new players have been added to the list: Tlr1 was the first protease of the Astacin family to be shown to be involved in axon guidance. It has a strong, but not exclusive, effect on *Drosophila* motor axon defasciculation at the ventral choice point. Dmp is the only multiplexin in *Drosophila*, and one of its few collagens. The previously uncharacterized gene was shown to moderately influence motor axon pathfinding, including the ventral choice point steering decision.

4.1. Tlr1 acts cell non-autonomously on axon pathfinding

In this work, *tlr1* expression was identified in a wide range of tissues, including mesoderm, stage 13 somatic muscles, ring gland, and stage 15 CNS. The work documented here shows that Tlr1 works in a cell non-autonomous way, as the range of tissues where Tlr1 overexpression could rescue the axon pathfinding phenotype is broad (muscles, postmitotic neurons, fat body, hemocytes, ubiquitous expression after heat shock) and not identical with endogenous *tlr1* expression. The identity of the actual source tissue of Tlr1 thus has proven irrelevant for its function in axon pathfinding.

4.2. Tlr1 is a modulatory cue

Adhesive and tropic cues that steer a growth cone, as defined by Raper and Mason (2010), act at the site of interaction between a growth cone and its substratum. Trophic cues may act on a neuronal soma to promote cell survival, or at the growth cone, to promote growth cone motility. Modulatory cues, as described by Raper and Mason, interfere with the interaction of a tropic cue and its receptor, thus altering growth cone behaviour compared to the uninfluenced situation.

The fact that the identity of Tlr1 source tissue is irrelevant for its function in axon pathfinding suggests that the function of Tlr1 does not depend on a specific spatial distribution pattern. Rather, it seems to be an extracellular, diffusible compound that has to be produced by some source tissue and then reaches its specific site of action by diffusion. This means that Tlr1 is not a tropic guidance cue, as for such a cue its expression domains are critical for axon steering. (See Table 1 for an overview of likely action mechanisms of Tlr1 and Dmp). Tlr1 is also not likely to be an adhesive cue, first because a protease would be a very atypical adhesion molecule, and second because adhesive or anti-adhesive surface properties that steer a growth cone need some specific spatial distribution, just as tropic cues do. Guidance through a trophic mechanism has a potential to act independently of a specific distribution pattern by improving neuron viability or growth cone motility in general, and thus support their reaction to a steering cue. However, a protease would be an atypical trophic factor, and neuron survival is not impaired in *tlr1* mutants. The *tlr1* loss-of-function phenotypes also do not give any indication of decreased growth cone motility, since growth cones often travel far, just not along the right path. Taken together, it is very unlikely that Tlr1 itself is a trophic cue, and moreover, it seems unlikely that the mechanism downstream of Tlr1 that eventually leads to growth cone steering works through a trophic mechanism.

Tlr1 rather has clear potential to fit into the category of modulatory guidance cues defined by Raper and Mason. By their definition, modulatory cues do not act as tropic cues themselves, but interfere with the molecular interaction cascade between the growth cone and a tropic cue. An extension to this category should probably be made by adding cues that modulate the properties of adhesive cues or their interpretation by the growth cone. When examined in detail, a large range of indirect action mechanisms can probably be distinguished and added to the modulatory cue category. It is easy to imagine that Tlr1 can modulate tropic or adhesive cues through its proteolytic function. It can activate or inactivate an attractant or a repellent, release a diffusible signalling domain from an immobile ECM or membrane-anchored molecule, or increase or decrease the adhesive properties of a molecule. Moreover, the molecule generated trough cleavage by Tlr1 could also be another modulatory cue, Tlr1 then being part of a modulatory cascade.

		Tlr1	Tlr1 downstream cue	Dmp	Dmp downstream cue
Adhesive cues	ECM components or CAMs, eg. laminin, fibronectin, fasciclins, cadherins	-		+ (fl)	
	o provide a permissive substratum, that gets preferred by growth cones	-	+	-	+
	o increase adherence of growth cones to substratum	-	+	-	+
	o influence the effect of other adhesive cues	n.a.	+	-	+
	o can be crucial accessory receptors in signalling (applies to CAMs, eg. L1 in Sema signalling)	n.a.	+	n.a.	+
Trophic signals	eg. Neurotrophins, HGF	-		+ (ES)	
	o stimulate growth cone motility and axon outgrowth	-	-	+	+
	o promote neuronal survival	-	-	-	-
	o stabilize neuron-target-interactions once they are established	-	-	+	+
Tropic cues	Secreted molecules or CAMs, eg. Sema, Ephrins, DSCAM	+		+ (ES)	
	o act as attractants or repellents, thus impart a directional value to growth cone motility	-	+	-	+
Modula-tory cues	eg. Laminin, fibronectin, neurotrophins	+		+	
	o affect how growth cones respond to tropic cues	+	+	+	+

Table 1: Likely action mechanisms of Tlr1 and Dmp
Left section, grey rows: cue category and examples according to Raper and Mason (2010)
Right section, grey rows: potential of Tlr1 and Dmp to belong to this category based on their sequence
Left section, white rows: action mechanism of the different cues according to Raper and Mason;
Right section, white rows: probability of Tlr1, Dmp or their putative downstream effectors to act through this mechanism, taking into account sequence information as well as experimental results from Meyer and Aberle (2006) and Meyer and Moussian (2009); especially, loss-of-function-phenotypes and rescue data.
- Disproved or unlikely
+ Possible or likely
ES: separate endostatin domain

4.3. Tlr1 and Mmp1 and 2 have distinct functions in motor axon pathfinding, but share the property of non cell-autonomy

In 2008, Matrix metalloproteases 1 and 2 were described as promoters of motor axon fasciculation in *Drosophila*, as a loss of function decreases motor axon fasciculation, but causes only relatively mild misrouting phenotypes (Miller et al., 2008). This is a

phenotype opposite to that caused by loss of Tlr1 function, as the ventral bypass phenotype seen here argues for an increased fasciculation; so these proteases have clearly distinct functions in motor axon pathfinding. But like Tlr1, Mmp1 and Mmp2 act cell non-autonomously. The diffusible Mmp1 is expressed in proventriculus and hindgut, and in different cells of the embryonic nervous system, but not in motor neurons. Mmp2 is membrane-bound, and the gene is exclusively expressed by some glial cells and some interneurons of the embryonic CNS, but not in motor neurons (Miller et al., 2008).

The example of the immobile Mmp2 shows that it is possible to modulate the behaviour of motor growth cones by producing cues in the vicinity of motor neuron cell bodies in the CNS. For *tlr1*, there is an onset of expression in individual cells in the CNS that are not motor neurons during embryonic stage 15, shortly before the event of growth cones altering growth direction at the ventral choice point and turning into the ventral muscle field (F. M., unpublished results). It thus seems possible that growth cone turning is a reaction to *tlr1* expression. However, because the spectrum of tissues from which the transgenic rescue of *tlr1* mutant phenotype could be driven was broad, none of the earlier *in vivo* expression of *tlr1* by other tissues, like somatic muscles or ring gland, can be excluded for *in vivo* relevance.

4.4. A range of proteins have been hypothesized as Tlr1 substrates

4.4.1. Cell adhesion molecules Beaten path, Sidestep and LAR

Drosophila embryos mutant for a Tlr1 substrate that is relevant to pathfinding may display a phenotype similar to that of *tlr1* mutants. Striking similarities exist between *tlr1*, *side*, *beatIa* and *lar* loss-of-function phenotypes (Fambrough and Goodman, 1996; Krueger et al., 1996; Sink et al., 2001). Between BeatIa and Side, both members of the immunoglobulin superfamily, an adhesive interaction has been demonstrated, where the secreted ligand BeatIa acts cell-autonomously on motor neuron surfaces, and Side non-autonomously, as it is a transmembrane molecule expressed on the muscle surfaces on which motor neurons migrate (Siebert et al., 2009). The phenotypic similarity between *side*, *beatIa* and *tlr1* lead to the theory that they act together. However, as documented in this work (Meyer and Aberle, 2006), phenotype penetrance of *tlr1,side* double null

mutants increased compared to the two single null mutants, indicating that the two gene products do not collaborate in the same pathway. Similarly, a double mutant of *tlr1* and *beatIa* displayed increased phenotype penetrance (H.A., unpublished observation). By contrast, in the double mutant of *side* and *beatIa* the phenotype penetrance does not exceed that of the single mutants, which was taken by the authors as an indication that the two gene products interact, and was subsequently demonstrated correct by S2 cell aggregation assays and side misexpression experiments (Siebert et al., 2009). So a model emerges where Side and BeatIa interact in a common pathway, whereas LAR remains as putative interactor for Tlr1. This also means that at least two parallel pathways exist that act on the same biological process, the same guidance decisions.

4.4.2. TGF-β/activin-like extracellular ligand Dawdle

Serpe and O'Connor (2006) believe to have identified a substrate for Tlr1 of functional relevance in motor axon pathfinding. They and others suggest that the activin-like extracellular ligand Dawdle (Daw) regulates pathfinding by signalling to motor neurons through the TGF-β/activin pathway via the receptor Baboon and the Smads dSmad2 and Medea (Parker et al., 2006). Serpe and O'Connor (2006) found Tlr1 to act proteolytically on Daw in conditioned S2 cell culture medium, and to activate Daw signalling through dSmad2 in an S2-cell-based assay. However, in both assays, Tlr1 and Tld were tested in parallel, and in both cases Tld had an effect similar to, but stronger than that of Tlr1. As documented in this work, *tld* mutant L3 larvae do not exhibit an axon pathfinding phenotype, and Tld overexpression could not rescue the *tlr1* mutant phenotype (Meyer and Aberle, 2006). It is surprising that proteolysis of a substrate that is not specific to Tlr1 should yield a phenotype that is Tlr1-specific. While it is possible to find explanations for this, the simplest explanation is that Daw is not a Tlr1 substrate of *in vivo* relevance for axon pathfinding. Serpe and O'Connor documented axon pathfinding phenotypes for mutants of *daw* and its suspected downstream interactors that are weaker in penetrance than defects found in *tlr1* mutants. To the unbiased observer it is also clear that they are dissimilar in quality. Neither of the mutants ever displays a ventral ISNb bypass phenotype, which is a hallmark of *tlr1* mutants, and the motor neuron defects

documented for *daw* mutants are extremely subtle. It seems possible that loss of Daw slightly delays the growth cone, and thus leads to the phenotype, as also noted by Serpe and O'Connor, and reflected by their choice for naming the gene. No data is shown that would either positively indicate or at least strongly suggest an *in vivo* interaction between Tlr1 and Daw. Hence, while not entirely ruling out the possibility for such an interaction, the publication does not show that it actually occurs. In any case, as also indicated by the authors, Daw will not be the only substrate of Tlr1 that is relevant for Tlr1's function in axon guidance. This conclusion directly follows from the fact that *daw* mutants have a much weaker phenotype than *tlr1* mutants, and the *daw* mutant phenotype does not persist into larval stages.

4.5. Dmp is a novel factor in motor axon pathfinding

Initial interest in *Drosophila* multiplexin stemmed from the fact that many heparan sulfate and chondroitin sulfate proteoglycans have been implicated in nervous system development, including axonal pathfinding (Bandtlow and Zimmermann, 2000; Carulli et al., 2005) and some publications indicating a role for multiplexins in neuronal migration processes in other organisms (Ackley et al., 2001; Kliemann et al., 2003; Schneider and Granato, 2006), as well as from the option of Dmp being a target substrate of Tlr1.

The results illustrate a relevance of Dmp for motor axon pathfinding, as the loss-of-function phenotype clearly exhibits motor axon pathfinding defects, including ISNb ventral bypass events and ISN misrouting. Interestingly, the results imply differential functions for the C-terminal ES domain as a function of its association with the main molecule and its trimerization. This finding is analogous with results from both *C. elegans* (Ackley et al., 2001; Kuo et al., 2001) and different vertebrate model systems (Clamp et al., 2006; Kuo et al., 2001; Sasaki et al., 2000), where different forms of endostatin can have very different effects, also varying with model systems and exact biological context. This is not very surprising considering the broad range of molecular interactors found for endostatin in vertebrates (Faye et al., 2009), and possibly finds a reflection in the wealth of different effects found in our rescue and overexpression experiments.

4.6. Dmp's action is cell non-autonomous,

In this work, using *in situ hybridization*, Dmp expression was found in a punctate pattern within the ventral nerve cord (VNC). In a recent publication (Momota et al., 2011), a Dmp-specific antibody was used, and these cells were determined not to be neurons. Interestingly, Momota et al. detected Dmp protein already at stage 14, and in additional tissues compared to this work, including midgut primordia and visceral musculature. In this work, the *dmp* mutant phenotype could be rescued by transgenic expression of full-length Dmp and monomeric ES through the driver line 24B-Gal4, that shows overlap with *dmp* with regard to tissues of expression, but also produces expression that has to be classified as ectopic with regard to *dmp*, as *dmp* does not show pan-mesodermal expression. However, in spite of this ectopic expression, the mutant phenotype was not aggravated, but rescued when using 24B-Gal4. This implies that Dmp acts cell non-autonomously, and that no spatial information is directly encoded in endogenous *dmp* expression.

4.7. Dmp is a trophic or modulatory cue

Non-cell-autonomy is a property Dmp shares with Tlr1, and the same arguments apply, from which can be concluded that Dmp or monomeric endostatin are not tropic or adhesive cues. Endostatin, as a signalling molecule, has a potential to act as a trophic signal, and support correct pathfinding by supporting e.g. growth cone motility. This notion is strongly supported by the fact that mono- and oligomeric ES showed strong motogenic and anti-motogenic activity, which is motility-dependent, in vertebrate tissue culture model systems, with often opposite effects caused by mono- and oligomeric ES (Clamp et al., 2006; Kuo et al., 2001; Sasaki et al., 2000). Moreover, vertebrate ES was recently found to be able to bind NGF and thus inhibit neurite outgrowth *in vitro* (Al Ahmad et al., 2010).

It further remains possible that Dmp or its released domains play a modulatory role in axon pathfinding, i.e. that they influence the action of tropic, adhesive or trophic cues, for example through binding interactions with a cue or a receptor that lead to its

activation or inactivation. This includes an option where Dmp or ES act in a network that modulates trophic signals to the growth cone, hence works as a modulatory cue on a trophic guidance mechanism. (See Table 1 for an overview of possible action mechanisms.)

4.8. The term Modulation has been applied to different concepts

The modulation of axon pathfinding accuracy described for Dmp refers to a different interpretation of the term modulation than the modulation of pathfinding by modulatory cues defined by Raper and Mason (2010). For Raper and Mason, modulatory cues by definition do not act directly on a growth cone. They can exert a function only when certain other cues by turning on or abolishing the effects of that cue, and this action was termed modulation.

The statement made in Meyer and Moussian (2009) about the modulatory activity Dmp, however, does not intend to say that the effect of Dmp depends on the presence of other specific molecules. It rather refers to the varying effects seen for different versions of the protein (full-length Dmp, mono- and trimeric ES) in different genetic backgrounds, and to the fact that phenotypic penetrance of these effects is not very high. This implies that Dmp has the capacity to influence guidance by different means, possibly through a pro-motile effect of monomeric ES, and an anti-motile effect of trimeric ES, but it does not suggest that Dmp has an all-or-nothing impact on the action of any specific cue. It may attenuate the effect of several cues present, and thus subtly affect the balance of all different guidance cues acting at once on a given growth cone.

In the current literature, functional differences in strength of effect between guidance cues are currently not taken into account. It may be useful to do so in order to elucidate the action network of all guidance cues.

4.9. RPTPs are putative receptors for Dmp signals

Different receptor protein tyrosine phosphatases (RPTPs) are encoded by a family of six genes in *Drosophila* (Desai et al., 1996; Desai et al., 1997; Jeon et al., 2008; Schindelholz et al., 2001; Sun et al., 2001). One of them, LAR, is well known for its strong ventral bypass mutant phenotype (Desai et al., 1996; Krueger et al., 1996). Those other than

LAR show weaker or no mutant phenotypes as single mutants. Double and triple mutants show phenotypic variations when analysed in detail and compared to each other (Jeon et al., 2008; Schindelholz et al., 2001; Sun et al., 2001) including a suggested counteraction of LAR through RPTP99A (Desai et al., 1997). Hence, like Dmp, RPTPs play roles of modulation to pathfinding and seem to be diverse in their effects. Collagen XVIII has been shown to act *in vitro* as a ligand for the avian RPTP cPTPσ (Aricescu et al., 2002). Taken together, these findings hint at a possible cooperation between multiplexins and RPTPs in axon pathfinding, and further investigation of this line of thought may prove interesting.

4.10. Dmp is a possible target of Tlr1

For vertebrate Collagen XVIII, a number of proteases from different classes, including matrix metalloproteases, have been identified that are capable of releasing monomeric ES *in vitro* (Felbor et al., 2000; Ferreras et al., 2000; Lin et al., 2001; Wen et al., 1999), and proteolytic ES release has been shown to activate biological function (Heljasvaara et al., 2005). Tlr1, as a BMP-1-like protein, is a member of the astacin family of metalloproteases, but no member of this family has been tested for its action on multiplexins.

The results presented here leave the option that proteolytic release plays a role in the action of Dmp, as transgenic monomeric ES as well as full length Dmp had similar rescue activities on the *dmp* mutant phenotype. Transgenic NC1, that probably forms trimeric ES domains, had no rescue activity in mutant background, suggesting that proteolytic release of monomeric ES is not possible from trimeric ES. The reason for this may be that the collagenous region of Dmp is necessary for enzyme-substrate recognition. Tlr1 has a multi-domain protein-protein interaction region located C-terminally of the protease domain that may be responsible for interaction with its substrate (Hopkins et al., 2007).

The *dmp* VNC expression pattern looks suspiciously similar to that of *tlr1*, leaving room for the speculation that the products of the two genes interact locally within the VNC and act on their target motor neurons there. At this point it should be mentioned that a number of genes exhibit a similar VNC expression pattern, including the Tlr1

substrate Dawdle postulated by Serpe and O'Connor (2006), illustrating the low significance this similarity has as evidence for an interaction.

A comparison of *tlr1* and *dmp* loss-of-function mutants shows that the penetrance of defects is different in both mutants, but that phenotypes observed are of a similar quality. For both genes, the effect most frequently observed in mutants is a lack of defasciculation of ISNb axons from the main nerve tract at the ventral choice point. The penetrance of ISNb ventral bypass, however, as well as the lack of dorsal innervation through the ISN observed in both mutants, is lower in *dmp* than in *tlr1*. The similarity in phenotype quality leaves room for the option that Tlr1 and Dmp are direct interactors, with Tlr1 presumably releasing fragments from Dmp that function as guidance cues.

Unpublished rescue experiments resulted in a beneficial influence of Dmp fragments on the *tlr1* mutant phenotype. The same Dmp-UAS-lines and the same Gal4 driver were used as in $dmp^{\Delta C12\text{-}25}$ rescue experiments. The ISNb error rate of 96% in *tlr1* mutant embryos (Meyer and Aberle, 2006) was reduced to 65% and 67% respectively by UAS-3hNC1 and UAS-ES, and the difference to *tlr1* mutant phenotype yielded clear statistical significance. With UAS-NC1, the error rate was only reduced to 84%, and statistical significance was low. Interestingly, this pattern of transgene effect on pathfinding exactly recapitulates that found for rescue of the *dmp* mutant ISNb phenotype.

Taken together, these findings show that Tlr1 and Dmp collaboratively act on axonal pathfinding of motor neurons. This collaboration may be direct or indirect; this remains to be determined. From the difference in phenotype penetrance it is clear, however, that Tlr1 must have more targets than Dmp alone.

5. References

Aberle, H., Haghighi, A. P., Fetter, R. D., McCabe, B. D., Magalhaes, T. R. and Goodman, C. S. (2002). wishful thinking encodes a BMP type II receptor that regulates synaptic growth in Drosophila. *Neuron* **33**, 545-58.

Ackley, B. D., Crew, J. R., Elamaa, H., Pihlajaniemi, T., Kuo, C. J. and Kramer, J. M. (2001). The NC1/Endostatin Domain of Caenorhabditis elegans Type XVIII Collagen Affects Cell Migration and Axon Guidance. *J. Cell Biol.* **152**, 1219-1232.

Al Ahmad, A., Lee, B., Stack, J., Parham, C., Campbell, J., Clarke, D., Fertala, A. and Bix, G. J. (2010). Endostatin binds nerve growth factor and thereby inhibits neurite outgrowth and neuronal migration in-vitro. *Brain Res* **1360**, 28-39.

Amano, S., Scott, I. C., Takahara, K., Koch, M., Champliaud, M. F., Gerecke, D. R., Keene, D. R., Hudson, D. L., Nishiyama, T., Lee, S. et al. (2000). Bone morphogenetic protein 1 is an extracellular processing enzyme of the laminin 5 gamma 2 chain. *J Biol Chem* **275**, 22728-35.

Araujo, S. J. and Tear, G. (2003). Axon guidance mechanisms and molecules: lessons from invertebrates. *Nat Rev Neurosci* **4**, 910-922.

Aricescu, A. R., McKinnell, I. W., Halfter, W. and Stoker, A. W. (2002). Heparan Sulfate Proteoglycans Are Ligands for Receptor Protein Tyrosine Phosphatase {sigma}. *Mol. Cell. Biol.* **22**, 1881-1892.

Bandtlow, C. E. and Zimmermann, D. R. (2000). Proteoglycans in the developing brain: new conceptual insights for old proteins. *Physiol Rev* **80**, 1267-90.

Blader, P., Rastegar, S., Fischer, N. and Strahle, U. (1997). Cleavage of the BMP-4 antagonist chordin by zebrafish tolloid. *Science* **278**, 1937-40.

Boehm, T., O'Reilly M, S., Keough, K., Shiloach, J., Shapiro, R. and Folkman, J. (1998). Zinc-binding of endostatin is essential for its antiangiogenic activity. *Biochem Biophys Res Commun* **252**, 190-4.

Bosman, F. T. and Stamenkovic, I. (2003). Functional structure and composition of the extracellular matrix. *J Pathol* **200**, 423-8.

Bozyczko, D. and Horwitz, A. F. (1986). The participation of a putative cell surface receptor for laminin and fibronectin in peripheral neurite extension. *J Neurosci* **6**, 1241-51.

Bulow, H. E. and Hobert, O. (2004). Differential Sulfations and Epimerization Define Heparan Sulfate Specificity in Nervous System Development. *Neuron* **41**, 723-736.

Canty, E. G., Garrigue-Antar, L. and Kadler, K. E. (2006). A complete domain structure of Drosophila tolloid is required for cleavage of short gastrulation. *J Biol Chem* **281**, 13258-67.

Carulli, D., Laabs, T., Geller, H. M. and Fawcett, J. W. (2005). Chondroitin sulfate proteoglycans in neural development and regeneration. *Curr Opin Neurobiol* **15**, 116-20.

Chilton, J. K. (2006). Molecular mechanisms of axon guidance. *Developmental Biology* **292**, 13-24.

Clamp, A., Blackhall, F. H., Henrioud, A., Jayson, G. C., Javaherian, K., Esko, J., Gallagher, J. T. and Merry, C. L. R. (2006). The Morphogenic Properties of Oligomeric Endostatin Are Dependent on Cell Surface Heparan Sulfate. *J. Biol. Chem.* **281**, 14813-14822.

Colamarino, S. A. and Tessier-Lavigne, M. (1995). The axonal chemoattractant netrin-1 is also a chemorepellent for trochlear motor axons. *Cell* **81**, 621-9.
Coleman, H. A., Labrador, J. P., Chance, R. K. and Bashaw, G. J. (2010). The Adam family metalloprotease Kuzbanian regulates the cleavage of the roundabout receptor to control axon repulsion at the midline. *Development* **137**, 2417-26.
Desai, C. and Purdy, J. (2003). The neural receptor protein tyrosine phosphatase DPTP69D is required during periods of axon outgrowth in Drosophila. *Genetics* **164**, 575-88.
Desai, C. J., Gindhart, J. G., Jr., Goldstein, L. S. and Zinn, K. (1996). Receptor tyrosine phosphatases are required for motor axon guidance in the Drosophila embryo. *Cell* **84**, 599-609.
Desai, C. J., Krueger, N. X., Saito, H. and Zinn, K. (1997). Competition and cooperation among receptor tyrosine phosphatases control motoneuron growth cone guidance in Drosophila. *Development* **124**, 1941-52.
Dickson, B. J. (2002). Molecular mechanisms of axon guidance. *Science* **298**, 1959-64.
Dickson, B. J. and Zou, Y. (2010). Navigating intermediate targets: the nervous system midline. *Cold Spring Harb Perspect Biol* **2**, a002055.
Dontchev, V. D. and Letourneau, P. C. (2002). Nerve growth factor and semaphorin 3A signaling pathways interact in regulating sensory neuronal growth cone motility. *J Neurosci* **22**, 6659-69.
du Lac, S., Bastiani, M. J. and Goodman, C. S. (1986). Guidance of neuronal growth cones in the grasshopper embryo. II. Recognition of a specific axonal pathway by the aCC neuron. *J Neurosci* **6**, 3532-41.
Esko, J. D. and Selleck, S. B. (2002). ORDER OUT OF CHAOS: Assembly of Ligand Binding Sites in Heparan Sulfate. *Annual Review of Biochemistry* **71**, 435-471.
Fambrough, D. and Goodman, C. S. (1996). The Drosophila beaten path gene encodes a novel secreted protein that regulates defasciculation at motor axon choice points. *Cell* **87**, 1049-58.
Fambrough, D., Pan, D., Rubin, G. Ä. and Goodman, C. Ä. (1996). The cell surface metalloprotease/disintegrin Kuzbanian is required for axonal extension in Drosophila. *Proceedings of the National Academy of Sciences* **93**, 13233-13238.
Faye, C. m., Chautard, E., Olsen, B. R. and Ricard-Blum, S. (2009). The First Draft of the Endostatin Interaction Network. *Journal of Biological Chemistry* **284**, 22041-22047.
Felbor, U., Dreier, L., Bryant, R. A., Ploegh, H. L., Olsen, B. R. and Mothes, W. (2000). Secreted cathepsin L generates endostatin from collagen XVIII. *Embo J* **19**, 1187-94.
Ferreras, M., Felbor, U., Lenhard, T., Olsen, B. R. and Delaisse, J. (2000). Generation and degradation of human endostatin proteins by various proteinases. *FEBS Lett* **486**, 247-51.
Finelli, A. L., Xie, T., Bossie, C. A., Blackman, R. K. and Padgett, R. W. (1995). The tolkin gene is a tolloid/BMP-1 homologue that is essential for Drosophila development. *Genetics* **141**, 271-81.
Fox, A. N. and Zinn, K. (2005). The Heparan Sulfate Proteoglycan Syndecan Is an In Vivo Ligand for the Drosophila LAR Receptor Tyrosine Phosphatase. *Current Biology* **15**, 1701-1711.

Gaetzner, S., Deckers, M. M. L., Stahl, S., Lowik, C., Olsen, B. R. and Felbor, U. (2005). Endostatin's heparan sulfate-binding site is essential for inhibition of angiogenesis and enhances in situ binding to capillary-like structures in bone explants. *Matrix Biology* **23**, 557-561.

Garcia-Alonso, L., Fetter, R. D. and Goodman, C. S. (1996). Genetic analysis of Laminin A in Drosophila: extracellular matrix containing laminin A is required for ocellar axon pathfinding. *Development* **122**, 2611-21.

Gonzalez, E. M., Reed, C. C., Bix, G., Fu, J., Zhang, Y., Gopalakrishnan, B., Greenspan, D. S. and Iozzo, R. V. (2005). BMP-1/Tolloid-like metalloproteases process endorepellin, the angiostatic C-terminal fragment of perlecan. *J Biol Chem* **280**, 7080-7.

Halfter, W., Dong, S., Schurer, B. and Cole, G. J. (1998). Collagen XVIII Is a Basement Membrane Heparan Sulfate Proteoglycan. *J. Biol. Chem.* **273**, 25404-25412.

Hartmann, U. and Maurer, P. (2001). Proteoglycans in the nervous system -- the quest for functional roles in vivo. *Matrix Biology* **20**, 23-35.

Hattori, M., Osterfield, M. and Flanagan, J. G. (2000). Regulated cleavage of a contact-mediated axon repellent. *Science* **289**, 1360-5.

Heljasvaara, R., Nyberg, P., Luostarinen, J., Parikka, M., Heikkila, P., Rehn, M., Sorsa, T., Salo, T. and Pihlajaniemi, T. (2005). Generation of biologically active endostatin fragments from human collagen XVIII by distinct matrix metalloproteases. *Experimental Cell Research* **307**, 292-304.

Hollyday, M. (1995). Chick wing innervation. I. Time course of innervation and early differentiation of the peripheral nerve pattern. *J Comp Neurol* **357**, 242-53.

Hong, K., Hinck, L., Nishiyama, M., Poo, M. M., Tessier-Lavigne, M. and Stein, E. (1999). A ligand-gated association between cytoplasmic domains of UNC5 and DCC family receptors converts netrin-induced growth cone attraction to repulsion. *Cell* **97**, 927-41.

Hopker, V. H., Shewan, D., Tessier-Lavigne, M., Poo, M. and Holt, C. (1999). Growth-cone attraction to netrin-1 is converted to repulsion by laminin-1. *Nature* **401**, 69-73.

Hopkins, D. R., Keles, S. and Greenspan, D. S. (2007). The bone morphogenetic protein 1/Tolloid-like metalloproteinases. *Matrix Biol* **26**, 508-23.

Iozzo, R. V., Zoeller, J. J. and Nystrom, A. (2009). Basement membrane proteoglycans: modulators Par Excellence of cancer growth and angiogenesis. *Mol Cells* **27**, 503-13.

Jeon, M., Nguyen, H., Bahri, S. and Zinn, K. (2008). Redundancy and compensation in axon guidance: genetic analysis of the Drosophila Ptp10D/Ptp4E receptor tyrosine phosphatase subfamily. *Neural Dev* **3**, 3.

Johnson, K. G., Ghose, A., Epstein, E., Lincecum, J., O'Connor, M. B. and Van Vactor, D. (2004). Axonal Heparan Sulfate Proteoglycans Regulate the Distribution and Efficiency of the Repellent Slit during Midline Axon Guidance. *Current Biology* **14**, 499-504.

Johnson, K. G., Tenney, A. P., Ghose, A., Duckworth, A. M., Higashi, M. E., Parfitt, K., Marcu, O., Heslip, T. R., Marsh, J. L., Schwarz, T. L. et al. (2006). The HSPGs Syndecan and Dallylike bind the receptor phosphatase LAR and exert distinct effects on synaptic development. *Neuron* **49**, 517-31.

Kadler, K. E., Baldock, C., Bella, J. and Boot-Handford, R. P. (2007). Collagens at a glance. *J Cell Sci* **120**, 1955-8.
Karumanchi, S. A., Jha, V., Ramchandran, R., Karihaloo, A., Tsiokas, L., Chan, B., Dhanabal, M., Hanai, J.-i., Venkataraman, G., Shriver, Z. et al. (2001). Cell Surface Glypicans Are Low-Affinity Endostatin Receptors. *Molecular Cell* **7**, 811-822.
Kessler, E., Takahara, K., Biniaminov, L., Brusel, M. and Greenspan, D. S. (1996). Bone morphogenetic protein-1: the type I procollagen C-proteinase. *Science* **271**, 360-2.
Kivirikko, S., Heinamaki, P., Rehn, M., Honkanen, N., Myers, J. C. and Pihlajaniemi, T. (1994). Primary structure of the alpha 1 chain of human type XV collagen and exon-intron organization in the 3' region of the corresponding gene. *J. Biol. Chem.* **269**, 4773-4779.
Kliemann, S. E., Waetge, R. T., Suzuki, O. T., Passos-Bueno, M. R. and Rosemberg, S. (2003). Evidence of neuronal migration disorders in Knobloch syndrome: clinical and molecular analysis of two novel families. *Am J Med Genet A* **119**, 15-9.
Krueger, N. X., Van Vactor, D., Wan, H. I., Gelbart, W. M., Goodman, C. S. and Saito, H. (1996). The transmembrane tyrosine phosphatase DLAR controls motor axon guidance in Drosophila. *Cell* **84**, 611-22.
Kuo, C. J., LaMontagne, K. R., Jr., Garcia-Cardena, G., Ackley, B. D., Kalman, D., Park, S., Christofferson, R., Kamihara, J., Ding, Y.-H., Lo, K.-M. et al. (2001). Oligomerization-dependent Regulation of Motility and Morphogenesis by the Collagen XVIII NC1/Endostatin Domain. *J. Cell Biol.* **152**, 1233-1246.
Landgraf, M., Bossing, T., Technau, G. M. and Bate, M. (1997). The origin, location, and projections of the embryonic abdominal motorneurons of Drosophila. *J Neurosci* **17**, 9642-55.
Letourneau, P. C. (1975). Cell-to-substratum adhesion and guidance of axonal elongation. *Dev Biol* **44**, 92-101.
Li, D., Clark, C. C. and Myers, J. C. (2000). Basement Membrane Zone Type XV Collagen Is a Disulfide-bonded Chondroitin Sulfate Proteoglycan in Human Tissues and Cultured Cells. *J. Biol. Chem.* **275**, 22339-22347.
Li, S. W., Sieron, A. L., Fertala, A., Hojima, Y., Arnold, W. V. and Prockop, D. J. (1996). The C-proteinase that processes procollagens to fibrillar collagens is identical to the protein previously identified as bone morphogenic protein-1. *Proc Natl Acad Sci U S A* **93**, 5127-30.
Lin, D. M., Auld, V. J. and Goodman, C. S. (1995). Targeted neuronal cell ablation in the Drosophila embryo: pathfinding by follower growth cones in the absence of pioneers. *Neuron* **14**, 707-15.
Lin, D. M. and Goodman, C. S. (1994). Ectopic and increased expression of Fasciclin II alters motoneuron growth cone guidance. *Neuron* **13**, 507-23.
Lin, H.-C., Chang, J.-H., Jain, S., Gabison, E. E., Kure, T., Kato, T., Fukai, N. and Azar, D. T. (2001). Matrilysin Cleavage of Corneal Collagen Type XVIII NC1 Domain and Generation of a 28-kDa Fragment. *Invest. Ophthalmol. Vis. Sci.* **42**, 2517-2524.
Marques, G., Musacchio, M., Shimell, M. J., Wunnenberg-Stapleton, K., Cho, K. W. and O'Connor, M. B. (1997). Production of a DPP activity gradient in the early Drosophila embryo through the opposing actions of the SOG and TLD proteins. *Cell* **91**, 417-26.

Matani, P., Sharrow, M. and Tiemeyer, M. (2007). Ligand, modulatory, and co-receptor functions of neural glycans. *Front Biosci* **12**, 3852-79.
McFarlane, S. (2003). Metalloproteases: Carving Out a Role in Axon Guidance. *Neuron* **37**, 559-562.
Meyer, F. and Aberle, H. (2006). At the next stop sign turn right: the metalloprotease Tolloid-related 1 controls defasciculation of motor axons in Drosophila. *Development* **133**, 4035-4044.
Meyer, F. and Moussian, B. (2009). Drosophila multiplexin (Dmp) modulates motor axon pathfinding accuracy. *Dev Growth Differ* **51**, 483-98.
Miller, C. M., Page-McCaw, A. and Broihier, H. T. (2008). Matrix metalloproteinases promote motor axon fasciculation in the Drosophila embryo. *Development* **135**, 95-109.
Mirre, C., Le Parco, Y. and Knibiehler, B. (1992). Collagen IV is present in the developing CNS during Drosophila neurogenesis. *J Neurosci Res* **31**, 146-55.
Momota, R., Naito, I., Ninomiya, Y. and Ohtsuka, A. (2011). Drosophila type XV/XVIII collagen, Mp, is involved in Wingless distribution. *Matrix Biol* **30**, 258-66.
Muragaki, Y., Abe, N., Ninomiya, Y., Olsen, B. R. and Ooshima, A. (1994). The human alpha 1(XV) collagen chain contains a large amino-terminal non-triple helical domain with a tandem repeat structure and homology to alpha 1(XVIII) collagen. *J. Biol. Chem.* **269**, 4042-4046.
Muragaki, Y., Timmons, S., Griffith, C. M., Oh, S. P., Fadel, B., Quertermous, T. and Olsen, B. R. (1995). Mouse Col18a1 is Expressed in a Tissue-Specific Manner as Three Alternative Variants and is Localized in Basement Membrane Zones. *PNAS* **92**, 8763-8767.
Nguyen, T., Jamal, J., Shimell, M. J., Arora, K. and O'Connor, M. B. (1994). Characterization of tolloid-related-1: a BMP-1-like product that is required during larval and pupal stages of Drosophila development. *Dev Biol* **166**, 569-86.
O'Reilly, M. S., Boehm, T., Shing, Y., Fukai, N., Vasios, G., Lane, W. S., Flynn, E., Birkhead, J. R., Olsen, B. R. and Folkman, J. (1997). Endostatin: An Endogenous Inhibitor of Angiogenesis and Tumor Growth. *Cell* **88**, 277-285.
Oh, S. P., Warman, M. L., Seldin, M. F., Cheng, S.-D., Knoll, J. H. M., Timmons, S. and Olsen, B. R. (1994). Cloning of cDNA and Genomic DNA Encoding Human Type XVIII Collagen and Localization of the [alpha]1(XVIII) Collagen Gene to Mouse Chromosome 10 and Human Chromosome 21. *Genomics* **19**, 494-499.
Pappano, W. N., Steiglitz, B. M., Scott, I. C., Keene, D. R. and Greenspan, D. S. (2003). Use of Bmp1/Tll1 doubly homozygous null mice and proteomics to identify and validate in vivo substrates of bone morphogenetic protein 1/tolloid-like metalloproteinases. *Mol Cell Biol* **23**, 4428-38.
Parker, L., Ellis, J. E., Nguyen, M. Q. and Arora, K. (2006). The divergent TGF-beta ligand Dawdle utilizes an activin pathway to influence axon guidance in Drosophila. *Development* **133**, 4981-91.
Parnas, D., Haghighi, A. P., Fetter, R. D., Kim, S. W. and Goodman, C. S. (2001). Regulation of postsynaptic structure and protein localization by the Rho-type guanine nucleotide exchange factor dPix. *Neuron* **32**, 415-24.
Piccolo, S., Agius, E., Lu, B., Goodman, S., Dale, L. and De Robertis, E. M. (1997). Cleavage of Chordin by Xolloid metalloprotease suggests a role for proteolytic processing in the regulation of Spemann organizer activity. *Cell* **91**, 407-16.

Pipes, G. C., Lin, Q., Riley, S. E. and Goodman, C. S. (2001). The Beat generation: a multigene family encoding IgSF proteins related to the Beat axon guidance molecule in Drosophila. *Development* **128**, 4545-52.
Raper, J. and Mason, C. (2010). Cellular strategies of axonal pathfinding. *Cold Spring Harb Perspect Biol* **2**, a001933.
Rattenholl, A., Pappano, W. N., Koch, M., Keene, D. R., Kadler, K. E., Sasaki, T., Timpl, R., Burgeson, R. E., Greenspan, D. S. and Bruckner-Tuderman, L. (2002). Proteinases of the bone morphogenetic protein-1 family convert procollagen VII to mature anchoring fibril collagen. *J Biol Chem* **277**, 26372-8.
Rawson, J. M., Dimitroff, B., Johnson, K. G., Rawson, J. M., Ge, X., Van Vactor, D. and Selleck, S. B. (2005). The Heparan Sulfate Proteoglycans Dally-like and Syndecan Have Distinct Functions in Axon Guidance and Visual-System Assembly in Drosophila. *Current Biology* **15**, 833-838.
Reddi, A. H. (1996). BMP-1: resurrection as procollagen C-proteinase. *Science* **271**, 463.
Rehn, M. and Pihlajaniemi, T. (1994). {alpha}1(XVIII), a Collagen with Frequent Interruptions in the Collagenous Sequence, a Distinct Tissue Distribution, and Homology with Type XV Collagen. *PNAS* **91**, 4234-4238.
Rehn, M. and Pihlajaniemi, T. (1995). Identification of Three N-terminal Ends of Type XVIII Collagen Chains and Tissue-specific Differences in the Expression of the Corresponding Transcripts. *J. Biol. Chem.* **270**, 4705-4711.
Rehn, M., Veikkola, T., Kukk-Valdre, E., Nakamura, H., Ilmonen, M., Lombardo, C., Pihlajaniemi, T., Alitalo, K. and Vuori, K. (2001). Interaction of endostatin with integrins implicated in angiogenesis. *Proc Natl Acad Sci U S A* **98**, 1024-9.
Reichardt, L. F. (2006). Neurotrophin-regulated signalling pathways. *Philos Trans R Soc Lond B Biol Sci* **361**, 1545-64.
Rhiner, C. and Hengartner, M. O. (2006). Sugar antennae for guidance signals: syndecans and glypicans integrate directional cues for navigating neurons. *ScientificWorldJournal* **6**, 1024-36.
Ricard-Blum, S. and Ruggiero, F. (2005). The collagen superfamily: from the extracellular matrix to the cell membrane. *Pathol Biol (Paris)* **53**, 430-42.
Sanchez-Soriano, N. and Prokop, A. (2005). The influence of pioneer neurons on a growing motor nerve in Drosophila requires the neural cell adhesion molecule homolog FasciclinII. *J Neurosci* **25**, 78-87.
Sasaki, T., Fukai, N., Mann, K., Gohring, W., Olsen, B. R. and Timpl, R. (1998). Structure, function and tissue forms of the C-terminal globular domain of collagen XVIII containing the angiogenesis inhibitor endostatin. *Embo J* **17**, 4249-56.
Sasaki, T., Larsson, H., Kreuger, J., Salmivirta, M., Claesson-Welsh, L., Lindahl, U., Hohenester, E. and Timpl, R. (1999). Structural basis and potential role of heparin/heparan sulfate binding to the angiogenesis inhibitor endostatin. *EMBO Journal* **18**, 6240-6248.
Sasaki, T., Larsson, H., Tisi, D., Claesson-Welsh, L., Hohenester, E. and Timpl, R. (2000). Endostatins derived from collagens XV and XVIII differ in structural and binding properties, tissue distribution and anti-angiogenic activity. *Journal of Molecular Biology* **301**, 1179-1190.

Schindelholz, B., Knirr, M., Warrior, R. and Zinn, K. (2001). Regulation of CNS and motor axon guidance in Drosophila by the receptor tyrosine phosphatase DPTP52F. *Development* **128**, 4371-4382.
Schneider, V. A. and Granato, M. (2003). Motor axon migration: a long way to go. *Dev Biol* **263**, 1-11.
Schneider, V. A. and Granato, M. (2006). The Myotomal diwanka (lh3) Glycosyltransferase and Type XVIII Collagen Are Critical for Motor Growth Cone Migration. *Neuron* **50**, 683-695.
Scott, I. C., Blitz, I. L., Pappano, W. N., Imamura, Y., Clark, T. G., Steiglitz, B. M., Thomas, C. L., Maas, S. A., Takahara, K., Cho, K. W. et al. (1999). Mammalian BMP-1/Tolloid-related metalloproteinases, including novel family member mammalian Tolloid-like 2, have differential enzymatic activities and distributions of expression relevant to patterning and skeletogenesis. *Dev Biol* **213**, 283-300.
Sepp, K. J., Schulte, J. and Auld, V. J. (2001). Peripheral glia direct axon guidance across the CNS/PNS transition zone. *Dev Biol* **238**, 47-63.
Serpe, M. and O'Connor, M. B. (2006). The metalloprotease Tolloid-related and its TGF-{beta}-like substrate Dawdle regulate Drosophila motoneuron axon guidance. *Development* **133**, 4969-4979.
Serpe, M., Ralston, A., Blair, S. S. and O'Connor, M. B. (2005). Matching catalytic activity to developmental function: tolloid-related processes Sog in order to help specify the posterior crossvein in the Drosophila wing. *Development* **132**, 2645-56.
Siebert, M., Banovic, D., Goellner, B. and Aberle, H. (2009). Drosophila motor axons recognize and follow a Sidestep-labeled substrate pathway to reach their target fields. *Genes Dev* **23**, 1052-62.
Sink, H., Rehm, E. J., Richstone, L., Bulls, Y. M. and Goodman, C. S. (2001). sidestep encodes a target-derived attractant essential for motor axon guidance in Drosophila. *Cell* **105**, 57-67.
Sink, H. and Whitington, P. M. (1991). Location and connectivity of abdominal motoneurons in the embryo and larva of Drosophila melanogaster. *J Neurobiol* **22**, 298-311.
Soderhall, C., Marenholz, I., Kerscher, T., Ruschendorf, F., Esparza-Gordillo, J., Worm, M., Gruber, C., Mayr, G., Albrecht, M., Rohde, K. et al. (2007). Variants in a novel epidermal collagen gene (COL29A1) are associated with atopic dermatitis. *PLoS Biol* **5**, e242.
Song, H. J., Ming, G. L. and Poo, M. M. (1997). cAMP-induced switching in turning direction of nerve growth cones. *Nature* **388**, 275-9.
Srinivasan, S., Rashka, K. E. and Bier, E. (2002). Creation of a Sog morphogen gradient in the Drosophila embryo. *Dev Cell* **2**, 91-101.
Steigemann, P., Molitor, A., Fellert, S., Jackle, H. and Vorbruggen, G. (2004). Heparan sulfate proteoglycan syndecan promotes axonal and myotube guidance by slit/robo signaling. *Curr Biol* **14**, 225-30.
Sterchi, E. E., St^cker, W. and Bond, J. S. (2008). Meprins, membrane-bound and secreted astacin metalloproteinases. *Molecular Aspects of Medicine* **29**, 309-328.
Stevens, A. and Jacobs, J. R. (2002). Integrins regulate responsiveness to slit repellent signals. *J Neurosci* **22**, 4448-55.

Sudhakar, A., Sugimoto, H., Yang, C., Lively, J., Zeisberg, M. and Kalluri, R. (2003). Human tumstatin and human endostatin exhibit distinct antiangiogenic activities mediated by alpha v beta 3 and alpha 5 beta 1 integrins. *Proc Natl Acad Sci U S A* **100**, 4766-71.

Sun, Q., Schindelholz, B., Knirr, M., Schmid, A. and Zinn, K. (2001). Complex genetic interactions among four receptor tyrosine phosphatases regulate axon guidance in Drosophila. *Mol Cell Neurosci* **17**, 274-91.

Takahara, K., Brevard, R., Hoffman, G. G., Suzuki, N. and Greenspan, D. S. (1996). Characterization of a novel gene product (mammalian tolloid-like) with high sequence similarity to mammalian tolloid/bone morphogenetic protein-1. *Genomics* **34**, 157-65.

Takahara, K., Lyons, G. E. and Greenspan, D. S. (1994). Bone morphogenetic protein-1 and a mammalian tolloid homologue (mTld) are encoded by alternatively spliced transcripts which are differentially expressed in some tissues. *J Biol Chem* **269**, 32572-8.

Tessier-Lavigne, M. and Goodman, C. S. (1996). The molecular biology of axon guidance. *Science* **274**, 1123-33.

Unsold, C., Pappano, W. N., Imamura, Y., Steiglitz, B. M. and Greenspan, D. S. (2002). Biosynthetic processing of the pro-alpha 1(V)2pro-alpha 2(V) collagen heterotrimer by bone morphogenetic protein-1 and furin-like proprotein convertases. *J Biol Chem* **277**, 5596-602.

Van Vactor, D., Wall, D. P. and Johnson, K. G. (2006). Heparan sulfate proteoglycans and the emergence of neuronal connectivity. *Curr Opin Neurobiol* **16**, 40-51.

Webber, C. A., Hocking, J. C., Yong, V. W., Stange, C. L. and McFarlane, S. (2002). Metalloproteases and Guidance of Retinal Axons in the Developing Visual System. *The Journal of Neuroscience* **22**, 8091-8100.

Weinstein, B. M. (2005). Vessels and Nerves: Marching to the Same Tune. *Cell* **120**, 299-302.

Wen, W., Moses, M. A., Wiederschain, D., Arbiser, J. L. and Folkman, J. (1999). The generation of endostatin is mediated by elastase. *Cancer Res* **59**, 6052-6.

Westerfield, M., McMurray, J. V. and Eisen, J. S. (1986). Identified motoneurons and their innervation of axial muscles in the zebrafish. *J Neurosci* **6**, 2267-77.

Wickstrom, S. A., Alitalo, K. and Keski-Oja, J. (2004). An Endostatin-derived Peptide Interacts with Integrins and Regulates Actin Cytoskeleton and Migration of Endothelial Cells. *J. Biol. Chem.* **279**, 20178-20185.

Yamaguchi, N., Anand-Apte, B., Lee, M., Sasaki, T., Fukai, N., Shapiro, R., I Que, C. L., Timpl, R. and Olsen, B. R. (1999). Endostatin inhibits VEGF-induced endothelial cell migration and tumor growth independently of zinc binding. *EMBO Journal* **18**, 4414-4423.

Yasothornsrikul, S., Davis, W. J., Cramer, G., Kimbrell, D. A. and Dearolf, C. R. (1997). viking: identification and characterization of a second type IV collagen in Drosophila. *Gene* **198**, 17-25.

Yurchenco, P. D., Amenta, P. S. and Patton, B. L. (2004). Basement membrane assembly, stability and activities observed through a developmental lens. *Matrix Biol* **22**, 521-38.

Zito, K., Parnas, D., Fetter, R. D., Isacoff, E. Y. and Goodman, C. S. (1999). Watching a synapse grow: noninvasive confocal imaging of synaptic growth in Drosophila. *Neuron* **22**, 719-29.

Own contribution to the manuscripts

Publication 1: Frauke Meyer and Hermann Aberle (2006). At the next stop sign turn right: the metalloprotease Tolloid-related 1 controls defasciculation of motor axons in *Drosophila*. Development 133, 4035-4044.

The *tlr1* mutant alleles were generated in a mutagenesis screen by Hermann Aberle, and their genomic position was mapped by Hermann Aberle and Dirk Beuchle. I sequenced the alleles. I performed the experiments depicted in Fig. 1 H-M, Fig. 2 A-F, Fig. 3, Fig. 4, Fig. 7 and Table1.

Preparation of the manuscript was shared equally between Hermann Aberle and myself.

Publication 2: Frauke Meyer and Bernard Moussian (2009). *Drosophila* multiplexin (Dmp) modulates motor axon pathfinding accuracy. Development, Growth and Differentiation 51, 483-498.

All experiments were performed by myself. Bernard Moussian gave strategic support for the design. The manuscript was prepared by myself with intellectual support by Bernard Moussian.

Development ePress online publication date 13 September 2006

Development 133, 4035-4044 (2006) doi:10.1242/dev.02580

At the next stop sign turn right: the metalloprotease Tolloid-related 1 controls defasciculation of motor axons in *Drosophila*

Frauke Meyer and Hermann Aberle*

Navigation of motoneuronal growth cones toward the somatic musculature in *Drosophila* serves as a model system to unravel the molecular mechanisms of axon guidance and target selection. In a large-scale mutagenesis screen, we identified *piranha*, a motor axon guidance mutant that shows strong defects in the neuromuscular connectivity pattern. In *piranha* mutant embryos, permanent defasciculation errors occur at specific choice points in all motor pathways. Positional cloning of *piranha* revealed point mutations in *tolloid-related 1* (*tlr1*), an evolutionarily conserved gene encoding a secreted metalloprotease. Ectopic expression of Tlr1 in several tissues of *piranha* mutants, including hemocytes, completely restores the wild-type innervation pattern, indicating that Tlr1 functions cell non-autonomously. We further show that loss-of-function mutants of related metalloproteases do not have motor axon guidance defects and that the respective proteins cannot functionally replace Tlr1. *tlr1*, however, interacts with *sidestep*, a muscle-derived attractant. Double mutant larvae of *tlr1* and *sidestep* show an additive phenotype and lack almost all neuromuscular junctions on ventral muscles, suggesting that Tlr1 functions together with Sidestep in the defasciculation process.

KEY WORDS: *Drosophila*, Neuromuscular junction, Motor axon guidance, Motoneuron, Metalloprotease, Tolloid, Tolkin, Tolloid-related 1, Sidestep, Kuzbanian

INTRODUCTION

Accurate innervation of somatic muscles is a prerequisite for coordinated movements in any higher organism. During embryogenesis, correct neuromuscular connectivity is established by the developmental processes of axon outgrowth, axon guidance, target selection and synapse formation (Tessier-Lavigne and Goodman, 1996). Despite the fact that motor axons initially form coherent nerve bundles, certain growth cones leave these tightly fasciculated nerves at specific peripheral locations in order to migrate into their target regions. Defasciculation, the exit of axons from a nerve track, is therefore a crucial process that needs to be strictly regulated. Failure to defasciculate at these choice points leads to axon guidance defects and muscle innervation errors (Araujo and Tear, 2003). Which molecules regulate the detachment of motor axons from adherent nerve bundles? How are choice points molecularly defined?

The *Drosophila* neuromuscular innervation pattern provides a powerful experimental system to genetically dissect the molecular mechanisms of defasciculation and motor axon guidance in vivo. Trajectories of motor axons and their branching patterns are stereotypic and segmentally repeated (Sink and Whitington, 1991), as are the positions of neuromuscular terminals on muscle fibers (Hoang and Chiba, 2001). This relatively simple anatomy, together with the available genetic tools in *Drosophila*, have been of great advantage to identify genes and gene families with roles in motor axon guidance, including the Semaphorins (Kolodkin et al., 1993) and Netrins (Mitchell et al., 1996). Furthermore, three molecules have been identified that seem to specifically control defasciculation of motor axons: the transmembrane tyrosine phosphatase Lar (leukocyte common antigen-related) and the members of the immunoglobulin superfamily Beaten path (Beat) and Sidestep (Side), all three of which give rise to highly penetrant motor axon guidance phenotypes (Desai et al., 1996; Fambrough and Goodman, 1996; Krueger et al., 1996; Sink et al., 2001). Sidestep is expressed in somatic muscles during the period of motor axon pathfinding and is thought to function as a muscle-derived attractant for motor nerves (Sink et al., 2001). In *sidestep* mutant embryos, motor axons frequently bypass their targets, as they fail to defasciculate from their nerve tracts. As Lar, Beat and Side give rise to similar bypass phenotypes when mutated, they all seem to be involved in the defasciculation process, but how they interact mechanistically, and whether additional regulators are required, is currently unknown.

Here, we describe *piranha*, a novel axon guidance mutant with defasciculation defects. In *piranha* mutants, we identified point mutations in the evolutionarily conserved gene *tolloid-related 1* (*tlr1*), also called *tolkin* (*tok*), which encodes an extracellular metalloprotease (Nguyen et al., 1994; Finelli et al., 1995). Mutations in *tlr1*, but not in related *Drosophila* metalloproteases, lead to stable innervation errors that persist into larval stages. Motor nerves stay attached to each other at places where they should diverge and consequently fail to reach their muscle targets or use irregular routes. Genetic rescue experiments demonstrate that Tlr1 functions non-cell-autonomously, possibly in the hemolymph. In addition, the proteolytic activity of Tlr1 is required in cooperation with other axon guidance molecules, such as Sidestep, to terminate coherent axon-axon interactions at choice points.

MATERIALS AND METHODS

Genetics and fly stocks

The mutant alleles of *tlr1* ($tlr1^{D427}$, $tlr1^{I678}$, $tlr1^{K598}$ and $tlr1^{K788}$) and *side* ($side^{C137}$, $side^{I306}$, $side^{I1563}$, $side^{K717}$) were isolated in an F2 methanesulfonic acid ethylester (EMS)-mutagenesis screen on the third chromosome for

Max-Planck-Institute for Developmental Biology, Department III/Genetics, Spemannstrasse 35, 72076 Tübingen, Germany.

*Author for correspondence (e-mail: hermann.aberle@tuebingen.mpg.de)

Accepted 10 August 2006

recessive mutations affecting the structure of neuromuscular junctions (NMJs) (Aberle et al., 2002). The *side, tlr1* double mutants were constructed by recombination using recessive markers of the rucuca-chromosome. *UAS-tlr1* and *UAS-tld*^{23A} were a kind gift of Michael O'Connor. The *tolloid* alleles *tld*^{10E95}, *tld*^{9B66}, *tld*^{6B69} and *tld*^{7074} and Heat shock-Gal4 were provided by the Tübingen stock collection. *tlr1*^{1}, *tlr1*^{3}, *kuz*^{E29}, *kuz*^{K01403}, *Mmp1*^{k04809}, *Mmp2*^{k00604} and *Mmp2*^{KG01263}, *UAS-kuz*^{F}, *UAS-dsRed2* (#6282) and CG-Gal4 were obtained from the Bloomington Stock Center (http://flystocks.bio.indiana.edu/). To assess neuromuscular phenotypes, mutants were crossed into the CD8-GFP-Sh background (Zito et al., 1999). The following Gal4-lines were used: Elav-Gal4, 24B-Gal4 (gifts of C. S. Goodman), G14-Gal4 (Aberle et al., 2002), Cha-Gal4 (Salvaterra and Kitamoto, 2001), Serpent-Gal4 (gift of R. Reuter), PPL-Gal4 (gift of M.J. Pankratz) and OK371-Gal4 (Mahr and Aberle, 2006). As wild-type control strains, y w^{1} or w;; CD8-GFP-Sh were used. Genotypes of larvae with transgenically labeled NMJs and motor nerves were OK371-Gal4/+; CD8-GFP-Sh,UAS-*dsRed2*/+ and OK371-Gal4/+; *tlr1*^{K788}/*tlr1*^{D427},UAS-*dsRed2*. Rescue crosses were performed according to the following scheme: *UAS-GeneX*; *tlr1*^{D427}/TM6B crossed to Tissue-specific-Gal4; *tlr1*^{K788}/TM6B. For heat shock experiments, flies were allowed to lay eggs into the food of their vials for 3 hours. Embryos were then stored for 3, 6 or 9 hours or overnight at room temperature before a heat shock (1 hour, 37°C water bath) was applied.

Complementation and mapping

Mutant lines with similar phenotypes were crossed to each other and judged for non-complementation by the presence of mislocalized NMJs. Mutations were mapped by meiotic recombination against the multiply marked rucuca-chromosome (Bloomington). Mapping was refined using available deficiencies. Df(3R)crb87-4, Df(3R)crb-F89-4 and Df(3R)96B did complement but Df(3R)crb87-5, Df(3R)slo3, Df(3R)XS and Df(3R)XTA1 failed to complement *tlr1* mutations. Database searches were performed at FlyBase (http://flybase.bio.indiana.edu/) and NCBI (http://www.ncbi.nlm.nih.gov/).

Quantification of axon guidance phenotypes

The innervation phenotypes were quantified in intact third instar CD8-GFP-Sh larvae. The locations of NMJs were evaluated through the translucent cuticle in abdominal segments A2-A7 using confocal microscopy. Embryonic guidance phenotypes were quantified in dissected embryos stained with anti-Fas II.

Molecular analysis

Genomic DNA of the *tlr1* alleles was isolated using the QIAamp DNA Mini Kit (Qiagen), amplified by PCR and sequenced on both strands with the BigDye Terminator kit (PE Applied Biosystems). Sequences were analyzed using the Lasergene software package (DNAStar). The partial *tlr1* cDNA clone RH04849 was obtained from BDGP (http://www.fruitfly.org/). Digoxigenin-labeled sense and antisense probes for in situ hybridizations were synthesized from RH04849 (Tautz and Pfeifle, 1989). In situ hybridizations were imaged with an Axiophot light microscope (Zeiss) equipped with a CCD-camera (ProgRes3012).

Immunohistochemistry

Embryos were stained as described (Mahr and Aberle, 2006), except that fluorescent labeling was performed with the TSA Cyanine-3 System (Perkin Elmer). Stained embryos were dissected with sharpened tungsten needles on microscope slides and imaged with an LSM510 confocal microscope (Zeiss) in the Cy3- and DIC channels. Signals in the Cy3-channel were depicted in black to enhance the contrast in overlays with the DIC images. Wandering third instar larvae were dissected in PBS on Sylgaard plates (Dow Corning Corporation) using spring scissors (Fine Science Tools) and insect pins (Emil Arlt). Larval fillets were fixed in 3.7% formaldehyde/PBS for 15 minutes, washed with PTx (PBS containing 0.1% Triton X-100) and blocked in PTx/5% normal goat serum. Primary antibodies were added overnight at 4°C. Fillets were washed with PTx and incubated with fluorescence-labeled secondary antibodies for 1 hour. Stained fillets were cleared in 70% glycerol/PBS and mounted onto microscope slides. The dilutions of the primary antibodies (supernatants) were as follows: mouse anti-Discs large (4F3) 1:100 and mouse anti-Fasciclin II (1D4) 1:5 (gifts of C. S. Goodman). The Cy3-conjugated secondary antibodies were diluted 1:400 (Molecular Probes or Jackson ImmunoResearch). Fluorescently-labeled larvae were examined with a TCS SPL (Leica) or LSM510 (Zeiss) confocal laser scanning microscope. Projections and single images were adjusted for brightness and contrast using Adobe Photoshop.

RESULTS

Piranha mutant larvae display a high degree of missing and mislocalized NMJs

In *Drosophila* embryos and larvae, the somatic musculature of abdominal segments A2-A7 consists of 30 muscles that are individually identifiable and innervated at invariant positions (Fig. 1A). Wiring of the neuromuscular system starts at stage 13 of embryogenesis, when motor axons begin to migrate toward the differentiating muscle fields (van Vactor et al., 1993). In each abdominal hemisegment, two major motor nerves defasciculate into five nerve branches (Fig. 1A). The segmental nerve (SN) bifurcates into the SNa and SNc, and the intersegmental nerve gives rise to a dorsal branch (ISN) and two ventral branches (ISNb and ISNd).

In a large-scale mutagenesis screen for genes that affect the structure and maintenance of NMJs (Parnas et al., 2001; Aberle et al., 2002), we discovered four alleles of a novel mutant, *piranha*, which showed missing and/or mislocalized NMJs. To visualize NMJs in *piranha* mutants, we used the transgenically encoded fusion protein CD8-GFP-Sh (Zito et al., 1999). CD8-GFP-Sh is controlled by a muscle-specific promotor and consists of the extracellular and transmembrane domain of human CD8, fused cytoplasmatically to GFP and a C-terminal domain of the Shaker potassium channel. It binds to the postsynaptic protein Discs large (Dlg) and highlights all NMJs consisting of type Ib and Is boutons (Zito et al., 1999). Using this synaptic marker, we could evaluate NMJs through the translucent cuticle of intact third instar larvae.

In wild-type larvae, the dorsalmost NMJs on muscle pairs 1/9 and 2/10 are normally arranged symmetrically relative to the axis of the ISN (Fig. 1A-C). In *piranha*^{D427}/*piranha*^{K788} mutants, however, we found that muscles 1 and 9 either lacked NMJs completely or were innervated at ectopic sites in 38.1% (muscle 1) or 25.0% (muscle 9) of hemisegments (Table 1, Fig. 1D). We observed even stronger defects in ventral muscle regions. In wild type, the ISNb defasciculates from the ISN and forms, among others, NMJs in the cleft between muscles 6/7 and on a ventral and medial position on muscles 12 and 13, respectively (Fig. 1E,F). In *piranha* mutants, we found that NMJs on muscle 12 and 13 were mislocalized or absent in 64.3 and 56.0% of hemisegments, respectively (Table 1, Fig. 1G). Muscles 6 and 7 showed an erroneous innervation pattern in 23.9 and 34.6% of hemisegments. It is important to note that the pattern and degree of misinnervation varied between hemisegments along the anterior-posterior axis and also between two hemisegments located on contralateral sides. We determined the total number of misinnervated muscles per hemisegment and found that between 7.1 and 46.4% of muscles were affected in *piranha* mutant hemisegments (n=84) compared with 0-14.3% in wild-type larvae (n=44). Thus, innervation errors occurred in all body wall regions and in every hemisegment, but the innervation pattern was unique for each hemisegment, indicating that the innervation process is largely autonomous within a given hemisegment.

As CD8-GFP-Sh is a transgenically encoded exogenous protein, it is possible that it does not accurately reflect the location of endogenous NMJs. To exclude this possibility, we stained *piranha* mutant larvae with antibodies that recognize synaptic marker

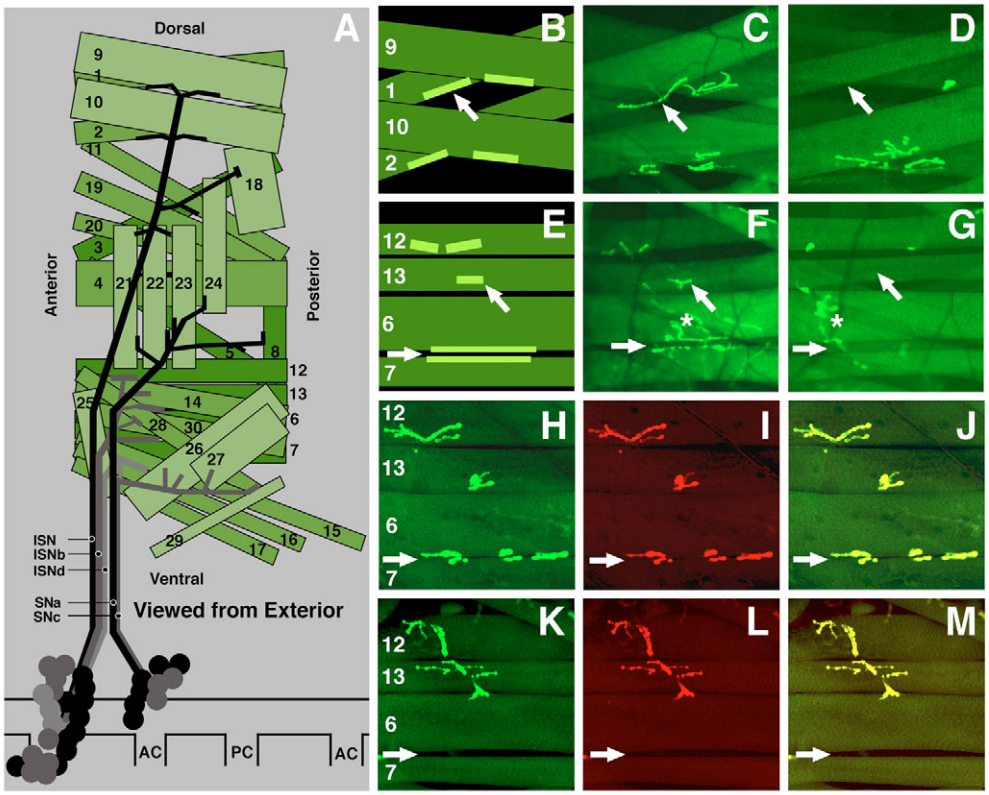

Fig. 1. Neuromuscular terminals are missing and mislocalized in *piranha* mutant third instar larvae. Arrows illustrate the normal localization of NMJs on muscles of wild-type larvae. (**A**) Schematic diagram of the innervation pattern of the somatic musculature of an abdominal hemisegment viewed from the exterior. The approximate branching pattern of the five motor nerves and the innervation sites are superimposed onto the muscle pattern. The approximate locations of motoneurons in the ventral nerve cord are indicated. (**B-D**) Innervation defects on dorsalmost muscles. (B) Schematic diagram and (C) confocal micrograph of NMJs (bright green) on muscle pairs 1/9 and 2/10 in undissected wild-type larvae as seen with the CD8-GFP-Sh marker (exterior view). (D) NMJs are missing on muscle 1 and reduced to a remnant on muscle 9 in this $piranha^{D427}/piranha^{K788}$ mutant hemisegment. (**E-G**) Innervation defects on ventral muscles. (E) Schematic diagram and (F) confocal micrograph depicting the locations of NMJs on ventral internal muscles 12, 13, 6 and 7 in an undissected wild-type larva expressing CD8-GFP-Sh. (G) In this $piranha^{D427}/piranha^{K788}$ mutant hemisegment, NMJs are missing on muscle 13 and rudimentary in the cleft of muscles 6/7. Muscle 12 displays innervation defects as well. Asterisks indicate NMJs and muscles outside of the intended focal plane. (**H-M**) Confocal images of the ventral innervation pattern of a dissected wild-type (H-J) and $piranha^{D427}/piranha^{K788}$ mutant larva (K-M) viewed from the interior. NMJs on muscles 12, 13, 6 and 7 are visualized with CD8-GFP-Sh (H,K) and anti-Dlg (I,L). Endogenous Dlg staining completely overlaps with transgenic CD8-GFP-Sh (J,M). Note the altered innervation pattern of muscles 12 and 13 and the lack of NMJs in the cleft between muscles 6 and 7 in the mutant animal (arrows in K-M). Dorsal is up and anterior is left in all figures. AC, anterior commissure; PC, posterior commissure.

proteins. Dlg is a postsynaptic protein that mediates the anchorage of transmembrane receptors to the underlying cytoskeleton (Budnik et al., 1996). We did not observe neuromuscular Dlg staining in places where CD8-GFP-Sh clusters were absent, neither in wild-type (Fig. 1H-J) nor in *piranha* mutant larvae (Fig. 1K-M). CD8-Sh-GFP therefore faithfully reflects the presence and positions of NMJs.

Misguided motor axons innervate muscles at ectopic locations in *piranha* mutants

As CD8-GFP-Sh visualizes only postsynaptic sides of NMJs but not motor nerves, we asked whether the unusual locations of NMJs in *piranha* mutants were caused by misguided axons. We stained dissected third instar larvae with anti-Fasciclin II antibodies (anti-Fas II). Fasciclin II is expressed by all motoneurons and accumulates

Table 1. Frequency of innervation errors in wild type, *tolloid-related 1* (*tlr1*, *piranha*) and *sidestep* (*side*) mutant animals

	ISN				SNa				ISNb				SNc			ISNd		
L3 larvae	M1	M9	M2	M10	M21	M22	M23	M24	M12	M13	M6	M7	M26	M27	M29	M15	M16	M17
Wild type (CD8-GFP-Sh) (*n*=44)	0	0	0	0	2.3	0	0	0	6.8	2.3	0	2.3	0	0	2.3	13.6	6.8	4.6
tlr^{D427}/tlr^{K788} (*n*=84)	38.1	25.0	7.1	3.6	8.4	1.2	1.2	34.5	64.3	56.0	23.9	34.6	21.7	74.7	71.1	83.4	27.4	34.6
$side^{C137}/side^{I1563}$ (*n*=60)	25.0	35.0	16.7	11.7	41.7	3.4	3.3	51.7	75.0	75.0	83.3	85.0	61.7	86.7	66.7	78.3	63.3	98.4
$tlr^{D427},side^{C137}/tlr^{K788},side^{C137}$ (*n*=65)	36.9	35.4	41.6	18.5	53.8	12.3	21.5	95.4	93.8	98.5	100	100	95.3	100	98.5	96.9	98.5	100

			ISNb bypass				
Stage 17 embryos	ISN defect	SNa defect	Fused full	Split full	Partial	SNc bypass	ISNd bypass
Wild type (CD8-GFP-Sh) (*n*=218)	1.4	2.8	0.9	1.8	3.7	1.8	14.7
tlr^{D427}/tlr^{K788} (*n*=211)	84.4	51.2	29.4	52.6	14.2	54.0	54.0
$side^{C137}$ (*n*=105)	14.3	22.9	36.2	15.2	32.4	67.6	65.7

(Top) Innervation defects in larvae. Numbers represent the percentage of hemisegments with innervation defects on the indicated muscles (mislocalized and missing NMJs) in third instar larvae stained with CD8-GFP-Sh. (Bottom) Innervation defects in embryos. Numbers represent percentage of hemisegments with guidance defects in the indicated motor nerves.
n, number of hemisegments quantified.

in their axons and presynaptic terminals, making it possible to selectively visualize motor nerves but not the afferent sensory nerves that project along similar pathways (van Vactor et al., 1993). In wild-type larvae, muscles 12 and 13 are innervated by a ventrodorsal projection of the ISNb pathway (Fig. 2A-C). In *piranha* mutants, we found that muscles 12 and 13 were often innervated via a dorsoventral projection of the ISN or SNa, which induced the formation of NMJs at ectopic sites (Fig. 2D-F). This suggests that motoneuronal growth cones of the ISNb pathway failed to navigate into the ventral muscle field via their normal route. Despite this initial failure, however, some growth cones eventually managed to detach from the ISN or SNa and innervated muscles 12 and 13 from the dorsal side (reach back phenotypes via a different nerve route). These experiments show that motor axons are misrouted in *piranha* mutants, which leads to the formation of synaptic terminals at ectopic locations.

During manual dissection of larvae, great care must be taken to preserve the trajectories of peripheral nerves. To circumvent this technical hurdle, we devised a genetic method that permits the visualization of both motor nerves and NMJs in living animals. Using the Gal4/UAS-system (Brand and Perrimon, 1993), we expressed the *Discosoma* Red Fluorescent Protein (UAS-dsRed2) specifically in motoneurons (OK371-Gal4) in the background of CD8-GFP-Sh wild-type or *piranha* mutant animals. Motor axons and presynaptic terminals were therefore highlighted in red and muscles and postsynaptic terminals in green (Fig. 2G-L). In wild-type larvae, the SN and ISN nerves form a single nerve bundle that defasciculates into five nerve branches at the ventralmost choice point (shown schematically in Fig. 2G). The ISNb and ISNd detach from the ISN, whereas the SNc detaches from the SNa (Fig. 2J). In *piranha* mutants, we observed that the ISNb frequently stayed attached to the ISN, sometimes as a separately identifiable axon bundle, and reached its target muscles via irregular routes (Fig. 2H,K). We found similar defasciculation errors in the SN pathway. As shown in Fig. 2I,L, the SN nerve often grew too far to the posterior, because the SNa defasciculates much too late. *piranha* mutant larvae display, therefore, severe bypass and misrouting phenotypes, primarily due to motor axons remaining attached to each other at choice points.

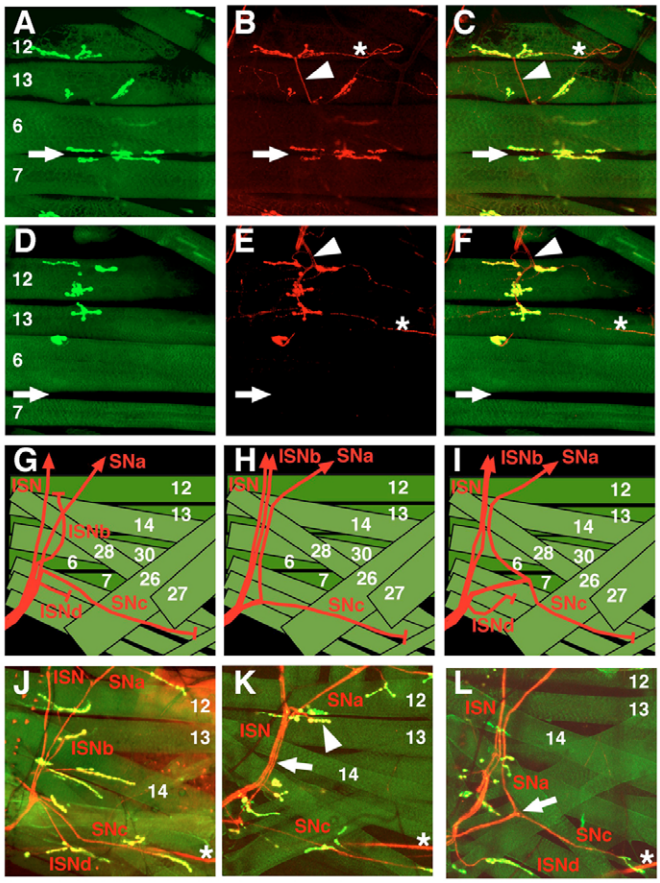

Fig. 2. Motor axons are misguided in *piranha*^{D427}/*piranha*^{K788} mutant larvae. (**A-F**) Confocal micrographs of the ISNb innervating ventral muscles 12, 13, 6 and 7 in dissected wild-type (A-C) and *piranha* mutant (D-F) larvae. Muscles and postsynaptic terminals are visualized with CD8-GFP-Sh (A,D), motor axons and presynaptic endings are stained with anti-Fasciclin II (B,E). The ISNb normally innervates muscle 12 on its ventral side via a ventrodorsal projection (arrowheads in B,C). In a *piranha* mutant hemisegment, muscles 12, 13 and 6 are innervated at ectopic sites by a dorsoventral nerve projection (arrowheads in E,F). Muscles 6 and 7 remain uninnervated (arrows in D-F). Arrows mark the cleft between muscles 6 and 7. Asterisks indicate type II boutons. (**G-L**) Transgenic labeling of motor axons reveals guidance defects in living *piranha*^{D427}/*piranha*^{K788} mutant larvae (exterior views). In addition to CD8-GFP-Sh, larvae express dsRed2 in all motoneurons using OK371-Gal4. (G,J) Schematic diagram (G) and confocal micrograph (J) of the hemisegmental nerve defasciculating into five nerve branches at the ventral choice point of a wild-type larva. (H,K) Schematic diagram (H) and confocal micrograph (K) of the defasciculation defects in a *piranha* mutant larva. The ISNb failed to branch into the ventral region and migrated in a parallel pathway along the ISN. The ISN, ISNb and SNa pathways are visible as separate nerve bundles (arrow). An axon branching out of the misguided ISNb innervates muscle 13 at an ectopic position (arrowhead). (I,L) Schematic diagram (I) and confocal micrograph (L) of the ventral muscle field of a *piranha* mutant larva. The SNa stays attached to the SNc and defasciculates too late (arrow). Asterisks in (J-L) indicate nerves innervating neighboring hemisegments.

Guidance errors in *piranha* mutants occur at embryonic stages

We asked next at which time point these projection errors develop, and we examined motoneuronal trajectories during stages 16-17 of embryonic development, when neuromuscular connectivity is established. The ISN of wild-type embryos has three clearly visible branch points (Fig. 3A). In *piranha* mutants, we observed in 84.4% of hemisegments (Table 1) that the branch points appeared underdeveloped and/or the ISN was stalled at the second branch point and barely reached the position of the third branch point (arrow in Fig. 3B). Within the developing SNa pathway, axons normally bifurcate into a dorsal and posterior branch at the dorsal edge of muscle 12 (Fig. 3C). In *piranha* mutant embryos, we found SNa defects in 51.2% of hemisegments, including, for example, two dorsal branches of the SNa (arrowheads in Fig. 3D). In ventral muscle regions, the ISNb failed to defasciculate from the ISN in 96.2% of hemisegments. The ISNb was either tightly attached to the ISN (fusion bypass, see left segment in Fig. 3D and Table 1) or formed a separated parallel nerve bundle (split bypass, middle and right segment in Fig. 3D and Table 1). In addition, we and others (M. Serpe and M. O'Connor, personal communication) observed defasciculation defects in Fasciclin II-positive nerve tracts in the embryonic central nervous system (data not shown). The innervation defects do not strongly compromise embryogenesis and larval development, because we recover *piranha*^{D427} mutant second and early third instar larvae at the expected ratios (data not shown).

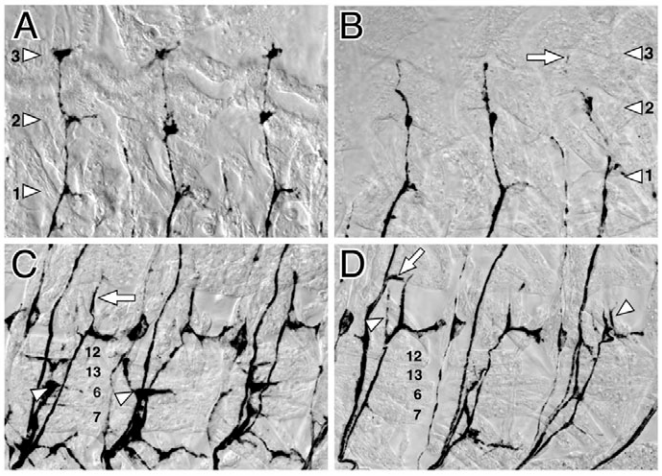

Fig. 3. Axon guidance defects in *piranha* mutants arise during embryonic development and affect all motor axon pathways. (**A-D**) Micrographs of motor axons in three consecutive hemisegments in dissected wild-type (A,C) and *piranha*^{D427}/*piranha*^{K788} mutant (B,D) embryos at stage 17 stained with anti-Fas II antibodies. (A) In the dorsal region of a wild-type embryo, the ISN has reached its terminal branch point at muscle pair 1/9 in all three hemisegments, and all three branch points are well developed (arrowheads 1-3). (B) The ISN fails to reach its final branch point properly (arrow) in *piranha* mutants, and most branch points appear underdeveloped (arrowheads 1-3). (C) Lateral and ventral body wall region of a wild-type embryo. The SNa bifurcates into a dorsal branch (arrow) and posterior branch. The ISNb (arrowheads) forms a clearly visible projection innervating muscles 12, 13, 6 and 7. (D) In *piranha* mutants, a bifurcated dorsal branch of the SNa is often observed (arrowheads). The ISNb fails to innervate muscles 12, 13, 6 and 7. In the left segment, the ISNb remains fused to the ISN and branches off at muscle 4 (arrow). In the middle and right segments, a split bypass occurs, with the ISNb temporarily detaching from the ISN (right) or fusing to different nerve tracts (middle).

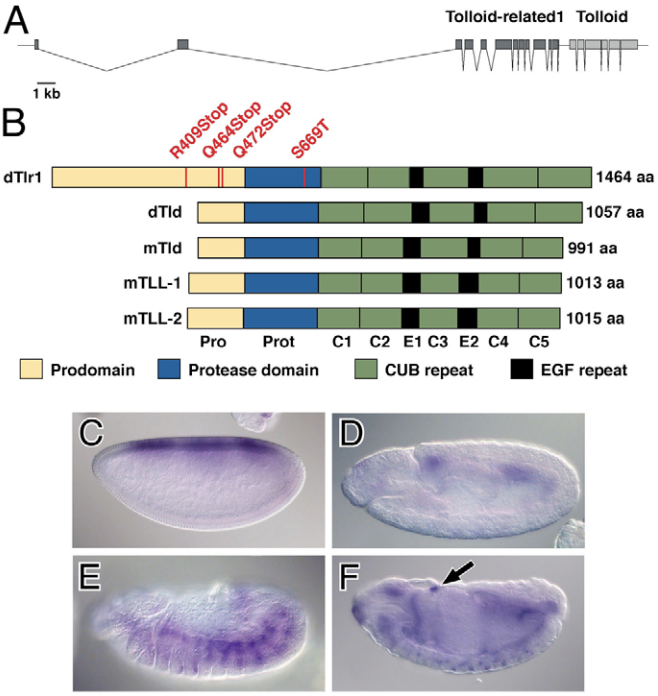

Fig. 4. Positional cloning of *piranha*. (**A**) Genomic organization of the *piranha* (*tolloid-related 1*, *tlr1*) locus. The 3′ end of the *tlr1* gene is less than 1 kb away from the 5′ end of its paralog *tolloid* (*tld*), limiting the 5′ regulatory region of *tld* to a minimum. (**B**) Domain structure of *Drosophila* Tlr1, Tld and their mouse homologs. The EMS-induced point mutations in the four *piranha* (*tlr1*) alleles are indicated (see text). (**C-F**) In situ hybridization using *tlr1* antisense probes. *tlr1* is expressed in the dorsal blastoderm at stage 5 (C), in progenitor cells of the visceral mesoderm at stage 10 (D), in somatic muscles at stage 13 (E) and in cells of the ventral nerve cord and ring gland (arrow) at stage 16 (F).

Based on these observations, we conclude that the *piranha* mutant guidance phenotype arises during embryogenesis, and the defects are quantitatively stronger but qualitatively similar to the larval defects.

Positional cloning of *piranha*

The *piranha* locus was mapped by meiotic recombination and deficiency mapping to the cytological region 96A2-A21 on the third chromosome. During meiotic mapping, we noticed homozygous mutant adult escapers that lacked the posterior crossvein of the wings. Literature and database searches revealed that mutants in *tlr1* [*tolkin* (*tok*)], located at 96A18-A19 (Fig. 4A), display a similar wing phenotype (Nguyen et al., 1994; Finelli et al., 1995). To examine if *piranha* is allelic to *tlr1,* we performed complementation crosses using existing *tlr1* alleles. Both *tlr1*^{1} and *tlr1*^{3} did not complement our *piranha* alleles, and the transheterozygous animals had both axon guidance and posterior crossvein defects. The *tlr1* cDNA encompasses 5.4 kb and encodes a predicted extracellular metalloprotease (Nguyen et al., 1994; Finelli et al., 1995). Consisting of 1464 amino acids, Tlr1 is composed of an N-terminal prodomain, a central metalloprotease domain and a C-terminal protein-protein interaction domain containing five CUB (complement subcomponents C1r/C1s, Uegf, BMP-1) and two EGF (epidermal growth factor) domains (Fig. 4B).

To identify potential molecular lesions, we sequenced the Tlr1-encoding exons and found single point mutations in all four *piranha* alleles. We therefore renamed our *piranha* alleles to *tlr1*^{K788}, *tlr1*^{D427}, *tlr1*^{K598} and *tlr1*^{I678}. Three of them contain nonsense mutations in the N-terminal prodomain: R409Stop in *tlr1*^{K788}, Q464Stop in *tlr*^{D427} and Q472Stop in *tlr1*^{K598} (Fig. 4B). Provided that the prodomain functions only in inhibiting the activity of the protease domain, these alleles are probably null alleles. Consistent with this assumption is the previous classification of *tlr1*^{1}, which contains a stop codon in the protease domain, as a null allele (Finelli et al., 1995). In the fourth allele, we identified a serine to threonine exchange within the protease domain (S669T in *tlr1*^{I678}). This highly conserved serine residue is located within the sequence motif ‘SIMHY’, which forms a characteristic loop, the Met-turn, that positions the terminal tyrosine residue to coordinate the zinc ion in the active site (Gomis-Ruth et al., 1993). Insufficient zinc coordination probably renders the protease domain non-functional in *tlr1*^{I678}. Indeed, a point mutation in the very same serine residue of the related metalloprotease Tolloid (S276F in *tolloid*^{10E}) has been isolated in a screen for new *tolloid* alleles (Finelli et al., 1994).

tolloid (*tld*) is a close sequence homolog and genomic neighbor of *tlr1*, with less than 1000 base pairs separating the two genes (Fig. 4A). Tolloid is involved in the determination of the dorsoventral body axis and functions as an activator of Decapentaplegic (Dpp) signaling in dorsal regions of blastoderm embryos (Shimell et al.,

1991; Marques et al., 1997). In mammals, four relatives of Tlr1 and Tld have been identified (Fig. 4B): mammalian Tolloid (Tld), bone morphogenetic protein 1 (Bmp1), Tolloid-like 1 (Tll1) and Tolloid-like 2 (Tll2), the first two of which are isoforms derived from the same gene (Takahara et al., 1994; Takahara et al., 1996; Scott et al., 1999). The metalloprotease domain of *Drosophila* Tlr1 is 64.5, 67.5 and 67.0% identical to its mouse relatives Tld, Tll1 and Tll2, respectively. The CUB/EGF protein-protein interaction domain is also well conserved and shows 42.0, 42.5 and 43.9% identity to these proteins.

To determine where *tlr1* is expressed during embryonic development, we synthesized Digoxigenin-labeled antisense probes using cDNA clone RH04849. *tlr1* showed a dynamic expression pattern during embryogenesis (Nguyen et al., 1994; Finelli et al., 1995). We observed *tlr1* expression first in the dorsal blastoderm (Fig. 4C). In the extended germ band stage, it was transcribed in progenitor cells of the visceral mesoderm (Fig. 4D). At stages 13-15, *tlr1* was expressed in somatic muscles and the midgut (Fig. 4E). Beginning with stage 15, *tlr1* transcripts also appeared in a few cells in the ventral nerve cord, the thoracic peripheral nervous system and the ring gland (Fig. 4F). Interestingly, *tlr1* was strongly expressed in muscles but not in neurons when motor axons leave the central nervous system, indicating that muscle-derived Tlr1 may be important for motor axon guidance.

Transgenic rescue experiments reveal that Tlr1 functions non-cell-autonomously

To determine in which tissue and during which developmental period Tlr1 is required, we performed transgenic rescue experiments using the Gal4/UAS system. We induced transcription of wild-type Tlr1 in a *tlr1* mutant background during different developmental stages using Heat shock-Gal4. Compared with wild-type animals (Fig. 5A), mutant animals transgenic for UAS-*tlr1* and Heat shock-Gal4 displayed strong innervation defects when reared at room temperature, because expression of Tlr1 is not induced (Fig. 5B). By contrast, mutant embryos that received a 1-hour heat shock (37°C) when they were 3-6, 6-9 or 9-12 hours old (stages 6-9, 10-12 or 12-15, respectively) developed into larvae with a normal innervation pattern (Fig. 5C). When we applied the heat shock at the end of embryogenesis (stage 17), however, we were unable to rescue the mislocalized NMJs in *tlr1* mutants, indicating that Tlr1 is ineffective after NMJs have formed. Hence, Tlr1 functions during mid- to late-embryonic stages, when neuromuscular connectivity is established.

To examine whether Tlr1 is required in nerves or muscles, we performed rescue experiments using tissue-specific Gal4-lines. As *tlr1* is strongly expressed in muscles during motor axon pathfinding, we reasoned that muscle-specific expression of Tlr1 might be sufficient for rescue. Indeed, expression of Tlr1 in all somatic muscles using G14-Gal4 completely restored the innervation pattern in homozygous mutant larvae (Fig. 5D). The rescued larvae were indistinguishable from wild-type animals with respect to the size and localization of their NMJs. Unexpectedly, however, expression of Tlr1 in all postmitotic neurons using Elav-Gal4 also completely restored the wild-type innervation pattern (Fig. 5E). When we expressed Tlr1 only in cholinergic neurons using Cha-Gal4, the mutant phenotype was not rescued, demonstrating that UAS-*tlr1* is not unspecifically expressed in the absence of a Gal4 driver (Fig. 5F). From these results, it appeared that Tlr1 could be expressed either in muscles or all neurons to fully rescue the guidance defects. As Tlr1 is likely to be a secreted protease, this finding could be explained by a non-cell-autonomous function of Tlr1. If secretion into the extracellular matrix or hemolymph is sufficient to deliver Tlr1 to the locations where its proteolytic activity is required, then expression of Tlr1 in tissues normally irrelevant for motor axon guidance should rescue the innervation defects. Using fat body-specific Pumpless-Gal4 (PPL-Gal4) or two different hemocyte-specific drivers (CG-Gal4 and Serpent-Gal4), we could completely restore the wild-type innervation pattern in *tlr1* mutants (data not shown), supporting a cell non-autonomous function for Tlr1.

To test whether Tlr1 is also sufficient to misdirect motor axons in a wild-type background, we overexpressed it either in the nervous system (Elav-Gal4) or in all muscles (G14-Gal4) but we did not observe any motor axon guidance phenotypes, as visualized with CD8-GFP-Sh (data not shown). We noticed, however, that overexpression of Tlr1 in wing discs (24B-Gal4) leads to a large central wing blister, suggesting that the function of Tlr1 during wing development is dosage sensitive: too little Tlr1 leads to missing posterior crossveins, whereas too much Tlr1 causes loss of adhesion between wing epithelia (data not shown).

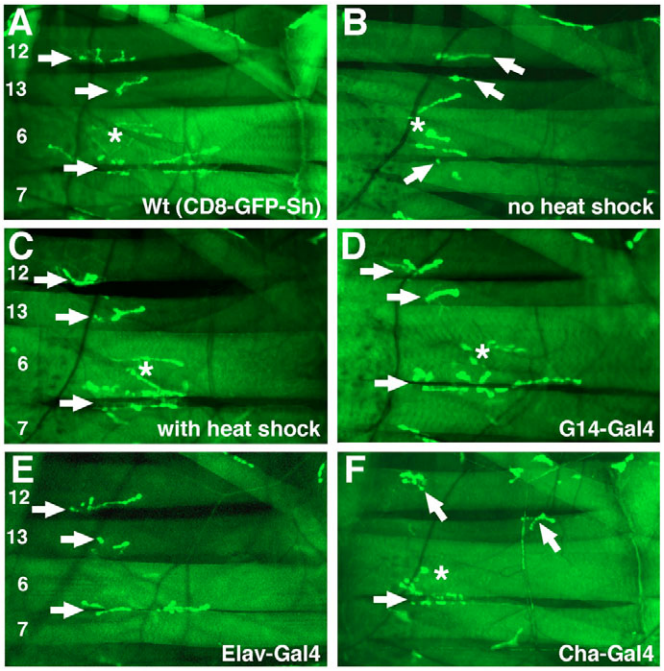

Fig. 5. The *tlr1* mutant phenotype can be rescued by expressing wild-type Tlr1 in various tissues. (**A-F**) Confocal micrographs of NMJs on ventral muscles 12, 13, 6 and 7 stained with CD8-GFP-Sh in undissected third instar larvae. Arrows indicate NMJs on muscles 12, 13, 6 and 7. (A) Wild type. (B) $tlr1^{D427}/tlr1^{K788}$ mutant larva carrying Heat shock-Gal4 and *UAS-tlr1* transgenes. When no heat shock is applied, the neuromuscular pattern is disrupted. Muscles 12 and 13 are innervated at wrong positions, and the cleft between muscles 6 and 7 is only marginally innervated (arrows). (C) Application of a heat shock during mid-embryogenesis completely rescues the innervation errors on all muscles. (D) Ventral muscle field of a $tlr1^{D427}/tlr1^{K788}$ mutant larva expressing Tlr1 in all somatic muscles using G14-Gal4. The innervation pattern appears wild-type. (E) Expression of Tlr1 in all postmitotic neurons using Elav-Gal4 similarly rescues the innervation errors in $tlr1^{D427}/tlr1^{K788}$ mutants. (F) The neuromuscular pattern is not restored in $tlr1^{D427}/tlr1^{K788}$ mutants expressing Tlr1 only in cholinergic neurons using Cha-Gal4. NMJs on muscles 12 and 13 are mislocalized (arrows). Asterisks indicate NMJs located on muscles that are outside the intended focal plane.

The metalloproteases Tolloid and Kuzbanian cannot functionally replace Tlr1

As mutations in *tlr1* affect a large subset, but not all, NMJs, we wondered whether the proteolytic activities of other metalloproteases are additionally required for pathway selection. As a closely related paralog of Tlr1, Tolloid may be required for the innervation of the remaining muscles. As strong alleles of *tld* are embryonic lethal, we searched for transheterozygous allelic combinations that would survive to third instar larvae. Compared with *tlr1* mutants (Fig. 6A), we were not able to detect mislocalized or structurally abnormal NMJs in tld^{6B69}/tld^{7074}, tld^{6B69}/tld^{9B66} or tld^{9B66}/tld^{10E95} mutants, indicating that Tolloid is not required for wiring and maintaining NMJs (Fig. 6B).

Both Tlr1 and Tld are members of the astacin family of metalloproteases, a subgroup of the metzincin superfamily, which comprises in addition the serralysins, the matrixins (matrix metalloproteases) and the adamlysins (ADAMs, metalloproteases with a disintegrin and metalloprotease domain) (Bond and Beynon, 1995; Stocker et al., 1995). Kuzbanian (Kuz), a member of the ADAM family in *Drosophila*, is expressed in neurons and has been shown to play a role in axon guidance at the ventral midline, raising the possibility that it may also regulate pathfinding of motor axons (Fambrough et al., 1996; Schimmelpfeng et al., 2001). When we examined kuz^{E29}/kuz^{K01403} mutant larvae, however, all NMJs were at their wild-type positions, indicating that motor axons project along correct trajectories (Fig. 6C). Other prime candidates for regulators of axonal pathfinding are matrix metalloproteases (Mmps). Mmps in general process extracellular matrix components, which is necessary for tissue remodeling and cell migration, but has also been shown to be crucial for axon guidance (Webber et al., 2002). *Drosophila* has only two Mmps, Mmp1 and Mmp2. During the time of motor axon pathfinding, Mmp1 is expressed in midline glial cells and Mmp2 in neurons and mesodermal cells, all tissues that are relevant for navigating growth cones (Llano et al., 2000; Llano et al., 2002; Page-McCaw et al., 2003). When we analyzed $Mmp1^{k04809}$, $Mmp2^{k00604}$ and $Mmp2^{KG01263}$ mutant larvae, however, we failed to detect any neuromuscular abnormalities (data not shown).

We next examined if Tlr1 and Tld could functionally replace each other if expressed in similar tissues. To test for functional redundancy, we crossed *UAS-tld* or UAS-*tlr1* into the *tlr1* mutant background and expressed either gene with Elav-Gal4 or 24B-Gal4. In contrast to experiments using *UAS-tlr1* (Fig. 6D), Tld was not able to substantially rescue the *tlr1* mutant phenotype, irrespective of whether we expressed it in neurons or muscles (Fig. 6E). Similarly, *UAS-kuz* failed to improve the projections errors in *tlr1* mutants (Fig. 6F), showing that neither Tld nor Kuz could functionally replace Tlr1. Thus, loss- and gain-of-function analysis of metalloproteases belonging to the matrixin, adamlysin and astacin families support a key-regulatory role of Tlr1 in motor axon guidance in *Drosophila*.

Axon guidance phenotypes are strongly enhanced in *tlr1,side* double mutants

To identify candidate molecules that might act in concert with Tlr1, we searched for mutants with related phenotypes. In our large-scale EMS mutagenesis screen of the larval NMJ, we identified four new alleles of *sidestep* ($side^{C137}$, $side^{I306}$, $side^{I1563}$, $side^{K717}$). Sidestep, originally identified by H. Sink and colleagues (Sink et al., 2001), is a transmembrane receptor of the immunoglobulin superfamily that functions as a muscle-derived attractant for motor axons. Similarly to *tlr1* mutants (Fig. 7A,7A'), we found missing and abnormally localized NMJs in $side^{C137}/side^{I1563}$ mutant larvae, regardless of whether we used CD8-GFP-Sh (Fig. 7B) or anti-Fas II antibodies (Fig. 7B') as detection methods. The immunohistochemical stainings also confirmed that the CD8-GFP-Sh marker reliably reflected the axon guidance defects in *side* mutants. In *side* mutant embryos, pathfinding of the ISNb was defective in 83.8% of hemisegments (Table 1). *tlr1* and *side* mutants therefore share a variety of phenotypic similarities: (1) embryonic defasciculation defects affect all pathways and persist into larval stages; (2) failures to reach final branch points; (3) innervation patterns vary between segments; (4) ventral muscles are more frequently affected; and (5) NMJs can be mislocalized or absent on an affected muscle fiber. For a majority of muscles, however, the *side* mutant phenotype was more penetrant (Fig. 7A'',B'').

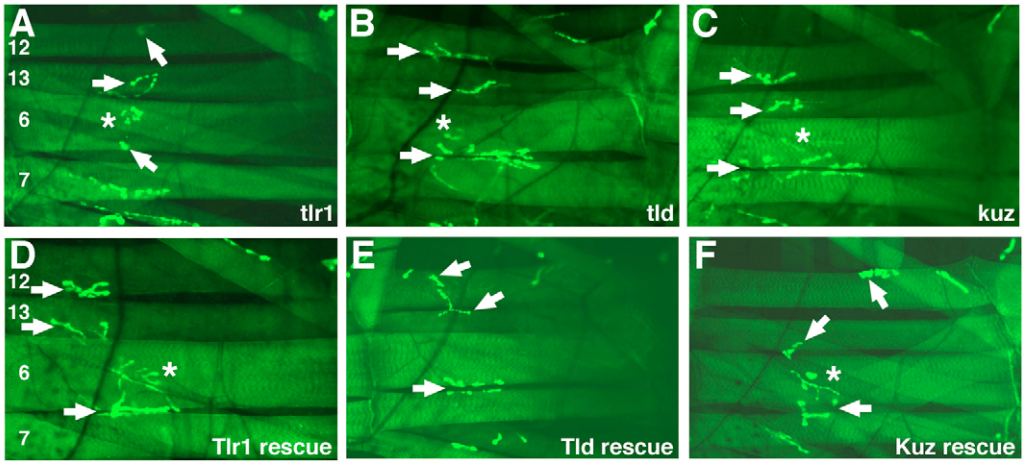

Fig. 6. Tolloid cannot functionally replace Tlr1. (**A-F**) Confocal images of the innervation patterns of ventral internal muscles in intact third instar larvae stained with CD8-GFP-Sh. Arrows indicate the locations of NMJs on muscles 12, 13, 6 and 7. (A) In a $tlr1^{D427}/tlr1^{K788}$ mutant animal, NMJs are mislocalized on muscle 12 and reduced to a remnant in the cleft of muscles 6 and 7. (B) All terminals are at their correct location and structured normally in a *tolloid* (tld^{10E95}/tld^{9B66}) mutant larva. (C) The neuromuscular innervation pattern appears wild-type in *kuzbanian* (kuz^{e29}/kuz^{K01403}) mutants. (D) Overexpression of Tlr1 in all neurons using Elav-Gal4 rescues the *tlr1* mutant phenotype. (E) Overexpression of Tld with Elav-Gal4 does not rescue the NMJ pattern in *tlr1* mutants. NMJs on muscles 12 and 13 are mislocalized in this hemisegment. (F) Overexpression of Kuzbanian in all neurons does not restore the innervation defects in *tlr1* mutants. NMJs are mislocalized on muscles 12 and almost absent on muscles 13, 6 and 7. Asterisks indicate NMJs located on muscles that are outside of the intended focal plane.

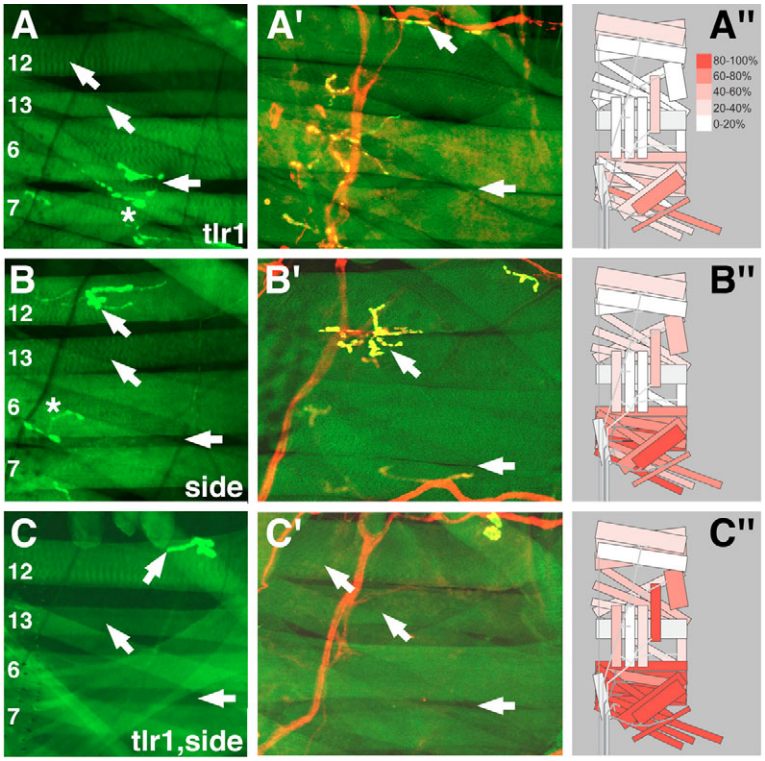

Fig. 7. Innervation defects are strongly enhanced in tlr1,side double mutants. Arrows indicate missing or mislocalized NMJs on muscles 12, 13, 6 and 7. Asterisks mark NMJs outside of the intended focal plane. (**A-C**) Confocal images of $tlr1^{D427}$ (A) and $side^{C137}/side^{l1563}$ (B) single and $tlr1^{D427},side^{C137}/tlr1^{K788},side^{C137}$ (C) double mutant third instar larvae stained with CD8-GFP-Sh. Double mutant larvae (C) show a strong enhancement of the innervation phenotype and lack almost all NMJs on ventral muscles, only muscle 12 is innervated at an unusual dorsal-posterior position in this example. (**A′-C′**) Confocal images of dissected $tlr1^{D427}/tlr1^{K788}$ (A′) and $side^{C137}/side^{l1563}$ (B′) single and $tlr1^{D427},side^{C137}/tlr1^{K788},side^{C137}$ (C′) double mutant third instar larvae stained with CD8-GFP-Sh (green) and anti-Fas II antibodies (red). In this double mutant hemisegment (C′), all NMJs are missing on ventral muscles, including NMJs formed by type II boutons. (**A″-C″**) Schematic representation of the quantitative evaluation of the larval innervation defects as presented in Table 1. The frequency of innervation errors for a respective muscle in wild type was subtracted from the frequency observed in mutants. Misinnervation frequencies were then transformed into a color code, as depicted in (A″). Muscles 4 and 25 were not evaluated. In tlr1 mutants (A″), the misinnervation phenotype is weaker than in side mutants (B″), and creation of a double mutant aggravates the innervation defects in ventral, lateral and dorsal body wall regions (C″).

As mutations in genes that function together in the same biological process often share phenotypic similarities, we created *side*,*tlr1* double mutants using genetic null alleles. If Tlr1 and Side function in a linear pathway, then double mutants would be predicted to exhibit a phenotype that resembles each single mutant phenotype. In $tlr1^{D427},side^{C137}/tlr1^{K788},side^{C137}$ double mutants, however, we observed a strong enhancement of each single mutant phenotype. Double mutant larvae lacked virtually all NMJs on all ventral muscles in all abdominal hemisegments (Fig. 7C,7C', Table 1). Muscles located in lateral or dorsal regions of the body wall also showed an increase in innervation errors, albeit less dramatically (Fig. 7C'', Table 1). The increase in phenotypic strength suggests that *tlr1* and *side* function in parallel pathways, or that their functions converge on shared components further downstream. Interestingly, *tlr1*,*side* double mutants were still capable of forming NMJs in lateral and dorsal regions, suggesting that additional gene products are involved in ensuring complete innervation of the musculature.

DISCUSSION

Motor axons are misrouted in *tlr1* mutants

In this paper, we show that *tlr1* is required for motor axons to defasciculate from other motor axons at specific choice points. *tlr1* encodes a secreted metalloprotease that functions non-cell-autonomously, possibly via secretion into the hemolymph. Mutations in *tlr1* lead to the permanent formation of NMJs at ectopic sites or to the absence of synaptic terminals. Only a few studies have examined whether embryonic motor axon guidance phenotypes persist into larval stages in *Drosophila* (Nose et al., 1994; Sink et al., 2001; de Jong et al., 2005). Apart from embryonic lethality, a possible reason is presumably that the detailed analysis of larval motor axon phenotypes is hampered by the availability of suitable methods other than manual dissection. We used transgenic methods for the visualization of the neuromuscular wiring pattern in intact larvae. The fluorescent CD8-GFP-Sh marker specifically highlights the postsynaptic apparatus of each muscle fiber, revealing the structure and location of each NMJ (Zito et al., 1999). As CD8-GFP-Sh is under the control of the myosin heavy chain promotor, we combined it with the Gal4/UAS-system to simultaneously express the red fluorescent protein dsRed2 in motoneurons. CD8-GFP-Sh by itself indirectly reflects the projection pattern of motor axons by reliably revealing the location of each NMJ. However, the combination of both CD8-GFP-Sh and motoneuron-specific dsRed2 highlights the entire neuromuscular connectivity pattern in living animals.

Supported by these non-invasive methods, we show that *tlr1* mutants have defects in motor axon guidance rather than in target recognition or innervation site selection. First, motor nerves show defasciculation defects already during embryogenesis, even before they reach their target muscles. Second, motor axons remain physically attached to each other beyond their destined branch points and until late larval stages. Third, the bypass, stall and misrouting phenotypes are similar to those found in *sidestep* mutants, a known regulator of motor axon guidance (Sink et al., 2001). As a result, motor axons fail to reach their targets in *tlr1* mutants or do so from unusual directions, which leads to anomalous muscle innervation. The formation of NMJs at ectopic locations suggests that the growth direction and entry point of the motor nerve may instruct the final location of an NMJ. Even if the position of an NMJ is predetermined by the muscle fiber, the incoming nerve terminal appears to be able to relocate postsynaptic components.

In *tlr1* mutants, all abdominal segments show innervation defects, and all pathways are affected. The intrasegmental phenotype, however, is quite variable, i.e. the innervation pattern of a given hemisegment differs visibly from the adjacent or contralateral hemisegment, indicating that neuromuscular wiring is largely autonomous for a given hemisegment. The variability further implies that Tlr1 may not regulate specific and invariable guidance decisions, but rather plays a general role in defasciculation.

Migrating growth cones in *tlr1* mutants apparently do not strictly rely on single molecular labels positioned at specific locations. These conclusions support the idea that exact target selection appears to be a rather stochastic process, in which the growth cones integrate attractive and repulsive cues provided by the microenvironment of surrounding cells (Winberg et al., 1998).

How does Tlr1 function?

Metalloproteases have been implicated in a variety of cellular processes, including cell migration, angiogenesis and metastasis (Sternlicht and Werb, 2001; Yong et al., 2001). Neuronal growth cones migrate through an environment that is rich in different extracellular surfaces and may thus exploit similar molecules and mechanisms as migrating cells. Despite the wealth of data on cell migration, only a few reports have been published implicating metalloproteases in axon outgrowth and guidance (Fambrough et al., 1996; Galko and Tessier-Lavigne, 2000; Hattori et al., 2000; Schimmelpfeng et al., 2001; Webber et al., 2002; McFarlane, 2003; Vaillant et al., 2003; VanSaun et al., 2003; Hehr et al., 2005; Jaworski et al., 2006). With regard to motor axons, only ADM-1 (*unc-71*), a member of the ADAM family in *Caenorhabditis elegans*, has been shown to regulate pathfinding (Huang et al., 2003). Tlr1 belongs to the astacin family of metalloproteases and is highly related to *Drosophila* Tolloid. Despite this high degree of conservation, we and others have shown that these two proteins have mutually exclusive functions (Nguyen et al., 1994; Serpe et al., 2005). While Tld cannot functionally replace Tlr1, it is still possible that other metalloproteases with redundant functions assist Tlr1 in defasciculation control, because not all guidance decisions are affected in *tlr1* mutants. Our loss- and gain-of-function analysis of related metalloproteases, however, did not support this possibility. In addition, no other metalloprotease has so far been recovered from mutant screens (van Vactor et al., 1993; Kraut et al., 2001; Sink et al., 2001). These observations support the idea that Tlr1 may be a key regulatory member of the metalloprotease family in *Drosophila* that controls motor axon guidance.

As a secreted metalloprotease, Tlr1 is predicted to function extracellularly, either in the extracellular matrix or in the interstitial fluid. Consistent with this prediction, overexpression of Tlr1 in hemocytes or cells of the fat body could fully rescue the *tlr1* mutant phenotype. Neither hemocytes nor fat-storing cells have so far been implicated in axon guidance. Hence, it is unlikely that Tlr1 remained associated with the extracellular matrix of these cells, but probably got released into the hemolymph. The circulating hemolymph then distributed it to where it was required. As endogenous Tlr1 is expressed in developing muscles during the period of axonal pathfinding, it is possibly secreted from there into the hemolymph to either proteolytically activate a repellent on motor nerves to induce defasciculation or to activate an attractant on muscles. The axon guidance receptor Sidestep is expressed on muscles and functions as an attractant for motor axons (Sink et al., 2001). Based on similarities in their loss-of-function phenotypes, Tlr1 could be required to activate the attractive function of Side. The phenotype of *tlr1,side* double mutants, however, was clearly stronger compared with each single mutant, indicating that they regulate the same biological process but that they function either independently or that the two functions converge further downstream. Tlr1 could therefore regulate the activity of an alternative pathway. Interestingly, M. O'Connor's group suggested that Tlr1 regulates motor axon guidance in part by activating latent TGF-β ligands (M. Serpe and M. O'Connor, unpublished). Although the exact molecular function of Tlr1 is currently not known, the data presented here clearly demonstrate that the evolutionarily conserved metalloprotease Tolloid-related 1 is necessary for motor axon guidance in *Drosophila*.

We are indebted to Mike O'Connor and Mihaela Serpe for sharing unpublished results. We also would like to thank Corey Goodman, in whose lab the EMS screen was performed, and Christiane Nüsslein-Volhard for support. We are grateful to Corey Goodmann, Mike O'Connor, Toshihiro Kitamoto, Rolf Reuter and Michael Pankratz for providing fly stocks and reagents. We thankfully appreciate the help of Dirk Beuchle for meiotic mapping, and Anne Spang and Matthew Harris for critically reading the manuscript. This project was funded by the Max-Planck Gesellschaft and the Deutsche Forschungsgemeinschaft (SFB446).

References

Aberle, H., Haghighi, A. P., Fetter, R. D., McCabe, B. D., Magalhaes, T. R. and Goodman, C. S. (2002). wishful thinking encodes a BMP type II receptor that regulates synaptic growth in Drosophila. *Neuron* **33**, 545-558.

Araujo, S. J. and Tear, G. (2003). Axon guidance mechanisms and molecules: lessons from invertebrates. *Nat. Rev. Neurosci.* **4**, 910-922.

Bond, J. S. and Beynon, R. J. (1995). The astacin family of metalloendopeptidases. *Protein Sci.* **4**, 1247-1261.

Brand, A. H. and Perrimon, N. (1993). Targeted gene expression as a means of altering cell fates and generating dominant phenotypes. *Development* **118**, 401-415.

Budnik, V., Koh, Y. H., Guan, B., Hartmann, B., Hough, C., Woods, D. and Gorczyca, M. (1996). Regulation of synapse structure and function by the Drosophila tumor suppressor gene dlg. *Neuron* **17**, 627-640.

de Jong, S., Cavallo, J. A., Rios, C. D., Dworak, H. A. and Sink, H. (2005). Target recognition and synaptogenesis by motor axons: responses to the sidestep protein. *Int. J. Dev. Neurosci.* **23**, 397-410.

Desai, C. J., Gindhart, J. G., Jr, Goldstein, L. S. and Zinn, K. (1996). Receptor tyrosine phosphatases are required for motor axon guidance in the Drosophila embryo. *Cell* **84**, 599-609.

Fambrough, D. and Goodman, C. S. (1996). The Drosophila beaten path gene encodes a novel secreted protein that regulates defasciculation at motor axon choice points. *Cell* **87**, 1049-1058.

Fambrough, D., Pan, D., Rubin, G. M. and Goodman, C. S. (1996). The cell surface metalloprotease/disintegrin Kuzbanian is required for axonal extension in Drosophila. *Proc. Natl. Acad. Sci. USA* **93**, 13233-13238.

Finelli, A. L., Bossie, C. A., Xie, T. and Padgett, R. W. (1994). Mutational analysis of the Drosophila tolloid gene, a human BMP-1 homolog. *Development* **120**, 861-870.

Finelli, A. L., Xie, T., Bossie, C. A., Blackman, R. K. and Padgett, R. W. (1995). The tolkin gene is a tolloid/BMP-1 homologue that is essential for Drosophila development. *Genetics* **141**, 271-281.

Galko, M. J. and Tessier-Lavigne, M. (2000). Function of an axonal chemoattractant modulated by metalloprotease activity. *Science* **289**, 1365-1367.

Gomis-Ruth, F. X., Stocker, W., Huber, R., Zwilling, R. and Bode, W. (1993). Refined 1.8 A X-ray crystal structure of astacin, a zinc-endopeptidase from the crayfish Astacus astacus L. Structure determination, refinement, molecular structure and comparison with thermolysin. *J. Mol. Biol.* **229**, 945-968.

Hattori, M., Osterfield, M. and Flanagan, J. G. (2000). Regulated cleavage of a contact-mediated axon repellent. *Science* **289**, 1360-1365.

Hehr, C. L., Hocking, J. C. and McFarlane, S. (2005). Matrix metalloproteinases are required for retinal ganglion cell axon guidance at select decision points. *Development* **132**, 3371-3379.

Hoang, B. and Chiba, A. (2001). Single-cell analysis of Drosophila larval neuromuscular synapses. *Dev. Biol.* **229**, 55-70.

Huang, X., Huang, P., Robinson, M. K., Stern, M. J. and Jin, Y. (2003). UNC-71, a disintegrin and metalloprotease (ADAM) protein, regulates motor axon guidance and sex myoblast migration in C. elegans. *Development* **130**, 3147-3161.

Jaworski, D. M., Soloway, P., Caterina, J. and Falls, W. A. (2006). Tissue inhibitor of metalloproteinase-2(TIMP-2)-deficient mice display motor deficits. *J. Neurobiol.* **66**, 82-94.

Kolodkin, A. L., Matthes, D. J. and Goodman, C. S. (1993). The semaphorin genes encode a family of transmembrane and secreted growth cone guidance molecules. *Cell* **75**, 1389-1399.

Kraut, R., Menon, K. and Zinn, K. (2001). A gain-of-function screen for genes controlling motor axon guidance and synaptogenesis in Drosophila. *Curr. Biol.* **11**, 417-430.

Krueger, N. X., Van Vactor, D., Wan, H. I., Gelbart, W. M., Goodman, C. S. and Saito, H. (1996). The transmembrane tyrosine phosphatase DLAR controls motor axon guidance in Drosophila. *Cell* **84**, 611-622.

Llano, E., Pendas, A. M., Aza-Blanc, P., Kornberg, T. B. and Lopez-Otin, C. (2000). Dm1-MMP, a matrix metalloproteinase from Drosophila with a potential

role in extracellular matrix remodeling during neural development. *J. Biol. Chem.* **275**, 35978-35985.
Llano, E., Adam, G., Pendas, A. M., Quesada, V., Sanchez, L. M., Santamaria, I., Noselli, S. and Lopez-Otin, C. (2002). Structural and enzymatic characterization of Drosophila Dm2-MMP, a membrane-bound matrix metalloproteinase with tissue-specific expression. *J. Biol. Chem.* **277**, 23321-23329.
Mahr, A. and Aberle, H. (2006). The expression pattern of the Drosophila vesicular glutamate transporter: A marker protein for motoneurons and glutamatergic centers in the brain. *Gene Expr. Patterns* **6**, 209-309.
Marques, G., Musacchio, M., Shimell, M. J., Wunnenberg-Stapleton, K., Cho, K. W. and O'Connor, M. B. (1997). Production of a DPP activity gradient in the early Drosophila embryo through the opposing actions of the SOG and TLD proteins. *Cell* **91**, 417-426.
McFarlane, S. (2003). Metalloproteases: carving out a role in axon guidance. *Neuron* **37**, 559-562.
Mitchell, K. J., Doyle, J. L., Serafini, T., Kennedy, T. E., Tessier-Lavigne, M., Goodman, C. S. and Dickson, B. J. (1996). Genetic analysis of Netrin genes in Drosophila: Netrins guide CNS commissural axons and peripheral motor axons. *Neuron* **17**, 203-215.
Nguyen, T., Jamal, J., Shimell, M. J., Arora, K. and O'Connor, M. B. (1994). Characterization of tolloid-related-1: a BMP-1-like product that is required during larval and pupal stages of Drosophila development. *Dev. Biol.* **166**, 569-586.
Nose, A., Takeichi, M. and Goodman, C. S. (1994). Ectopic expression of connectin reveals a repulsive function during growth cone guidance and synapse formation. *Neuron* **13**, 525-539.
Page-McCaw, A., Serano, J., Sante, J. M. and Rubin, G. M. (2003). Drosophila matrix metalloproteinases are required for tissue remodeling, but not embryonic development. *Dev. Cell* **4**, 95-106.
Parnas, D., Haghighi, A. P., Fetter, R. D., Kim, S. W. and Goodman, C. S. (2001). Regulation of postsynaptic structure and protein localization by the Rho-type guanine nucleotide exchange factor dPix. *Neuron* **32**, 415-424.
Salvaterra, P. M. and Kitamoto, T. (2001). Drosophila cholinergic neurons and processes visualized with Gal4/UAS-GFP. *Gene Expr. Patterns* **1**, 73-82.
Schimmelpfeng, K., Gogel, S. and Klämbt, C. (2001). The function of leak and kuzbanian during growth cone and cell migration. *Mech. Dev.* **106**, 25-36.
Scott, I. C., Blitz, I. L., Pappano, W. N., Imamura, Y., Clark, T. G., Steiglitz, B. M., Thomas, C. L., Maas, S. A., Takahara, K., Cho, K. W. et al. (1999). Mammalian BMP-1/Tolloid-related metalloproteinases, including novel family member mammalian Tolloid-like 2, have differential enzymatic activities and distributions of expression relevant to patterning and skeletogenesis. *Dev. Biol.* **213**, 283-300.
Serpe, M., Ralston, A., Blair, S. S. and O'Connor, M. B. (2005). Matching catalytic activity to developmental function: tolloid-related processes Sog in order to help specify the posterior crossvein in the Drosophila wing. *Development* **132**, 2645-2656.
Shimell, M. J., Ferguson, E. L., Childs, S. R. and O'Connor, M. B. (1991). The Drosophila dorsal-ventral patterning gene tolloid is related to human bone morphogenetic protein 1. *Cell* **67**, 469-481.
Sink, H. and Whitington, P. M. (1991). Location and connectivity of abdominal motoneurons in the embryo and larva of Drosophila melanogaster. *J. Neurobiol.* **22**, 298-311.
Sink, H., Rehm, E. J., Richstone, L., Bulls, Y. M. and Goodman, C. S. (2001). sidestep encodes a target-derived attractant essential for motor axon guidance in Drosophila. *Cell* **105**, 57-67.
Sternlicht, M. D. and Werb, Z. (2001). How matrix metalloproteinases regulate cell behavior. *Annu. Rev. Cell Dev. Biol.* **17**, 463-516.
Stocker, W., Grams, F., Baumann, U., Reinemer, P., Gomis-Ruth, F. X., McKay, D. B. and Bode, W. (1995). The metzincins-topological and sequential relations between the astacins, adamalysins, serralysins, and matrixins (collagenases) define a superfamily of zinc-peptidases. *Protein Sci.* **4**, 823-840.
Takahara, K., Lyons, G. E. and Greenspan, D. S. (1994). Bone morphogenetic protein-1 and a mammalian tolloid homologue (mTld) are encoded by alternatively spliced transcripts which are differentially expressed in some tissues. *J. Biol. Chem.* **269**, 32572-32578.
Takahara, K., Brevard, R., Hoffman, G. G., Suzuki, N. and Greenspan, D. S. (1996). Characterization of a novel gene product (mammalian tolloid-like) with high sequence similarity to mammalian tolloid/bone morphogenetic protein-1. *Genomics* **34**, 157-165.
Tautz, D. and Pfeifle, C. (1989). A non-radioactive in situ hybridization method for the localization of specific RNAs in Drosophila embryos reveals translational control of the segmentation gene hunchback. *Chromosoma* **98**, 81-85.
Tessier-Lavigne, M. and Goodman, C. S. (1996). The molecular biology of axon guidance. *Science* **274**, 1123-1133.
Vaillant, C., Meissirel, C., Mutin, M., Belin, M. F., Lund, L. R. and Thomasset, N. (2003). MMP-9 deficiency affects axonal outgrowth, migration, and apoptosis in the developing cerebellum. *Mol. Cell. Neurosci.* **24**, 395-408.
van Vactor, D., Sink, H., Fambrough, D., Tsoo, R. and Goodman, C. S. (1993). Genes that control neuromuscular specificity in Drosophila. *Cell* **73**, 1137-1153.
VanSaun, M., Herrera, A. A. and Werle, M. J. (2003). Structural alterations at the neuromuscular junctions of matrix metalloproteinase 3 null mutant mice. *J. Neurocytol.* **32**, 1129-1142.
Webber, C. A., Hocking, J. C., Yong, V. W., Stange, C. L. and McFarlane, S. (2002). Metalloproteases and guidance of retinal axons in the developing visual system. *J. Neurosci.* **22**, 8091-8100.
Winberg, M. L., Mitchell, K. J. and Goodman, C. S. (1998). Genetic analysis of the mechanisms controlling target selection: complementary and combinatorial functions of netrins, semaphorins, and IgCAMs. *Cell* **93**, 581-591.
Yong, V. W., Power, C., Forsyth, P. and Edwards, D. R. (2001). Metalloproteinases in biology and pathology of the nervous system. *Nat. Rev. Neurosci.* **2**, 502-511.
Zito, K., Parnas, D., Fetter, R. D., Isacoff, E. Y. and Goodman, C. S. (1999). Watching a synapse grow: noninvasive confocal imaging of synaptic growth in Drosophila. *Neuron* **22**, 719-729.

Develop. Growth Differ. (2009) **51**, 000–000 doi: 10.1111/j.1440-169X.2009.01111.x

Original Article

Drosophila multiplexin (Dmp) modulates motor axon pathfinding accuracy

Frauke Meyer and Bernard Moussian*

Max-Planck-Institute for Developmental Biology, Department III – Genetics, Spemannstrasse 35, 72076 Tübingen, Germany

Multiplexins are multidomain collagens typically composed of an N-terminal thrombospondin-related domain, an interrupted triple helix and a C-terminal endostatin domain. They feature a clear regulatory function in the development of different tissues, which is chiefly conveyed by the endostatin domain. This domain can be found in proteolytically released monomeric and trimeric versions, and their diverse and opposed effects on the migratory behavior of epithelial and endothelial cell types have been demonstrated in cell culture experiments. The only *Drosophila* multiplexin displays specific features of both vertebrate multiplexins, collagens XV and XVIII. We characterized the *Drosophila* multiplexin (*dmp*) gene and found that three main isoforms are expressed from it, one of which is the monomeric endostatin version. Generation of *dmp* deletion alleles revealed that Dmp plays a role in motor axon pathfinding, as the mutants exhibit ventral bypass defects of the intersegmental nerve b (ISNb) similar to other motor axon guidance mutants. Transgenic overexpression of monomeric endostatin as well as of full-length Dmp, but not trimeric endostatin, were able to rescue these defects. In contrast, trimeric endostatin increased axon pathfinding accuracy in wild type background. We conclude that Dmp plays a modulating role in motor axon pathfinding and may be part of a buffering system that functions to avoid innervation errors.

Key words: collagen XVIII and XV, *Drosophila*, endostatin, extracellular matrix, motoaxon guidance.

Introduction

The extracellular environment provides numerous cues that direct the behavior of many migratory cell types, including pathfinding decisions of neuronal axons and dendrites. While being exposed to multiple guidance signals at the same time, a growth cone has to integrate these signals, and a guidance decision thus results from the interplay of multiple attractive and repulsive signals of different strength. During the last two decades, a large number of extracellular proteins that act in the process of motor axon pathfinding have been identified and functionally characterized in several vertebrate and invertebrate model systems. In the limelight of genetic and biochemical studies were almost exclusively transmembrane molecules of adhesive or signaling function and their diffusible or membrane-bound ligands, like Robo and Slit, semaphorins and their plexin-containing receptor complexes, netrins and deleted in colorectal cancer (DCC)/frazzled receptors, ephrins and their receptors, fasciclinII/neuronal cell adhesion molecule (NCAM) and DsCam (Araujo and Tear 2003; Chilton 2006). Other components of the extracellular matrix (ECM) have received much less attention.

Abundant ECM constituents are glycosaminoglycans (GAGs); especially heparan sulfates (HS) and chondroitin sulfates (CS) that are covalently linked to a core protein. In the nervous system, both HS and CS proteoglycans (HSPGs and CSPGs) have been implicated in various aspects of development, including axonal pathfinding (Bandtlow and Zimmermann 2000; Carulli *et al*. 2005). Additional sulfation, epimerization and deacetylation of HS and CS side chains can create microdomains of high specificity for certain binding partners, thus adding a high degree of functional specificity to their core protein (Bulow and Hobert 2004). To date, it has been shown that a loss of enzymes involved in HS biosynthesis and modification causes axon guidance defects (Bulow and Hobert 2004; Lee *et al*. 2004) and that the guidance function of the Robo/Slit pathway requires HS (Bulow and Hobert 2004).

*Author to whom all correspondence should be addressed.
Email: bernard.moussian@tuebingen.mpg.de
Received 22 September 2008; revised 20 March 2009; accepted 20 March 2009
Author contributions: Experiments were designed by FM and BM and carried out by FM. Manuscript was prepared by FM and BM.

In *Drosophila*, four classes of HSPG core proteins are present. The membrane-bound ECM components syndecan (Sdc) and, to a lesser extent, the glypican Dally-like (Dlp) have been shown to function in axonal guidance at the ventral midline and in the visual system via the action of the Slit/Robo signaling system, but seem to play a minor role in the motor axon guidance system (Johnson *et al*. 2004; Steigemann *et al*. 2004; Fox and Zinn 2005; Rawson *et al*. 2005). Of the two basement membrane HSPG core proteins encoded in the *Drosophila* genome, only perlecan has been studied so far, and found to be involved in neuromuscular junction (NMJ) development (Arikawa-Hirasawa *et al*. 2002; Voigt *et al*. 2002), but it has not been implicated in axonal guidance. The only potential *Drosophila* HSPG core protein entirely uncharacterized to date is a homologue of vertebrate collagens XV and XVIII.

Collagens XV and XVIII are the only two members of a vertebrate collagen family termed multiplexins (Oh *et al*. 1994). While collagen XVIII is an HSPG, collagen XV is modified with CS side chains (Li *et al*. 2000). Both molecules are characterized by a collagen triple helix region that is interrupted by several non-collagenous stretches, as well as a C-terminal non-triple helical NC1 domain (Oh *et al*. 1994; Rehn and Pihlajaniemi 1995). The NC1 domain is composed of three functionally distinct regions: an association region in its most N-terminal part that trimerizes NC1 monomers, a protease-sensitive hinge region, and the C-terminal globular endostatin (ES) domain (Sasaki *et al*. 1998).

Biochemical work on vertebrate collagen XVIII has identified a number of proteases capable of releasing monomeric ES (Wen *et al*. 1999; Felbor *et al*. 2000; Ferreras *et al*. 2000; Lin *et al*. 2001; Heljasvaara *et al*. 2005) and proteolytic release has also been shown to be necessary to activate biological ES function *in vitro* (Heljasvaara *et al*. 2005). Free monomeric ES domains occur *in vivo* and have been extensively studied as inhibitors of endothelial cell migration and thus as angiogenesis inhibitors (O'Reilly *et al*. 1997; Sasaki *et al*. 1999; Yamaguchi *et al*. 1999; Rehn *et al*. 2001; Abdollahi *et al*. 2004; Hurskainen *et al*. 2005; Marneros *et al*. 2007). It has also become clear in several experimental systems that the association of two or three NC1 domains, forming dimeric or trimeric ES, changes the effects of ES: In tissue cultures of different endothelial and other cell types, ES dimers or trimers activate migratory cell behavior, whereas free ES monomers produce an inhibitory effect even in the presence of multimeric ES (Kuo *et al*. 2001; Clamp *et al*. 2006). Similarly, in *Caenorhabditis elegans* lacking the NC1-encoding region of the multiplexin gene *cle-1*, migration of several cell types is defective, including that of mechanosensory neurons. This phenotype can be restored to wild type by overexpressing NC1, but not by ES, and ES overexpression in wild type impairs mechanosensory neuron migration (Ackley *et al*. 2001).

The *Drosophila* neuromuscular system is a very powerful and extensively used genetic model for studying axonal pathfinding. Neuromuscular connectivity gets established during embryogenesis, starting with the outgrowth of pioneer axons from the central nervous system towards the regions where the respective target muscles develop. Ensuing events are guidance of the growth cone towards its target region, target recognition and synapse formation (Tessier-Lavigne and Goodman 1996). We believe that the results summarized above suggest a role for the collagen XV/XVIII homologue in this process. To the end of characterizing this role of the protein and its subdomains, we generated both mutant and overexpression fly strains, and assayed them for motor nerve misrouting phenotypes. Our observations indicate that Dmp is involved in axonal navigation decisions, and possibly by more than one mechanism. We also analyzed the gene, its expression and products on the sequence level.

Materials and methods

Molecular biology

RNA was isolated from pools of stage 1–17 w^{1118} embryos using the RNeasy tissue kit (Qiagen). After oligo-dT-primed reverse transcription, *dmp* transcripts were polymerase chain reaction (PCR)-amplified, cloned into TOPO pCRII and sequenced using the BigDye Terminator kit (PE Applied Biosystems). Transcript 14 indicated in Figure 1(B) is BDGP clone GH14382. Sequences of Transcripts 1–13 were submitted to GenBank (Accession numbers EU523228–EU523240). Primer sequences are available in Supplement 1.

In situ *hybridization*

Digoxygenin (DIG)-labeled RNA probes were generated using the following templates: an AflIII-digest of BDGP-clone GH14382 (ES antisense), a cDNA clone containing *dmp* exons 1 and 2 generated by ourselves (TSP antisense), and a PCR product of exon 3 using GH14382 as template and a reverse primer containing the sequence of the T7 promoter (exon 3 antisense). *In situ* hybridizations were carried out following the standard protocol (Tautz and Pfeifle 1989) and sense probes used for control purposes.

Genetics and fly stocks

Strains carrying deletions in the *dmp* locus were generated by recombination between piggyBac transposable

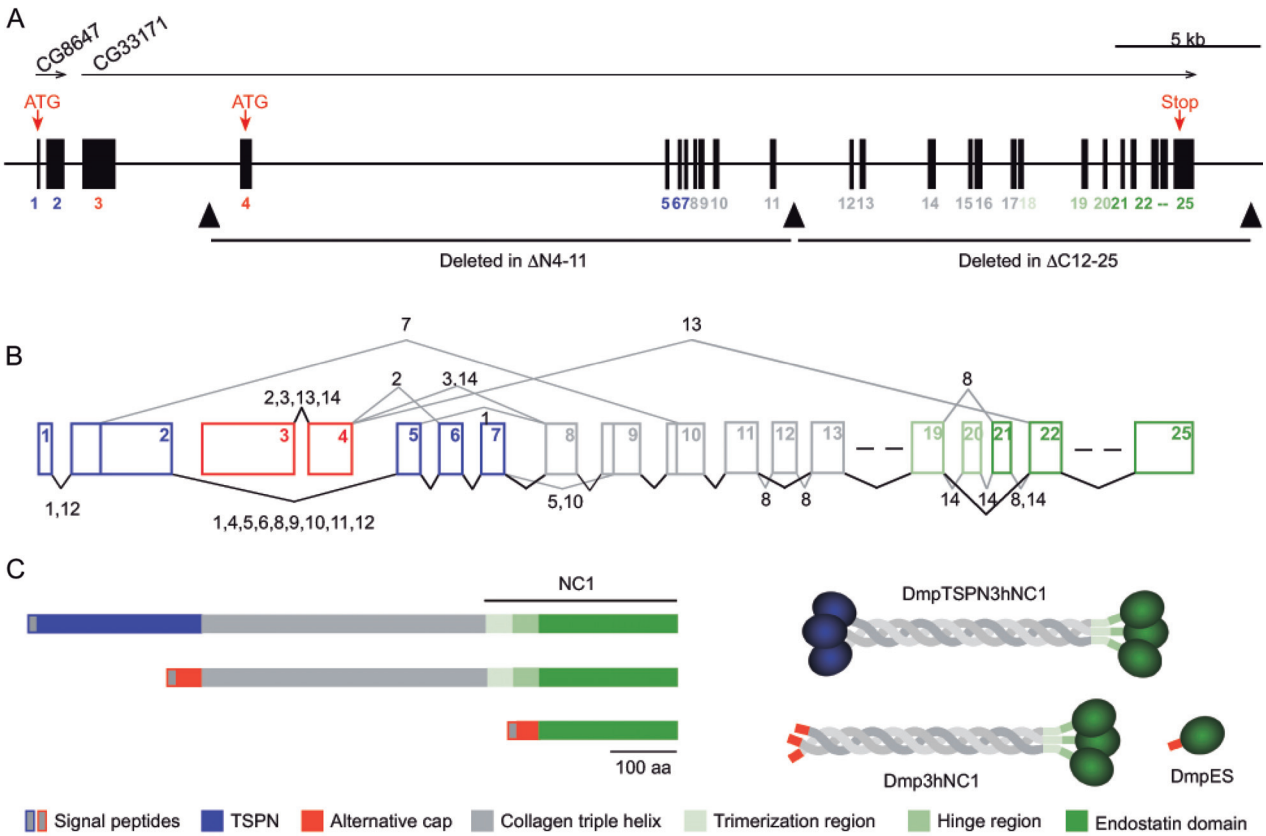

Fig. 1. Dmp gene, transcript and protein structures. Colour codes refer to protein domains as depicted in (C) and their respective coding sequences. (A) Genomic structure of the *dmp* gene. Exons are numbered in colours according to (B) and (C). Open reading frames of *CG8647* and *CG33171* are indicated as currently annotated in FlyBase. Triangles refer to PiggyBac insertion sites; they were used to generate *dmp* deletion alleles as indicated. (B) Summary of splicing patterns observed from 14 different transcripts that were fully or partly sequenced. Within these 14 transcripts, eight different splice variants occur, some of which are varied only by the in- or exclusion of very short exons. Exons are numbered as in (A). Sequences of transcripts 1–13 have been submitted to GenBank (Accession nos. EU523228-EU523240). Transcript 14 represents the RH14382 cDNA clone from BDGP. For a detailed description of the alternative splicing events, refer to Supplement 1. (C) Domain structure of the three major protein isoforms produced from the *dmp* locus. Left: Primary structures drawn to scale. Right: Schematic quartenary structures. The longest isoform DmpTSPN3hNC1 contains a domain with similarity to the N-terminal domain of thrombospondin (TSPN), which is absent from the middle isoform Dmp3hNC1. The shortest isoform DmpES is a single monomeric ES domain.

elements inserted within the *dmp* locus, as described by Parks *et al*. (2004). This method includes crossing together two different FLP recombination target (FRT)-bearing P-element or piggyBac insertion lines and a heat shock inducible FLP recombinase. Larvae were heat shocked at 37°C for 1 h daily on five consecutive days. As a result, it was possible to recover chromosomes where a recombination has taken place between the two FRT-bearing insertions, thus containing a deletion as well as a residual P-element or piggyBac insertion. For the $dmp^{\Delta N4-11}$ strain, PBac{WH}CG33171^{f07253} and PBac{WH}CG33171^{f03008} were recombined, while PBac{WH}CG33171^{f03008} and PBac{PB}c06608a were recombined for the $dmp^{\Delta C12-25}$ strain. PiggyBac insertion lines used were generated by Thibault *et al*. (2004) and obtained from Bloomington Drosophila Stock Center (PBac{WH}CG33171^{f07253}, http://flystocks.bio.indiana.edu/) and from the Exelixis collection at Harvard (PBac{WH}CG33171^{f03008} and PBac{PB}c06608a, http://drosophila.med.harvard.edu/). Successful deletions were identified by PCR screening for the correct intersections between piggyBac element and genomic DNA, as well as by carrying out long-range PCRs spanning the whole residing piggyBac element. Note that we successfully used piggyBac elements of the PB type, which were not used in the work published by Parks *et al*. (2004).

For overexpression constructs, respective *dmp* fragments were PCR-amplified from GH14382 and cloned into pUAST (Brand and Perrimon 1993). In this vector,

coding sequences were placed under the control of the so-called upstream activating sequence (UAS), so that *in vivo* their expression could be controlled by the Gal4 transcriptional activator binding to its UAS target site. The construct of the middle isoform Dmp3hNC1 contained the endogenous extracellular localization signal, while for the NC1 and ES constructs the signal sequence of wingless (Zecca *et al*. 1996) was PCR-amplified with primers introducing EcoRI restriction sites. These were then used to clone the signal sequence to the 5′ end of NC1 and ES coding sequences, to which an EcoRI site had also been introduced by using respective PCR primers. Transgenic lines were generated by construct injection into w^{1118} fertilized eggs using standard methods.

Wild-type flies used in all experiments were w^{1118}, which were also the background used for generating the rescue lines. The Gal4 driver line used for overexpressing the different Dmp fragments was 24B-Gal4 (Brand and Perrimon 1993; Fyrberg *et al*. 1997). Rescue crosses were carried out by crossing stocks of 24B-Gal4/24BGal4; $dmp^{\Delta C12-25}/dmp^{\Delta C12-25}$ genotypes to UAS-x/UAS-x; $dmp^{\Delta C12-25}/dmp^{\Delta C12-25}$ flies.

Immunohistochemistry and embryo staging

The nervous system of late embryos was stained as described (Meyer and Aberle 2006) using a murine fasciclinII (FasII) antibody (1D4, DSHB). Embryos were dissected on microscope slides and imaged with an LSM510 confocal microscope (Zeiss) using the Cy3- and DIC channels. Signals from the Cy3 channel were converted to black to enhance their contrast in overlays with DIC images.

Embryos for dissection (stage 16/17) were selected based on the FasII signal under a UV light dissection scope. Since the ventral nerve cord (VNC) contracts during development, the maturity of the nervous system can be inferred from VNC length. As a second step, each resulting embryo filet was only included into statistical analysis if in some of its segments the ISNb had already invaded the ventral muscle field, making sure that the developmental time point for the ISNb steering decision was already past.

Quantification of axon guidance phenotypes and statistical analysis

Innervation phenotypes were quantified in abdominal segments A2–A7 of dissected FasII-stained embryos. Upon phenotypic evaluation, genotypic identity of all embryos was masked to avoid bias.

Statistical significance of error rate differences between different lines was evaluated using a χ^2 test for independence or Fisher's exact test. Fisher's exact test is designed to deal with rare events. Comparisons between genotypes were carried out pairwise, one partner of the pair being the wild type or $dmp^{\Delta C12-25}$, depending on the phenotype of the pair's second partner: A mutant phenotype was compared to the wild type, while a rescue phenotype was compared to $dmp^{\Delta C12-25}$. Theoretically expected frequencies of correct and defective hemisegments were calculated using a contingency table. Values used were the absolute numbers of correct and defective hemisegments observed for each genotype and nerve. If any expectancy value in the table was below 10, Fisher's exact test was applied, which complies with the more rigorous of statistic standards (Becker and Genschel 2005; Bortz 2005). This was the case for most data presented here, exceptions being Figure 4(D) and all genotypes of Figure 5(A) except for 24B-Gal4xUAS-ES; $dmp^{\Delta C12-25}$. Here, all expectancy values were above 10 and therefore the χ^2 test for independence was used. *p*-values were calculated by JUMBO (Java-using Münster Biometry Online-System, http://imib.uni-muenster.de/fileadmin/template/conf/imib/lehre/skripte/biomathe/jumbo.html) using Java-Applet '4.8 Vierfeldertafel'.

Results

CG8647 *and* CG33171 *are one gene from which various isoforms of Dmp are expressed*

CG33171 is one of only three conserved collagen genes annotated in the *Drosophila* genome and the only one that encodes an endostatin domain. The ES domain is positioned at the protein's C-terminus and qualifies it as a multiplexin. But in contrast to vertebrate and *C. elegans* multiplexin genes (Kivirikko *et al*. 1994; Muragaki *et al*. 1994; Muragaki *et al*. 1995; Rehn and Pihlajaniemi 1995; Ackley *et al*. 2001), *CG33171* lacks the coding sequence for any N-terminal globular domain. This annotation is supported by 14 BDGP cDNA clones, one of which is full-length, and three more of which confirm this N-terminus. *CG8647* is predicted as the next gene upstream of *CG33171*, and its two exons encode a moiety related to the N-terminal domain of thrombospondin (TSPN), as found at the N-terminus of vertebrate and *C. elegans* multiplexins. This suggests that the two annotated genes *CG8647* and *CG33171* really are only one gene from which several different transcripts are produced, including a fusion transcript of the two predicted loci. Indeed, we were able to amplify respective cDNAs from the pooled stage 1–17 wild-type embryos and found that a variety of alternative transcripts are produced from *CG8647* and *CG33171*, which we now refer to as the *Drosophila* multiplexin (*dmp*) gene.

We found transcripts having the two exons of *CG8647*, now referred to as exons 1 and 2 of *dmp*, as their 5′

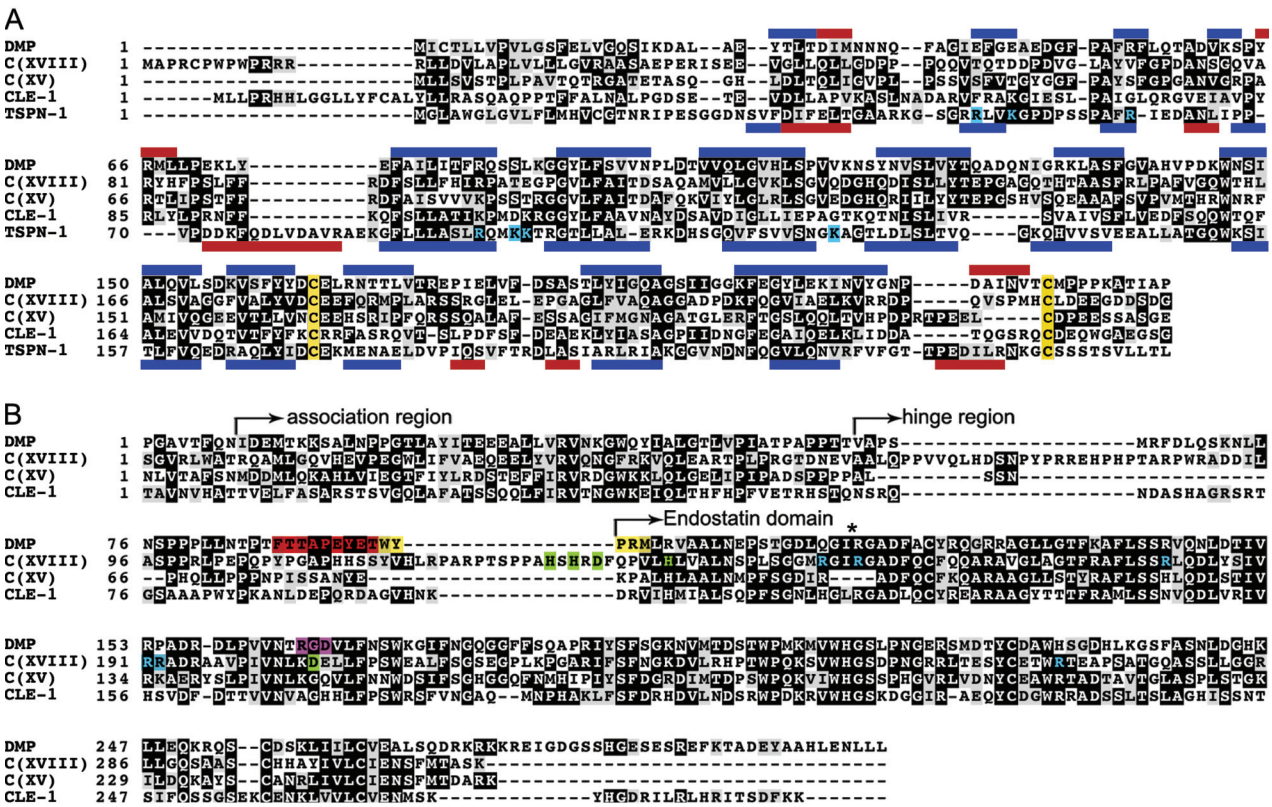

Fig. 2. Protein sequence alignment of Dmp domains and their *C. elegans* and human homologues. (A) TSPN domains of Dmp, human collagen XVIII and XV, *C. elegans* Cle-1, and human thrombospondin-1. Sequence identity on the amino acid level is low (around 20–25%). However, according to HHpred structure prediction, Dmp-TSPN has the same topology as reported for TSPN-1 (Tan *et al*. 2006). Here, Dmp-TSPN and TSPN-1 β-sheets (dark blue) and α-helices (red) as described by these two sources are indicated above and below the two sequences. Yellow: Two cysteine residues that stabilize the typical TSPN fold by forming a disulphide bond are conserved. Light blue: Basic residues that contribute to the major heparin binding site in TSPN-1 (Tan *et al*. 2006) are not conserved. (B) C-terminal NC1 domain of Dmp, human collagen XVIII and XV, and *C. elegans* Cle-1. Within the ES domain, identity between fly and human sequences is around 50%. *: 4-residue-loop that distinguishes collagen XV and XVIII. Light blue: Arginine residues that make important contributions to heparin binding in collagen XVIII (Sasaki *et al*. 1999). Green: zinc coordination residues (Sasaki *et al*. 2000). Purple: Putative integrin-binding RGD motif. Red and yellow: residues encoded by alternative exons 20 and 21 (see Fig. 1). They are omitted in the majority of transcripts we recovered, and their sequence provides no cue about their function.

ends, which then skip the first two exons of *CG33171* (now exons 3 and 4 of *dmp*), as well as transcripts beginning with exons 3 and 4 (see Figure 1A,B). Hence, one of the alternative transcripts will produce a protein carrying a TSPN domain at its N-terminus, the other will result in a multiplexin molecule starting with the collagen triple helix domain; we call the two DmpTSPN3hNC1 and Dmp3hNC1, respectively (see Fig. 1C).

We also detected one alternative transcript where exon 4 is directly joined to the first exon encoding the C-terminal endostatin domain. So the protein product of this transcript will be a single globular ES domain (Fig. 1C), which is a multiplexin isoform that has not been described previously. We refer to it as DmpES.

We additionally found a number of splicing variations that affect only short sequence stretches (see Fig. 1B). In summary, the alternative splicing events we observed fall into three classes: There are two alternative 5′ ends, each of which is made of two exons, there are seven exons (exons 5, 6, 7, 8, 12, 20, and 21) that individually participate in cassette-type alternative splicing, and there are three alternative 5′- or 3′ splice sites, within exons 2, 9, and 10.

Drosophila *Dmp shares characteristic features with both vertebrate collagen XV and XVIII*

Sequence alignment illustrates the relatively distant relatedness between TSPN domains of the different multiplexins and the N-terminal domain of human TSP-1 (TSPN-1) on the primary structure level (Fig. 2A). Sequence identity is around 25% between multiplexin TSPN

sequence stretches, depending on the alignment program used. Identity between multiplexin TSPN domains and TSPN-1 is well below 20%, but secondary structure prediction using the homology detection tool HHpred (Soding *et al*. 2005) suggests Dmp TSPN adopts the same structure as shown for TSPN-1 (Tan *et al*. 2006), as the prediction shows the 13 beta strands that form the beta sandwich structure of human TSPN-1. The two cysteine residues that form an intradomain disulfide bond are also conserved, while the arginine and lysine residues involved in heparin binding in TSPN-1 (Tan *et al*. 2006) are only partially conserved (Fig. 2A).

There are further alternative N-terminal domains found in nematode and vertebrate collagen XVIII. In *Drosophila*, the next predicted gene upstream of *dmp* encodes the transcription factor Biniou, and the intergenic sequence stretch of 17.8kb has been subjected to extensive use of gene prediction programs and BLAST searching. No additional putative exons could be identified. We therefore expect that the TSPN domain is the only N-terminal globular domain occurring in Dmp. This is a feature that the *Drosophila* multiplexin shares with vertebrate collagen XV (Kivirikko *et al*. 1994; Muragaki *et al*. 1994).

For the C-terminal NC1 domains of type XV and XVIII collagens of different organisms, homology is much higher already on sequence level (Fig. 2B). The *Drosophila* ES domain is 52% and 49% identical to that of human collagen XV and XVIII in a conserved core region of 164 residues, respectively. Of the two vertebrate multiplexins, only collagen XVIII carries the N-terminal Zn^{2+} coordination motif, and collagen XVIII also possesses a longer hinge region compared to collagen XV, as well as a four-residue loop that is thought to be important for heparin binding (Sasaki *et al*. 1999). Sequence alignment with the *Drosophila* and *C. elegans* homologues shows that for the first two features, both of the fly and worm multiplexins are more similar to vertebrate collagen XV. However, both the fly and worm multiplexins also possess the four-residue loop within the ES domain. Hence, the single multiplexin gene present in the fly genome exhibits characteristic features of both of the two vertebrate multiplexin types, and we therefore refrain from categorizing it as any of the two, but continue to refer to it as *Drosophila* multiplexin (Dmp).

Multiplexins are qualified as collagens by a region of triple helix repeats that is interrupted several times by a non-triple helix sequence. In Dmp this region spans about 290 amino acids and is thus considerably shorter than in human collagen XV and XVIII, where it extends over 570 and 690 amino acids, respectively. In contrast, the two type IV structural collagens of *Drosophila* possess triple helix regions of 1900 and 1560 amino acids. So the structural domain of Dmp is small both in relation to the rest of the molecule and to the same domain in other molecules, and this suggests that Dmp does not play an important role as a structural molecule.

Collagen XVIII has been shown to be a heparan sulfate proteoglycan (Halfter *et al*. 1998), while collagen XV is modified with chondroitin sulfate side chains (Li *et al*. 2000). Both types of modification occur via a Ser-Gly consensus sequence (Whitelock and Iozzo 2005) with acidic residues nearby, and a couple of such motifs are present in the Dmp core protein. The first of them is situated in the last part of the TSPN domain, encoded by one of the variably spliced exons. Additional putative attachment sites are present in the remainder of the molecule, with one of them being situated within the ES domain, giving ample potential for posttranslational glycosylation.

Transcription of dmp *begins in late stages of embryonic development*

We carried out *in situ* hybridization experiments using antisense probes for different characteristic regions of *dmp* transcripts in order to shed light on the different gene products' possible spatial and temporal requirement during development.

Using a probe against the region encoding the TSPN domain of the DmpTSPN3hNC1 isoform produces weak signals at embryonic stage 16 from head skeleton, filzkörper, dorsal vessel, and central nervous system (CNS) (Fig. 3A). All earlier embryonic stages do not show any TSPN expression. However, the TSPN probe yields a very weak signal, possibly reflecting a low expression level of the TSPN domain. In a ventral view of a stage 16 embryo, a symmetric, dotted and segmentally repeated pattern within the ventral region of the VNC is discernible (Fig. 3B), where each dot presumably corresponds to an individual cell. The identity of these cells is unknown.

The expression of the 5′-UTR of the non-globular N-terminus of Dmp3hNC1 and DmpES, encoded by exon 3, has a tissue distribution similar to that seen for TSPN, (Fig. 3C), but the signal is considerably stronger. Expression onset is during stage 16 as well. In contrast to the TSPN probe, there is a detectable expression in the CNS of late stage 17 embryos and early larvae (Fig. 3F). In these stages, the cell-wise expression of stage 16 VNCs (Fig. 3D) is lost, and the remaining signal has its main focus in the dorsal VNC, where the neuropil is located. Expression in the dorsal vessel is strongest within its posterior part, also referred to as the heart. In strongly stained embryos, there is also an expression in the aorta, reaching as far anterior as segment A2 (Fig. 3E,L). Dorsal vessel expression occurs in an interrupted, segmented fashion, so it seems that only a subset of cardioblasts produces Dmp.

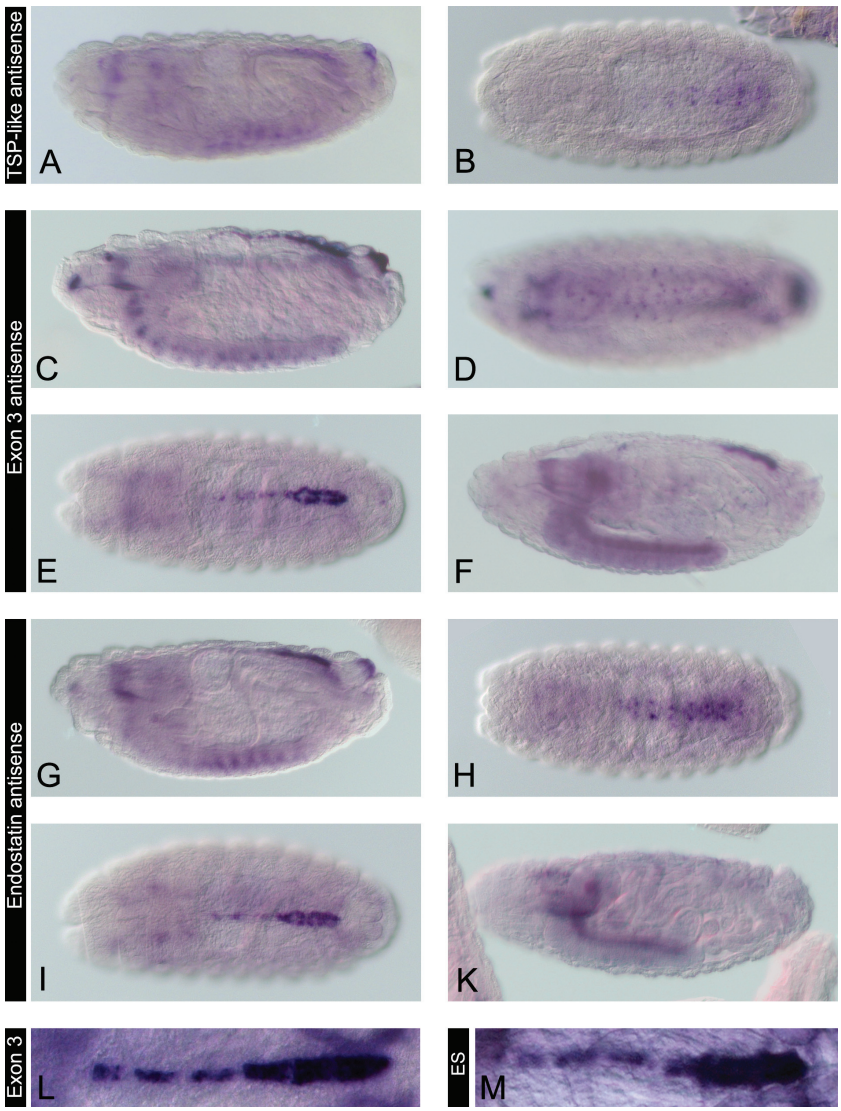

Fig. 3. mRNA expression patterns from different regions of *dmp*. All embryos are stage 16, except for (F) and (K) that are early (F) and late (K) 17. (A, B) TSPN-like region antisense probe, (C-F, L) exon 3 antisense probe, (G-K, M) endostatin antisense probe. With all probes, we detected expression in head skeleton, filzkörper, dorsal vessel, and CNS beginning at stage 16 (A, C, G). All tested regions of the gene were expressed in single cells of unknown identity within the VNC (B, D, H). Dorsal vessel expression for the TSPN-like region was very weak, whereas for exon 3 and the ES region, strong signals of a segmentally interrupted fashion were detected for the heart and the aorta (E, I, L, M). CNS expression persisted into stage 17, but the cell-wise pattern observed at stage 16 was lost (F, K). Note that ISNb invasion of the ventral muscle field as well as ISN dorsal development occurs throughout embryonic stage 16, i. e. before the onset of strong expression inside the CNS. In the mutant, we did not observe any strong heart or CNS defects in spite of the gene's strong expression in these two tissues.

Using an ES antisense probe yields an equally strong signal as the exon 3 probe, and from the same tissues as the two 5′ probes: the dorsal vessel, the central nervous system, the head skeleton, and the filzkörper starting at stage 16 (Fig. 3G–I) and lasting until the end of embryogenesis. During stages 16 and 17, expression occurs in the whole central nervous system, and with similar expression peaks in single cells of the VNC as the TSPN and exon 3 region (Fig. 3G,H). Like with the exon 3 probe, ES expression in the CNS persists into early larval stages, but loses its single-cell pattern. Instead, CNS expression is strongest within the neuropil region (Fig. 3K). Also the segmented staining pattern from the dorsal vessel is identical to that observed with the exon 3 probe (Fig. 3I,M). These results indicate that there is no tissue-specific usage of the different Dmp isoforms.

Dmp *partial deletion mutants are homozygous viable and the* dmp$^{\Delta N4-11}$ *deletion does not abolish NC1 transcription and processing*

Wanting to investigate the contribution of Dmp to *Drosophila* development in general and specifically to motor axon pathfinding, we generated two strains that carry partial deletions of the *dmp* gene by making use of FLP recombinase-induced recombination between FRT sites present in piggyBac transposons, as described by Parks *et al*. (2004). In the first strain, *dmp*$^{\Delta N4-11}$, 21.26 kbp of genomic DNA were removed, that encode the second alternative start codon and 759 bp of the triple helix repeat region (exons 4 to 11, see Fig. 1A). The second strain, *dmp*$^{\Delta C12-25}$, lacks a genomic stretch of 19.89 kbp, including the whole coding sequence for NC1 (exons 12 to 25, see Fig. 1A).

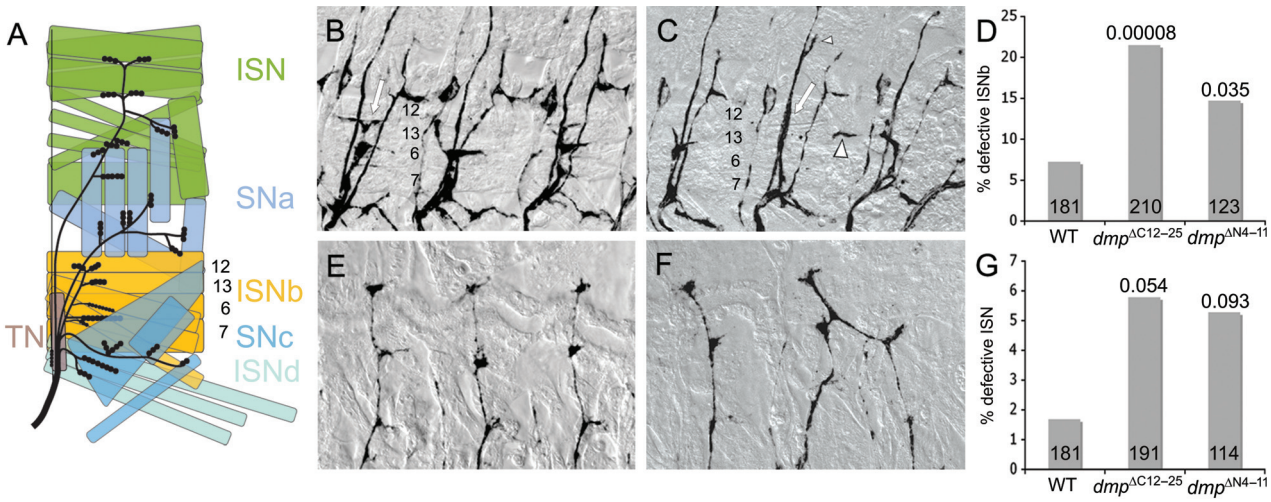

Fig. 4. Motor axon guidance phenotypes caused by deleting the parts of the anterior ($dmp^{\Delta N4-11}$) or the posterior ($dmp^{\Delta C12-25}$) region of the *dmp* gene locus. (A) Schematic of the larval hemisegmental set of muscles and the five motor nerves that innervate them. The target muscle fields of the five different nerves are depicted in different colours and the names of the respective nerves are given on the right. Phenotypes studied in this work concern the ISNb, that innervates one of the three ventral muscle fields (yellow) and the ISN, innervating the dorsalmost muscle field (green). (B–D) ISNb wild type and deletion phenotypes. (B) Ventral region of two wild type hemisegments, displaying the characteristic nervous structures that innervate muscles 12, 13, 6 and 7, formed by the ISNb (arrow in left hemisegment). (C) Ventral region of three $dmp^{\Delta C12-25}$ hemisegments. In the left hemisegment, the ISNb behaves similar to wild type. In the middle segment, it braches off the ISN at the ventral choice point, but instead of invading the ventral muscle field, it steers back to the ISN and fuses with it for part of its length (arrow), but detaches again later (small arrowhead). In the right hemisegment, the ISNb also detaches from the other nerves at the ventral choice point, but then steers to the anterior, even crossing the segment boundary and invading the anterior segment (large arrowhead). This may be an attempt to substitute for the missing ventral innervation in the anterior segment. (E–G) ISN wild type and deletion phenotypes. (E) Dorsal region of three wild type hemisegments and (F) dorsal region of three $dmp^{\Delta C12-25}$ hemisegments. In contrast to wild type, mutant ISN nerves bifurcate and cross segment boundaries. (D, G) Statistical evaluation of the incidence of ISNb (D) and ISN (G) guidance mistakes in wild type, $dmp^{\Delta C12-25}$, and $dmp^{\Delta N4-11}$. Deletion of the 3' portion of the *dmp* gene, encoding the NC1 region, leads to a significant increase in ISNb error frequency, while deletion of the 5' region, starting with exon 4, leads to a less penetrant phenotype. These tendencies are identical for the ISN, although statistical significance is on a lower level, due to the lower absolute error number. Absolute numbers of hemisegments evaluated are given at the base of each bar. Figures above the bars are *p*-values calculated by the χ^2 test for independence for (D) and by Fisher's exact test for (G).

We found that both deletions are homozygous viable, causing no obvious defects apart from a general developmental retardation of homozygous mutant animals compared with their heterozygous siblings, since homozygous adults start eclosing several days later than their balancer-bearing siblings, but then appear at the expected ratio. So in spite of the strong expression of Dmp by cardioblasts, it is not vital for a functional heart. Nonetheless, it is possible that a lack of Dmp affects its morphogenesis or has other functional consequences for the dorsal vessel. Likewise, in spite of the *dmp* expression inside the CNS, we did not observe any malformation of the CNS in *dmp* mutants, neither in conventional light microscopy nor when using the FasII marker (see below) that labels peripheral motoneurons as well as six characteristic longitudinal fascicles inside the CNS.

We detected some residual transcription of the ES domain from the $dmp^{\Delta N4-11}$ allele (see Supplement 2) and consequently, only $dmp^{\Delta C12-25}$, but not $dmp^{\Delta N4-11}$, can be considered as a functional null mutant with respect to the protein's C-terminus.

Deletion of different regions of the dmp *gene causes axon guidance errors in ISNb and ISN nerve tracts*

We then turned to a close examination of motor axon guidance accuracy in *dmp* mutants. Each of the abdominal hemisegments A2 to A7 of the *Drosophila* larva contains 30 different, individually identifiable muscles, which are innervated by five different nerves (Fig. 4A) that are FasII-positive. Branching sites of these nerves and the resulting innervation patterns are stereotypically reproduced in each wild type abdominal hemisegment. A ventral bypass phenotype can affect the ISNb as well as the other two nerves that innervate the ventral muscle field, the SNc and the ISNd. In these cases the affected nerves fail to detach from the main nerve tract and to invade the ventral muscle field. Instead, they continue

to travel dorsally together with the main nerve tract, with the distance travelled varying between segments. Several molecules have already been recognized for the regulation of this process, and many of the molecules influencing ISNb guidance also affect pathfinding of other motor nerves, reflecting the complex interplay between different guidance cues and their differential effects on different cells. These include fasciclinII (FasII), Integrins, the Leukocyte antigen related (LAR) family of receptor protein tyrosine phosphatases (RPTPs), and the extracellular protease Tlr1 and matrix metalloproteases (Lin and Goodman 1994; Lin *et al*. 1994; Desai *et al*. 1997; Hoang and Chiba 1998; Sun *et al*. 2001; Meyer and Aberle 2006; Miller *et al*. 2008).

We analyzed stage 16 and 17 embryos of both *dmp* deletion strains, that were FasII-stained and fileted. Our quantitative mutant analysis was focused on one of the nerves innervating part of the ventral muscle region, the ISNb, and the nerve leading to the dorsalmost muscles, the ISN. All quantifications were carried out blindfolded with respect to the genotypic identity of each sample, and by a single person. The other nerves, the SNa, SNc and ISNd did not show any phenotype that could be reliably distinguished from wild type. To the eye it appeared that in $dmp^{\Delta C12-25}$ mutants the third, most anterior SNa branch sometimes gave a stronger FasII signal than in wild type, where it was hardly visible in the embryo. This trait, however, could not be evaluated in quantitative terms.

Both the ISNb and the ISN showed an increased rate of guidance errors in homozygous mutants of both deletion strains. In the C-terminal deletion $dmp^{\Delta C12-25}$, ISNb pathfinding errors, leading to a lack of innervation of the ventral muscle field, were found in 21.4% of all examined hemisegments ($n = 210$, derived from 41 embryo filets). In a wild type genetic background, similar ISNb errors were observed at a rate of around 7.1% ($n^{segment} = 181$, $n^{embryo} = 30$, Fig. 4D), which is in accordance with rates described in other studies (Meyer and Aberle 2006; Yu *et al*. 2000; Miller *et al*. 2008). A χ^2 test for independence qualifies this difference as clearly statistically significant ($p = 0.00008$). Hence, Dmp does play a role in ensuring motor axon guidance quality. For $dmp^{\Delta N4-11}$, we observed an error rate of 14.6% ($n^{segment} = 123$, $n^{embryo} = 22$, $p = 0.035$), so the removal of one of the alternative N-termini from the gene and the at least reduced dosage of the protein's C-terminal NC1 domain impair axon guidance accuracy, but less strongly than the complete loss of the endostatin region. In both deletion strains, ISNb pathfinding errors are of the same quality. They include full ISNb bypass relative to the ventral muscle field that it is due to innervate, so that, instead of steering off into the ventral muscle field, an additional nerve tract can be seen travelling along the ISN (Fig. 4C, middle segment), or the disposition of the ISNb axon bundle remains entirely obscure. A partial bypass behavior has also been observed, where very faint FasII-positive structures have left the main nerve tract and adhered to muscle surfaces within the ventral muscle field immediately adjacent to the ISN. In this case, it seems that the ISNb fails to branch off the main nerve tract, but individual axon tips still follow a guiding mechanism towards the muscle field. Another type of guidance error is an overgrowth of the ISNb or parts of it towards the transversal nerve (TN) of either the adjacent anterior or posterior hemisegment, sometimes including intrusion into an adjacent hemisegment (Fig. 4C, right segment) and/or fusion of the ISNb to the TN.

For the ISN, similar tendencies were observed as for the ISNb. In both deletion strains, the ISN error rate is about threefold higher than in the wild type: 5.8% in $dmp^{\Delta C12-25}$ (with $n^{segment} = 191$, $n^{embryo} = 40$) and 5.3% in $dmp^{\Delta N4-11}$ (with $n^{segment} = 114$, $n^{embryo} = 22$), compared with 1.7% ($n^{segment} = 181$, $n^{embryo} = 30$, see Fig. 4G). For rare events, for example, those found in all experiments relating to the ISN, Fisher's exact test was used for assessing probabilities (see Materials and methods). This results in $p = 0.054$ for $dmp^{\Delta C12-25}$. This formally means that the observed differences of ISN phenotypes between wild type and $dmp^{\Delta C12-25}$ are not significant, but note that statistical significance is hard to achieve in this context due to the low absolute number of ISN errors, and a p-value of 0.054 is sufficiently small to let true differences between the genotypes seem possible. One of the ISN pathfinding mistakes we observed is its intrusion into an adjacent segment, leading to a fusion of ISN neighbors (Fig. 4F). This can result either from a premature deviation of the ISN from its route, or occur together with an ISN overgrowth, where the respective axonal growth cone(s) do not stop at the dorsalmost site of synapse formation, but continue growing perpendicular to the previous direction. We also observed bifurcation events of single ISNs, with either both new branches remaining in their original segment or the branches invading the neighboring segments. Taken together, the results from the two deletion strains strongly suggest a functional role for Dmp in ensuring motor axon guidance accuracy, and point at a specific relevance of the molecule's C-terminal NC1 domain in the process.

Different rescue activities on the $dmp^{\Delta C12-25}$ *guidance phenotype are exerted by different Dmp fragments*

In vertebrate tissue culture it has been shown that monomeric and oligomeric (as produced by natural trimerization of NC1 domains) ES has converse effects on migratory behavior of endothelial and other cells, with oligomeric ES activating migration and monomeric ES

having no impact (Kuo *et al*. 2001). Similarly, only NC1 constructs were able to restore defective migratory behavior of mechanosensory neurons in *C. elegans* (Ackley *et al*. 2001). We therefore wanted to test the effect of different Dmp fragments on motoaxon pathfinding in wild type and in our $dmp^{\Delta C12-25}$ mutant.

The *dmp* gene is highly expressed in the mesodermal heart and in some yet unidentified cells within the VNC at the end of mid-embryogenesis. The driver line 24B-Gal4 (Brand and Perrimon 1993; Fyrberg *et al*. 1997) produces an expression pattern that is partially similar to that of *dmp*, as it drives expression in somatic mesoderm, heart and some cells within the VNC (see Supplement 3).

The basement membrane is a continuous ECM covering all organs of the embryo and has been shown to be formed by non-cell-autonomous distribution of ECM components. For example, the classic basement membrane component Collagen IV is expressed by hemocytes and fat body in *Drosophila* embryos (Mirre *et al*. 1992; Yasothornsrikul *et al*. 1997), but in spite of this is present in the basement membranes of all tissues, including muscles and nerves (Fessler and Fessler 1989). Mirre *et al*. (1992) show that Collagen IV protein is present inside the VNC. A good example of non-cell-autonomous action in motoaxon guidance is Tlr1, an extracellular protease, mutants of which exhibit a motoaxon pathfinding phenotype similar to that of Dmp. In *tlr1* mutants, pathfinding defects can be rescued using Gal4 driver lines of various different tissue specificities, clearly indicating non-cell-autonomous action (Meyer and Aberle 2006). Therefore, we believed that a perfect match between endogenous *dmp* expression and Gal4 used to express transgenic Dmp is unlikely to be necessary for rescue, and hence did not hesitate to use 24B-Gal4 for the rescue crosses.

We produced UAS lines for overexpressing the endostatin domain (UAS-ES), NC1 domain (UAS-NC1) and Dmp3hNC1 (UAS-3hNC1) and assessing their potential rescue effect on the $dmp^{\Delta C12-25}$ motor axon guidance phenotype. Upon systematic quantitative evaluation, we found a reduction of ISNb guidance inaccuracies to wild type level when overexpressing UAS-3hNC1 ($n^{segment}$ = 79, n^{embryo} = 15, $p(dmp^{\Delta C12-25})$ = 0.0003) or UAS-ES ($n^{segment}$ = 291, n^{embryo} = 43, $p(dmp^{\Delta C12-25}) < 0.00001$). By contrast, overexpression of UAS-NC1, that is expected to create ES trimers, had no effect on the $dmp^{\Delta C12-25}$ phenotype ($n^{segment}$ = 67, n^{embryo} = 13, p = 0.002, Fig. 5A). So in this context, the monomeric version of ES is the active compound in conferring correct guidance instructions to axonal growth cones, whereas the NC1 version is inactive. This opens up the possibility that this active compound can be proteolytically generated from the Dmp3hNC1 molecule, but not from the UAS-NC1 product, that lacks the triple helix region.

In contrast to the ISNb, UAS-3hNC1 did not alter ISN error frequency (Fig. 5C), whereas both nerves experienced an error rate reduction to the wild type level by UAS-ES (for ISN: p = 0.045). This suggests that different fragments or isoforms of Dmp act through different mechanisms in ventral and dorsal regions of the embryo.

Different effects on wild type embryos are exerted by different Dmp fragments

We used the same UAS lines and the 24B-Gal4 driver line to overexpress the different Dmp fragments in a wild type background. Overexpression of UAS-3hNC1 did not have a significant impact on motoaxonal pathfinding, neither for the ISNb nor for the ISN nerve (Fig. 5B,D). Conversely, overexpression of the NC1 domain in wild type background reduced the number of ISNb pathfinding errors from 7.2% in wild type ($n^{segment}$ = 181, n^{embryo} = 30), that is typically observed in wild type (Yu *et al*. 2000; Meyer and Aberle 2006; Miller *et al*. 2008) to an extremely low error rate of 0.75% ($n^{segment}$ = 134, n^{embryo} = 19) that is significantly different from that in wild type (p = 0.005, Fig. 5B). For the ISN, a low error rate was found as well, but since ISN guidance mistakes are rare in wild type as well, there is no significance in this figure. For overexpression of the ES domain alone we found an impairment of ISNb and ISN pathfinding, and the resulting error rates we recovered are 14.6% ($n^{segment}$ = 88, n^{embryo} = 12) and 11.5% ($n^{segment}$ = 78, n^{embryo} = 11), respectively (p = 0.12 and 0.0012, Fig. 5B,D). These figures, however, do not reflect the full impact of ES overexpression on embryonic development, as a high proportion of individuals of this genotype showed a generally defective body morphology. It was the healthier fraction that was used for dissection and assessment of axon pathfinding, which is thus not representative of the genotype as a whole. Defective embryos possessed strands of FasII-positive cells that did not at all resemble a functional nervous system. Other embryos showed a recognizable, but disordered nervous system and a somewhat deformed general morphology (see Supplement 4). But on any account, it has become clear that a monomeric ES domain has a disadvantageous impact on axonal pathfinding, in contrast to trimeric ES, which is actually enhancing guidance accuracy.

Discussion

Axonal pathfinding is a complex process depending on the balance of various attractive and repulsive guidance cues that act on an individual growth cone. The C-terminal domains of vertebrate multiplexins have received ample attention as activators and inhibitors of endothelial and epithelial cell migration, and some evidence also

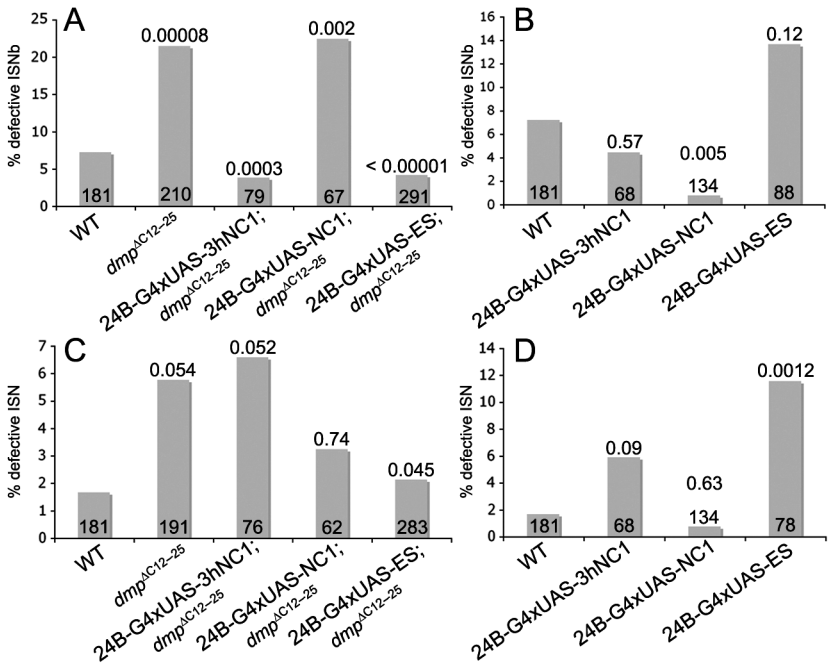

Fig. 5. Overexpression effects of different Dmp fragments in *dmp*$^{\Delta C12–25}$ and wild type background. (A, B) Effect on ISNb guidance accuracy in mutant (A) and wild type (B) background. A rescue effect of the mutant phenotype is evident for the longest construct UAS-3hNC1 and for the ES domain alone. With UAS-NC1, there is no rescue activity, since the error rate is still significantly different from that in wild type. In a wild type background, UAS-NC1 significantly reduces the wild type error rate. UAS-ES has a disruptive effect on the general morphology of some embryos which get not fully reflected by motor nerve error statistics (see text and supplementary data). (C, D) Effect on ISN guidance accuracy in mutant (C) and wild type (D) background. In contrast to the ISNb, UAS-3hNC1 does not exert a rescue effect on the ISN deletion phenotype. In contrast, the error rate reduction observed in the 24BxUAS-ES; *dmp*$^{\Delta C12–25}$ genotype statistically significant ($p = 0.045$). In wild type background, there is a clear disruptive effect of UAS-ES on the ISN (see above and text). At the base of each column, absolute numbers of hemisegments evaluated are given; figures above columns indicate p-values. The χ^2 test for independence was applied to all genotypes in (A) except for 24B-Gal4xUAS-ES;*dmp*$^{\Delta C12–25}$. Here, and to all data represented in (B), (C), and (D), Fisher's exact test was applied.

exists for a role of multiplexins as modulators of neuronal migratory behavior (Ackley *et al*. 2001; Kliemann *et al*. 2003; Schneider and Granato 2006). Multiplexins are multidomain proteins, containing an N-terminal domain with homology to the N-terminal domain of thrombospondin (TSPN), an interrupted collagen triple helix domain and a C-terminal non-collagenous domain (NC1), that subdivides into a trimerization region, a protease-sensitive hinge region and a globular endostatin (ES) domain. One of the two vertebrate multiplexins, collagen XVIII, and *C. elegans* collagen XVIII occur in three different isoforms that can contain further N-terminal domains (Muragaki *et al*. 1995; Rehn and Pihlajaniemi 1995; Ackley *et al*. 2001). We found that the *Drosophila melanogaster* multiplexin (Dmp) is encoded by a complex locus, comprising *CG8647* and *CG33171*, that encodes a TSPN domain (Tan *et al*. 2006), but no further N-terminal moieties.

We have generated two deletions within the *dmp* gene, and both deletion strains show pathfinding deficiencies of the same quality. ISNb growth cones fail to detach from the main nerve tract and steer into the ventral muscle field but continue to grow on dorsally. Additionally, ISNb as well as ISN nerves sometimes disrespect segment boundaries and fuse to nerves of adjacent segments. The two deletion strains differ by the incidence of pathfinding errors, as *dmp*$^{\Delta C12–25}$, lacking the larger part of the gene, including part of the triple helix repeat region and the NC1-encoding region, shows greater penetrance than *dmp*$^{\Delta N4–11}$, where the second alternative N-terminus and the following triple helical repeat regions are missing. We have shown that *dmp*$^{\Delta N4–11}$ is not likely to be a null mutation since there is wild type-like transcript present from the NC1-encoding region of the gene. This situation suggests that a low dosage of a truncated Dmp version leads to an improved phenotype compared with *dmp*$^{\Delta C12–25}$. However, an effect caused by the absence of the protein's N-terminal portion cannot be completely ruled out. For example, one can speculate about a function of a putative integrin-interacting RGD motif present therein.

The role of multiplexin is clearly distinct from that of the classic structural collagen IV

The spatially and temporally very restricted expression of *dmp* contrasts with the landmarks of the two collagen IV molecules, that are the only other conserved collagens in *Drosophila* and general important ECM constituents. In *Drosophila*, their expression begins in embryonic stage 12 (Mirre *et al*. 1988) or even earlier (Natzle *et al*. 1982)

and hemocytes produce and disperse them all over the embryo while circulating in the hemolymph throughout the rest of embryonic development. During late embryogenesis, specific hemocytes also migrate along the ventral midline between the CNS and the epidermis, but these midline hemocytes are dispersed very asymmetrically (Wood *et al*. 2006), and we do not believe that any of the *dmp* expression we observed originates from these cells. Hence, Dmp production is largely different from collagen IV expression, since it is restricted to limited domains of immobile cells and occurs markedly later in development.

Both *dmp* deletion strains we generated are homozygous viable. This is in correlation with collagen XV and XVIII single knockouts in mice (Eklund *et al*. 2001; Fukai *et al*. 2002) and even with the double knockout (Ylikarppa *et al*. 2003), as well as the *C. elegans cle-1* mutation (Ackley *et al*. 2001), none of which are lethal. However, the *dmp* gene and two type IV collagen genes (Natzle *et al*. 1982; Yasothornsrikul *et al*. 1997) are the only collagen genes in the *Drosophila* genome, whereas vertebrates and nematodes possess a far greater number of collagen types and genes (Myllyharju and Kivirikko 2004). This renders the dispensability of Dmp in flies even more surprising than in other organisms, and underlines that its role is very different from that of collagen IV.

Endostatin monomers harbor a specific activity in axon pathfinding, and their dosage is critical

It was possible to rescue the $dmp^{\Delta C12-25}$ ISNb phenotype by overexpressing the Dmp3hNC1 isoform in $dmp^{\Delta C12-25}$ mutant background, while its overexpression in wild type had no effect on axon pathfinding. This indicates that the protein product from the transgene functions in a fashion similar to the endogenous protein. Monomeric ES had a rescue effect on the $dmp^{\Delta C12-25}$ ISNb phenotype that is indistinguishable from the effect of UAS-3hNC1, whereas UAS-NC1, which is expected to lead to the formation of trimeric ES, did not improve the phenotype. We conclude from this that a beneficial activity resides specifically within the monomeric ES version, which is necessary and sufficient for ensuring ISNb pathfinding accuracy. Biochemical work on vertebrate collagen XVIII has identified a number of proteases capable of releasing monomeric ES (Wen *et al*. 1999; Felbor *et al*. 2000; Ferreras *et al*. 2000; Lin *et al*. 2001; Heljasvaara *et al*. 2005) and proteolytic release has also been shown to be necessary to activate biological function (Heljasvaara *et al*. 2005). In our *dmp* mutants, a proteolytic release of monomeric ES might account for the rescue effect of UAS-3hNC1. This implies that ES release is not possible from UAS-NC1, since this construct does not improve the mutant phenotype. A possible explanation for this is that the triple helix region of the molecule is needed for specific enzyme-substrate recognition.

The overexpression effect of ES in wild type background is qualitatively different from its impact on the *dmp* mutant phenotype. While ES overexpression was largely beneficial in the mutant, it caused a variety of phenotypes in wild type background, ranging from a defective body morphology giving the impression that morphogenesis was hampered on a general level, to wild type looking individuals and such that appeared to exhibit a specific motor axon guidance phenotype. We suggest that the phenotypic differences between the two genotypes are due to an ES dosage effect. ES overexpression in *dmp* mutant background produces an ES quantity that can be fully absorbed by the standard interaction partners, whereas the ES excess in the wild type overexpression situation leads to an ES overcharge of standard or non-standard interaction partners that inhibits vital interactions with other molecules. In an alternative scenario, the detrimental effect of ES in wild type background would arise from an interaction between ectopic ES and the trunk of the Dmp molecule.

When overexpressing Dmp3hNC1, no detrimental effect is observed, so the full-length protein dosage increase over wild type level apparently does not pose a problem. This can be due to the endogenous mechanisms that balance proteolytic generation of monomeric ES, such as the characteristics of the proteases involved, which can include their spatial and temporal distribution, quantity, substrate affinity and the resulting turnover numbers.

NC1 does not function without endogenous Dmp and might differ in its action mechanism from monomeric ES

Transgenic expression of trimeric ES, as formed by the NC1 transgene product, and monomeric ES had exactly converse effects on the ISNb phenotypes of wild type and $dmp^{\Delta C12-25}$ mutants. Free ES was able to rescue the pathfinding defects observed in $dmp^{\Delta C12-25}$ and had a detrimental effect in wild type background. In contrast, the NC1 transgene, while having no impact in the mutant background, significantly reduced the wild type ISNb error rate of 7.2% to a virtually flawless ISNb guidance with 0.75% errors. These observations indicate that the function of NC1 depends on the presence of endogenous Dmp. In one scenario, endogenous Dmp plays a role in creating a microenvironment or architecture in the basement membrane that is permissive for NC1 activity. Conversely, a basement membrane without Dmp deteriorates in quality resulting in an inactive form of NC1. Alternatively, a direct interaction between Dmp or parts

of it and NC1 may be required for NC1 function. Each feature of Dmp may potentially convey the relevant interactions, including the collagen triple helix region, the TSPN-1 domain, the NC1 portion, or several of these domains cooperate. Since both the Dmp triple helix region and the ES domain contain putative GAG attachment sites (Dong *et al*. 2003), options for functional moieties include heparan sulfate side chains.

Another question concerns the mode of action of NC1. One possibility is that it acts, if supported by the presence of functional Dmp, by releasing ES. In this scenario, NC1 simply is an inhibited version of ES. This option, however, is contradicted by the observation that neither overexpression of ES nor of 3hNC1 improved pathfinding in wild type background. An alternative idea is that ES monomers and NC1 trimers play distinct roles. In this setting, ES cannot be released from NC1, but NC1 exerts its own action as a trimer when Dmp is present. One option for NC1 activity is that its trivalence is used to crosslink different ECM components. This might stabilize structures that contain guidance information and eventually enhance the stringency of guidance interactions.

The modulating capacity of Dmp derivatives may buffer guidance processes against perturbations

Our results show that the wild type ISNb error rate of 7.2% can be reduced by 10-fold by the expression of additional trimeric endostatin from the UAS-NC1 transgene. This illustrates that Dmp possesses a capacity to influence pathfinding accuracy that is not fully taken advantage of in the normal wild type situation. This could be explained in that a low rate of statistically no more than one error per individual does not decrease the affected individual's fitness and hence does not exert any selective pressure.

Another possible reason is that increasing the fidelity of guidance interactions would interfere with the system's error prevention and/or correction mechanisms. As already described, correct pathfinding depends on the appropriate balance of attractive and repulsive forces, and this system is susceptible to perturbations. The observation that nerves are occasionally misrouted in wild type is a reflection of this fact. An ability to correct errors would therefore convey a certain degree of robustness in dealing with such perturbations. Indeed, error correction has been described in the Drosophila motor axon guidance system for SNa misrouting phenotypes that occur due to axonal overexpression of FasII. In third instar larvae, incidence of this phenotype is much lower than in embryos, suggesting that errors can get corrected during larval stages (Lin and Goodman 1994). For zebrafish retinal axons, it has also been stated that errors occur in wild type, but get corrected (Hutson and Chien 2002). In the example of ISNb pathfinding, excess trimeric endostatin might impair the system's plasticity by overly stabilizing misleading guidance interactions, and thus impair correction mechanisms, and by consequence reduces plasticity of the system.

Our observation that *dmp* mutations lead to pathfinding defects shows that certain features of Dmp do normally act to improve guidance accuracy. Hence, Dmp seems to play a dual modulating role, and as detailed above, these roles are likely exerted by different mechanisms. On the one hand, Dmp helps leading nerves where they belong, but on the other hand, does normally not make full use of its capacity to do so. This opens up the possibility that Dmp is an agent that has multiple means to modulate axon guidance accuracy by buffering axonal navigation against perturbations. It will be interesting to see if excess NC1 is able to improve guidance phenotypes of mutants other than Dmp.

Opposed effects of mono- and trimeric endostatin are a widespread phenomenon and differ in a context-dependent manner

Different effects of monomeric versus oligomeric endostatin have also been observed in *C. elegans* (Ackley *et al*. 2001), but contrarily to our results, the *C. elegans cle-1* neuronal migratory phenotype gets rescued by the putatively trimeric NC1 domain, whereas the ES domain does not provide rescue activity.

Mono- and oligomeric ES have also been tested in vertebrate tissue culture systems for their effects on tubule formation and angiogenesis. Oligomeric ES is an inhibitor of tube morphogenesis in HUVEC (human umbilical vein endothelial cell) cultures, since an addition of oligomeric ES to the culture before tube formation inhibited the process, which is motility-dependent, whereas after completion of tube formation, oligomeric ES had a motogenic activity leading to dispersal of the tubular structures. Monomeric ES alone did not have any effect on cell behavior, but pre-incubation with ES inhibited the motogenic effect of oligomeric ES (Kuo *et al*. 2001). In a CAM (chorioallantoic membrane) angiogenesis assay system, mono- and oligomeric ES of collagen XV and XVIII are converse in their inhibitory activity, that also depends on the cytokine used for stimulating angiogenesis (Sasaki *et al*. 2000). In another context, using IBE cells (intrahepatic biliary epithelial), monomeric ES even enhanced tubule formation (Dixelius *et al*. 2000). Hence, the action of mono- and trimeric ES seems to greatly depend on the biological context, on the cell types involved and additional signals they receive from their environment. The only common theme seems to be an antagonistic action of monomeric versus oligomeric ES. In this light,

it is not surprising that the rescue activity we observed on the *Drosophila* motor axon guidance phenotype is exactly opposite to the results for mechanosensory neuron (MSN) migration in *C. elegans* (Ackley *et al*. 2001). Notably, the biological process of axonal growth cone steering depends on directional cues and their correct interpretation, which is a fundamental difference to all other experimental systems that compared the action of mono- and oligomeric ES so far, as these systems all focused on the presence or absence of migratory activity per se. This includes the observations made for *C. elegans* MSN migration, as the phenotypes described by Ackley *et al*. (2001) mainly consist of errors in migration distance of whole neurons and not direction. So the observations of ES effects we made are placed in a novel biological context, and differences compared with other contexts are not surprising.

For murine multiplexins biochemical interactions with several other ECM components have been observed (Sasaki *et al*. 2000). Together with the variety of biological effects described for multiplexin fragments by us and others, it seems likely that its exact mechanisms of action depends very much on the biological context. We have here provided the starting point for functionally integrating *Drosophila* multiplexin into the biological process of motor axon pathfinding.

Acknowledgments

Bernard Moussian was supported by Deutsche Forschungsgemeinschaft (DFG). We would like to thank Christiane Nüsslein-Volhard for her extensive support. We also thank Andrew Renault, Jana Krauss, Uwe Irion and Hermann Aberle for many helpful discussions.

References

Abdollahi, A., Hahnfeldt, P., Maercker, C., Grone, H.-J., Debus, J., Ansorge, W., Folkman, J., Hlatky, L. & Huber, P. 2004. Endostatin's antiangiogenic signaling network. *Mol. Cell* **13**, 649–663.

Ackley, B. D., Crew, J. R., Elamaa, H., Pihlajaniemi, T., Kuo, C. J. & Kramer, J. M. 2001. The NC1/endostatin domain of *Caenorhabditis elegans* type XVIII collagen affects cell migration and axon guidance. *J. Cell Biol*. **152**, 1219–1232.

Araujo, S. J. & Tear, G. 2003. Axon guidance mechanisms and molecules: Lessons from invertebrates. *Nat. Rev. Neurosci*. **4**, 910–922.

Arikawa-Hirasawa, E., Rossi, S. G., Rotundo, R. L. & Yamada, Y. 2002. Absence of acetylcholinesterase at the neuromuscular junctions of perlecan-null mice. *Nat. Neurosci*. **5**, 119–123.

Bandtlow, C. E. & Zimmermann, D. R. 2000. Proteoglycans in the developing brain: New conceptual insights for old proteins. *Physiol. Rev*. **80**, 1267–1290.

Becker, C. & Genschel, U. 2005. 5.2 Parametrische tests. In *Schliessende Statistik*. Springer-Verlag, Berlin Heidelberg.

Bortz, J. 2005. 5.3.1 vergleich der häufigkeiten eines zweifach gestuften merkmals. In *Statistik für Human- und Sozialwissenschaftler*. Springer Medizin-Verlag, Heidelberg.

Brand, A. H. & Perrimon, N. 1993. Targeted gene expression as a means of altering cell fates and generating dominant phenotypes. *Development* **118**, 401–415.

Bulow, H. E. & Hobert, O. 2004. Differential sulfations and epimerization define heparan sulfate specificity in nervous system development. *Neuron* **41**, 723–736.

Carulli, D., Laabs, T., Geller, H. M. & Fawcett, J. W. 2005. Chondroitin sulfate proteoglycans in neural development and regeneration. *Curr. Opin. Neurobiol*. **15**, 116–120.

Chilton, J. K. 2006. Molecular mechanisms of axon guidance. *Dev. Biol*. **292**, 13–24.

Clamp, A., Blackhall, F. H., Henrioud, A., Jayson, G., Javaherian, K., Esko, J., Gallagher, J., Merry, C. 2006. The morphogenic properties of oligomeric endostatin are dependent on cell surface heparan sulfate. *J. Biol. Chem*. **281**, 14813–14822.

Desai, C. J., Krueger, N. X., Saito, H. & Zinn, K. 1997. Competition and cooperation among receptor tyrosine phosphatases control motoneuron growth cone guidance in Drosophila. *Development* **124**, 1941–1952.

Dixelius, J., Larsson, H., Sasaki, T., Holmqvist, K., Lu, L., Engstrom, A., Timpl, R., Welsh, M. & Claesson-Welsh, L. 2000. Endostatin-induced tyrosine kinase signaling through the Shb adaptor protein regulates endothelial cell apoptosis. *Blood* **95**, 3403–3411.

Dong, S., Cole, G. J. & Halfter, W. 2003. Expression of collagen XVIII and localization of its glycosaminoglycan attachment sites. *J. Biol. Chem*. **278**, 1700–1707.

Eklund, L., Piuhola, J., Komulainen, J., Sormunen, R., Ongvarrasopone, S., Fassler, R., Muona, A., Ilves, M., Ruskoaho, H., Takala, T. & Pihlajaniemi, T. 2001. Lack of type XV collagen causes a skeletal myopathy and cardiovascular defects in mice. *Proc. Natl Acad. Sci. USA* **98**, 1194–1199.

Felbor, U., Dreier, L., Bryant, R. A., Ploegh, H. L., Olsen, B. R. & Mothes, W. 2000. Secreted cathepsin L generates endostatin from collagen XVIII. *EMBO J*. **19**, 1187–1194.

Ferreras, M., Felbor, U., Lenhard, T., Olsen, B. R. & Delaisse, J. 2000. Generation and degradation of human endostatin proteins by various proteinases. *FEBS Lett*. **486**, 247–251.

Fessler, J. H. & Fessler, L. I. 1989. Drosophila extracellular matrix. *Ann. Rev. Cell Biol*. **5**, 309–339.

Fox, A. N. & Zinn, K. 2005. The heparan sulfate proteoglycan syndecan is an *in vivo* ligand for the drosophila LAR receptor tyrosine phosphatase. *Curr. Biol*. **15**, 1701–1711.

Fukai, N., Eklund, L., Marneros, A. G., Oh, S. P., Keene, D. R., Tamarkin, L., Niemela, M., Ilves, M., Li, E., Pihlajaniemi, T. & Olsen, B. R. 2002. Lack of collagen XVIII/endostatin results in eye abnormalities. *EMBO J*. **21**, 1535–1544.

Fyrberg, C., Becker, J., Barthmaier, P., Mahaffey, J. & Fyrberg, E. 1997. A drosophila muscle-specific gene related to the mouse quaking locus. *Gene* **197**, 315–323.

Halfter, W., Dong, S., Schurer, B. & Cole, G. J. 1998. Collagen XVIII is a basement membrane heparan sulfate proteoglycan. *J. Biol. Chem*. **273**, 25404–25412.

Heljasvaara, R., Nyberg, P., Luostarinen, J., Parikka, M., Heikkila, P., Rehn, M., Sorsa, T., Salo, T. & Pihlajaniemi, T. 2005. Generation of biologically active endostatin fragments from human collagen XVIII by distinct matrix metalloproteases. *Exp. Cell. Res*. **307**, 292–304.

Hoang, B. & Chiba, A. 1998. Genetic analysis on the role of integrin during axon guidance in drosophila. *J. Neurosci*. **18**, 7847–7855.

Hurskainen, M., Eklund, L., Hagg, P. O., Fruttiger, M., Sormunen, R., Ilves, M. & Pihlajaniemi, R. 2005. Abnormal maturation of the

retinal vasculature in type XVIII collagen/endostatin deficient mice and changes in retinal glial cells due to lack of collagen types XV and XVIII. *FASEB J*. **19**, 1564–1566.

Hutson, L. D. & Chien, C. B. 2002. Pathfinding and error correction by retinal axons: The role of astray/robo2. *Neuron* **33**, 205–217.

Johnson, K. G., Ghose, A., Epstein, E., Lincecum, J., O'connor, M. B. & Van Vactor, D. 2004. Axonal heparan sulfate proteoglycans regulate the distribution and efficiency of the repellent slit during midline axon guidance. *Curr. Biol*. **14**, 499–504.

Kivirikko, S., Heinamaki, P., Rehn, M., Honkanen, N., Myers, J. C. & Pihlajaniemi, T. 1994. Primary structure of the alpha 1 chain of human type XV collagen and exon-intron organization in the 3′ region of the corresponding gene. *J. Biol. Chem*. **269**, 4773–4779.

Kliemann, S. E., Waetge, R. T., Suzuki, O. T., Passos-Bueno, M. R. & Rosemberg, S. 2003. Evidence of neuronal migration disorders in Knobloch syndrome: Clinical and molecular analysis of two novel families. *Am. J. Med. Genet. A*. **119**, 15–19.

Kuo, C. J., Lamontagne, K. R. Jr, Garcia-Cardena, G., Ackley, B. D., Kalman, D., Park, S., Christofferson, R., Kamihara, J., Ding, Y.-H., Lo, K.-M., Gillies, S., Folkman, J., Mulligan, R. C. & Javaherian, K. 2001. Oligomerization-dependent regulation of motility and morphogenesis by the collagen XVIII NC1/endostatin domain. *J. Cell Biol*. **152**, 1233–1246.

Lee, J.-S., Von Der Hardt, S., Rusch, M. A., Stringer, S. E., Stickney, H., Talbot, W., Geisler, R., Nusslein-Volhard, C., Selleck, S. B., Chien, C.-B. & Roehl, H. 2004. Axon sorting in the optic tract requires HSPG synthesis by ext2 (dackel) and extl3 (boxer). *Neuron* **44**, 947–960.

Li, D., Clark, C. C. & Myers, J. C. 2000. Basement membrane zone type XV collagen is a disulfide-bonded chondroitin sulfate proteoglycan in human tissues and cultured cells. *J. Biol. Chem*. **275**, 22339–22347.

Lin, H.-C., Chang, J.-H., Jain, S., Gabison, E., Kure, T., Kato, T., Fukai, N. & Azar, D. T. 2001. Matrilysin cleavage of corneal collagen type XVIII NC1 domain and generation of a 28-kDa fragment. *Invest. Ophthalmol. Vis. Sci*. **42**, 2517–2524.

Lin, D. M., Fetter, R. D., Kopczynski, C., Grenningloh, G. & Goodman, C. S. 1994. Genetic analysis of fasciclin II in drosophila: Defasciculation, refasciculation, and altered fasciculation. *Neuron* **13**, 1055–1069.

Lin, D. M. & Goodman, C. S. 1994. Ectopic and increased expression of fasciclin II alters motoneuron growth cone guidance. *Neuron* **13**, 507–523.

Marneros, A. G., She, H., Zambarakji, H., Hashizume, H., Connolly, E. J., Kim, I., Gragoudas, E., Miller, J. W. & Olsen, B. R. 2007. Endogenous endostatin inhibits choroidal neovascularization. *FASEB J*. **41**, 3809–3818.

Meyer, F. & Aberle, H. 2006. At the next stop sign turn right: The metalloprotease tolloid-related 1 controls defasciculation of motor axons in Drosophila. *Development* **133**, 4035–4044.

Miller, C. M., Page-Mccaw, A. & Broihier, H. T. 2008. Matrix metalloproteinases promote motor axon fasciculation in the Drosophila embryo. *Development* **135**, 95–109.

Mirre, C., Cecchini, J. P., Le Parco, Y. & Knibiehler, B. 1988. De novo expression of a type IV collagen gene in Drosophila embryos is restricted to mesodermal derivatives and occurs at germ band shortening. *Development* **102**, 369–376.

Mirre, C., Le Parco, Y. & Knibiehler, B. 1992. Collagen IV is present in the developing CNS during Drosophila neurogenesis. *J. Neurosci. Res*. **31**, 146–155.

Muragaki, Y., Abe, N., Ninomiya, Y., Olsen, B. R. & Ooshima, A. 1994. The human alpha 1 (XV) collagen chain contains a large amino-terminal non-triple helical domain with a tandem repeat structure and homology to alpha 1(XVIII): Collagen. *J. Biol. Chem*. **269**, 4042–4046.

Muragaki, Y., Timmons, S., Griffith, C. M., Oh, S. P., Fadel, B., Quertermous, T. & Olsen, B. R. 1995. Mouse Col18a1 is expressed in a tissue-specific manner as three alternative variants and is localized in basement membrane zones. *Proc. Natl Acad. Sci. USA* **92**, 8763–8767.

Myllyharju, J. & Kivirikko, K. I. 2004. Collagens, modifying enzymes and their mutations in humans, flies and worms. *Trends Genet*. **20**, 33–43.

Natzle, J. E., Monson, J. M. & Mccarthy, B. J. 1982. Cytogenetic location and expression of collagen-like genes in Drosophila. *Nature* **296**, 368–371.

Oh, S. P., Kamagata, Y., Muragaki, Y., Timmons, S. & Ooshima, A. 1994. Isolation and sequencing of cDNAs for proteins with multiple domains of Gly-Xaa-Yaa repeats identify a distinct family of collagenous proteins. *Proc. Natl Acad. Sci. USA* **91**, 4229–4233.

O'Reilly, M. S., Boehm, T., Shing, Y., Fukai, N., Vasios, G., Lane, W. S., Flynn, E., Birkhead, J. R., Olsen, B. R. & Folkman, J. 1997. Endostatin: An endogenous inhibitor of angiogenesis and tumor growth. *Cell* **88**, 277–285.

Parks, A. L., Cook, K. R., Belvin, M., Dompe, N. A., Fawcett, R., Huppert, K., Tan, L. R., Winter, C. G., Bogart, K. P., Deal, J. E., Deal-Herr, M. E., Grant, D., Marcinko, M., Miyazaki, W. Y., Robertson, S., Shaw, K. J., Tabios, M., Vysotskaia, V., Zhao, L., Andrade, R. S., Edgar, K. A., Howie, E., Killpack, K., Milash, B., Norton, A., Thao, D., Whittaker, K., Winner, M. A., Friedman, L., Margolis, J., Singer, M. A., Kopczynski, C., Curtis, D., Kaufman, T. C., Plowman, G. D., Duyk, G. & Francis-Lang, H. L. 2004. Systematic generation of high-resolution deletion coverage of the *Drosophila melanogaster* genome. *Nat. Genet*. **36**, 288–292.

Rawson, J. M., Dimitroff, B., Johnson, K. G., Rawson, J. M., Ge, X., Van Vactor, D. & Selleck, S. B. 2005. The heparan sulfate proteoglycans dally-like and syndecan have distinct functions in axon guidance and visual-system assembly in drosophila. *Curr. Biol*. **15**, 833–838.

Rehn, M. & Pihlajaniemi, T. 1995. Identification of three n-terminal ends of type XVIII collagen chains and tissue-specific differences in the expression of the corresponding transcripts. *J. Biol. Chem*. **270**, 4705–4711.

Rehn, M., Veikkola, T., Kukk-Valdre, E., Nakamura, H., Ilmonen, M., Lombardo, C., Pihlajaniemi, T., Alitalo, K. & Vuori, K. 2001. Interaction of endostatin with integrins implicated in angiogenesis. *Proc. Natl Acad. Sci. USA* **98**, 1024–1029.

Sasaki, T., Fukai, N., Mann, K., Gohring, W., Olsen, B. R. & Timpl, R. 1998. Structure, function and tissue forms of the C-terminal globular domain of collagen XVIII containing the angiogenesis inhibitor endostatin. *EMBO J*. **17**, 4249–4256.

Sasaki, T., Larsson, H., Kreuger, J., Salmivirta, M., Claesson-Welsh, L., Lindahl, U., Hohenester, E. & Timpl, R. 1999. Structural basis and potential role of heparin/heparan sulfate binding to the angiogenesis inhibitor endostatin. *EMBO J*. **18**, 6240–6248.

Sasaki, T., Larsson, H., Tisi, D., Claesson-Welsh, L., Hohenester, E. & Timpl, R. 2000. Endostatins derived from collagens XV and XVIII differ in structural and binding properties, tissue distribution and anti-angiogenic activity. *J. Mol. Biol*. **301**, 1179–1190.

Schneider, V. A. & Granato, M. 2006. The myotomal diwanka (lh3) glycosyltransferase and type XVIII collagen are critical for motor growth cone migration. *Neuron* **50**, 683–695.

Soding, J., Biegert, A. & Lupas, A. N. 2005. The HHpred interactive server for protein homology detection and structure prediction. *Nucleic Acids Res*. **33**, W244–W248.

Steigemann, P., Molitor, A., Fellert, S., Jackle, H. & Vorbruggen, G. 2004. Heparan sulfate proteoglycan syndecan promotes axonal and myotube guidance by slit/robo signaling. *Curr. Biol*. **14**, 225–230.

Sun, Q., Schindelholz, B., Knirr, M., Schmid, A. & Zinn, K. 2001. Complex genetic interactions among four receptor tyrosine phosphatases regulate axon guidance in Drosophila. *Mol. Cell. Neurosci*. **17**, 274–291.

Tan, K., Duquette, M., Liu, J. H., Zhang, R., Joachimiak, A., Wang, J. H. & Lawler, J. 2006. The structures of the thrombospondin-1 N-terminal domain and its complex with a synthetic pentameric heparin. *Structure* **14**, 33–42.

Tautz, D. & Pfeifle, C. 1989. A non-radioactive *in situ* hybridization method for the localization of specific RNAs in drosophila embryos reveals translational control of the segmentation gene hunchback. *Chromosoma* **98**, 81–85.

Tessier-Lavigne, M. & Goodman, C. S. 1996. The molecular biology of axon guidance. *Science* **274**, 1123–1133.

Thibault, S. T., Singer, M. A., Miyazaki, W. Y., Milash, B., Dompe, N. A., Singh, C. M., Buchholz, R., Demsky, M., Fawcett, R., Francis-Lang, H. L., Ryner, L., Cheung, L. M., Chong, A., Erickson, C., Fisher, W. W., Greer, K., Hartouni, S. R., Howie, E., Jakkula, L., Joo, D., Killpack, K., Laufer, A., Mazzotta, J., Smith, R. D., Stevens, L. M., Stuber, C., Tan, L. R., Ventura, R., Woo, A., Zakrajsek, I., Zhao, L., Chen, F., Swimmer, C., Kopczynski, C., Duyk, G., Winberg, M. L. & Margolis, J. 2004. A complementary transposon tool kit for *Drosophila melanogaster* using P and piggyBac. *Nat. Genet*. **36**, 283–287.

Voigt, A., Pflanz, R., Schäfer, U. & Jäckle, H. 2002. Perlecan participates in proliferation activation of quiescent drosophila neuroblasts. *Dev. Dyn*. **224**, 403–412.

Wen, W., Moses, M. A., Wiederschain, D., Arbiser, J. L. & Folkman, J. 1999. The generation of endostatin is mediated by elastase. *Cancer Res*. **59**, 6052–6056.

Whitelock, J. M. & Iozzo, R. V. 2005. Heparan sulfate: A complex polymer charged with biological activity. *Chem. Rev*. **105**, 2745–2764.

Wood, W., Faria, C. & Jacinto, A. 2006. Distinct mechanisms regulate hemocyte chemotaxis during development and wound healing in *Drosophila melanogaster*. *J. Cell Biol*. **173**, 405–416.

Yamaguchi, N., Anand-Apte, B., Lee, M., Sasaki, T., Fukai, N., Shapiro, R., Que, I., Lowik, C., Timpl, R. & Olsen, B. R. 1999. Endostatin inhibits VEGF-induced endothelial cell migration and tumor growth independently of zinc binding. *EMBO J*. **18**, 4414–4423.

Yasothornsrikul, S., Davis, W. J., Cramer, G., Kimbrell, D. A. & Dearolf, C. R. 1997. Viking: Identification and characterization of a second type IV collagen in drosophila. *Gene* **198**, 17–25.

Ylikarppa, R., Eklund, L., Sormunen, R., Muona, A., Fukai, N., Olsen, B. R. & Pihlajaniemi, T. 2003. Double knockout mice reveal a lack of major functional compensation between collagens XV and XVIII. *Matrix Biol*. **22**, 443–448.

Yu, H. H., Huang, A. S. & Kolodkin, A. L. 2000. Semaphorin-1a acts in concert with the cell adhesion molecules fasciclin II and connectin to regulate axon fasciculation in drosophila. *Genetics* **156**, 723–731.

Zecca, M., Basler, K. & Struhl, G. 1996. Direct and long-range action of a wingless morphogen gradient. *Cell* **87**, 833–844.

Supporting information

Additional Supporting information may be found in the online version of this article:

Supplement 1. Sequences of transcripts submitted to GenBank

Supplement 2. NC1 cDNA detection from wild type and *dmp*$^{\Delta N4-11}$

Supplement 3. Images of 24B-Gal4 driving expression of UAS constructs in somatic musculature, heart and ventral nerve cord

Supplement 4. Images of individuals overexpressing 24B-Gal4-driven UAS-ES, showing a generally defective body morphology, and impaired head development

Please note: Wiley-Blackwell are not responsible for the content or functionality of any supporting materials supplied by the authors. Any queries (other than missing material) should be directed to the corresponding author for the article.

Supplement 1:

Note on Fig. 1B

Numbers above or below splice bars indicate individual transcripts that made use of that particular splice site. Black splice bars were used in the majority of transcripts, while grey splice bars indicate exceptional events. If no number is give below a splice bar, these splice sites were used in all transcripts that come into question. Sequences of transcripts 1 – 13 have been submitted to GenBank (Accession nos. EU523228-EU523240). Transcript 14 represents the RH14382 cDNA clone from BDGP.

The two exons of CG8647, together with three novel exons, are spliced to different exons of the CG33171 ORF. These splicing events skip exons 3 and 4, and this finding is consistent for all 10 sequenced cDNA clones that were derived from a PCR primed within CG8647, now referred to as exons 1 or 2 of the *dmp* gene. We also amplified cDNAs that had exons 1 and 2 of CG33171 (now exons 3 and 4 of *dmp*) as their 5' termini, and found those to be joined to different exons. In summary, exons 1 and 2 and exons 3 and 4 code for two alternatively used 5' ends of *dmp* transcripts, and each of these alternative 5' ends contains its own start codon. Exon 1 as presented here starts with a translational start codon, and its 5' UTR is unknown at present. A large part of exons 3 and 4 is predicted as a 5' UTR, with a start codon positioned only 150 bp upstream of the end of exon 4. Exons 5, 6, 7, and 12 are novel exons, that all participate in alternative splicing events. Exons 5, 6, and 7 seem to be constitutive exons in cases where the transcript starts with the TSPN coding sequence, with only one

exception to this rule (transcript No. 1). Sequence analysis reveals that these exons encode part of the TSPN domain. A major splicing pattern variation is represented by cDNA No. 13, where exon 4 is directly joined to the first exon encoding the C-terminal ES domain. So the protein product of this transcript will be a single globular ES domain.

Exons 2, 9 and 10 contain new alternative 5'- or 3' splice sites. The utilisation of the alternative splice site in exon 9, as found in two different cDNAs, will result in a frameshift mutation and an early stop codon in exon 11.

Note that transcipts 1, 2, and 3 were amplified with a reverse primer in exon 8, so no statement can be made about their sequence further downstream. Similarly, transcripts 4-12 were amplified with a forward primer in exon 2, so it is well possible that exon 1 was part of the original transcripts. Dashed lines indicate exons that were left out from the illustration, because they were spliced to each other in an invariant pattern.

cDNAs were amplified using the following primers:

150for GGTGGCAGCTGGCACTAC, 152for ATGATTTGCACGCTCCTGG, 176for ATGCCCTGGCCGAATACACAC, 154re CGTCGAAGATGTCTGTCGC, 162re CCAGATTCTGTACCCTGGATG, 163re GCTGCATACTCATCGGCCGTC, 174ESre CGATAGCAGGCGAAATCC, 175re AGCTTGCTGTCGCAGGACTG.

Primers were paired as follows: 152for/154re (Transcript 1), 150for/154re (Transcripts 2 and 3), 176for/174re (Transcripts 4 and 5), 176for/175re (Transcripts 6 and 7), 176for/162re (Transcripts 8 and 9), 176for/163re

(Transcripts 10 and 11), 152for/175re (Transcript 12), 150for/175re (Transcript 13).

Supplement 2

NC1 cDNA detection from wild type and *dmp*$^{\Delta N4\text{-}11}$. We amplified the NC1 region from wild-type and homozygous *dmp*$^{\Delta N4\text{-}11}$ oligo-dT-primed cDNA, and yielded a strong band from wild type, whereas a weak band was obtained from *dmp*$^{\Delta N4\text{-}11}$ cDNA. We used a forward primer hybridizing with exon 19 and a reverse primer binding to exon 24. The weak band was eluted from the gel and subjected to another round of PCR using the same primers as before. The resulting amplificate turned out to consist of three products of slightly different length. These products were separated and sequenced, and we found that the wild type splicing variations for the 3' region of the gene are recapitulated with perfect fidelity in the deletion strain, as the three splice variants include either exons 20 and 21, exon 21 only, or none of the two. This led us to the conclusion that the splicing machinery is able to cope with the truncation of the locus to some extent and a certain amount of NC1-encoding functional transcript is present in the *dmp*$^{\Delta N4\text{-}11}$ allele.

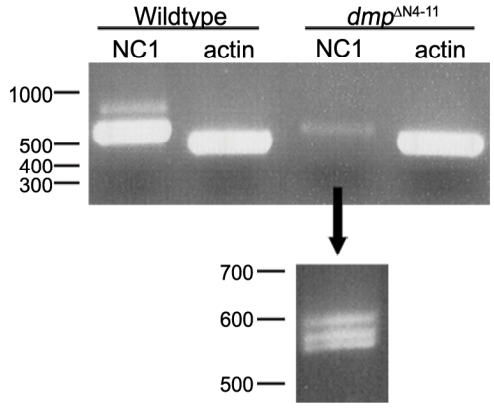

Supplement 3

24B-Gal4 drives expression of UAS constructs in somatic musculature, heart and ventral nerve cord. Images show one embryo of late stage 15 in dorsal (A) and ventral view (B). Arrowheads in A and B mark somatic musculature. Arrow in A indicates cardioblasts. Small arrows in B mark three rows of cells within the ventral nerve cord. For these images, 24B-Gal4 females were crossed to UAS-CD8-GFP males, and their progeny was fixed and stained with an anti-GFP antibody as mentioned in (Meyer & Aberle, 2006). In both images, anterior is to the left.

Meyer, F. & Aberle, H. 2006. At the next stop sign turn right: the metalloprotease Tolloid-related 1 controls defasciculation of motor axons in Drosophila. *Development,* **133,** 4035-4044.

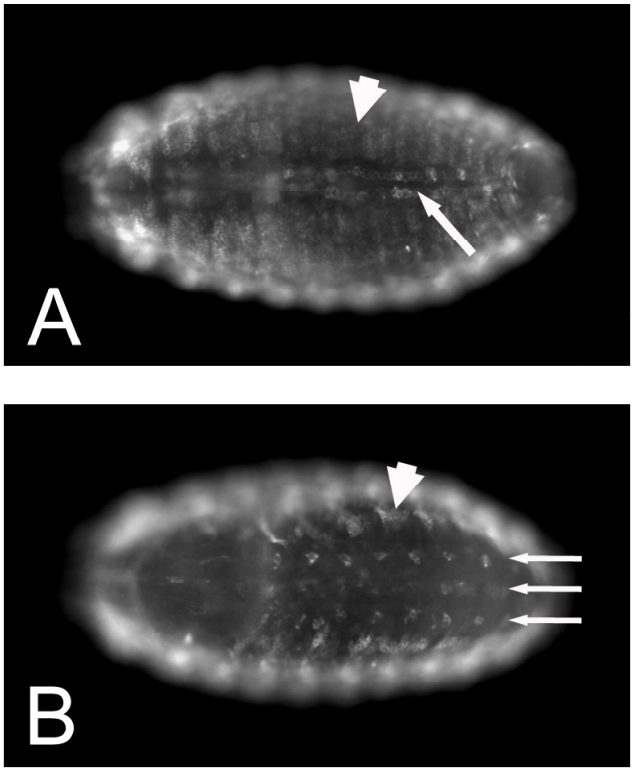

Supplement 4

A proportion of individuals overexpressing 24B-Gal4-driven UAS-ES showed a generally defective body morphology, and head development is impaired. Embryos depicted here are of stages 16 to 17. A: Healthy wild-type embryo. Arrow designates pharynx, that is a structure produced by head involution. B-D: Different examples of defective embryos overexpressing UAS-ES. In B, a head is not visible, while in C and D, head involution failed (arrows). Head involution is a morphogenetic event typical of acephalic insect larvae. It involves complex cell migration processes (VanHook & Letsou, 2008). In all images, anterior is to the left. In A-C, dorsal is up; D is a ventral view. Asterisks mark midgut.

Vanhook, A. & Letsou, A. 2008. Head involution in Drosophila: genetic and morphogenetic connections to dorsal closure. *Dev Dyn,* **237,** 28-38.